NASA/CR—2003-212361 91TM11

Users' Manual for Computer Code SPIRALG

Gas Lubricated Spiral Grooved Cylindrical and Face Seals

Jed A. Walowit
Jed A. Walowit, Inc., Clifton Park, New York

October 2005

The NASA STI Program Office . . . in Profile

Since its founding, NASA has been dedicated to the advancement of aeronautics and space science. The NASA Scientific and Technical Information (STI) Program Office plays a key part in helping NASA maintain this important role.

The NASA STI Program Office is operated by Langley Research Center, the Lead Center for NASA's scientific and technical information. The NASA STI Program Office provides access to the NASA STI Database, the largest collection of aeronautical and space science STI in the world. The Program Office is also NASA's institutional mechanism for disseminating the results of its research and development activities. These results are published by NASA in the NASA STI Report Series, which includes the following report types:

- TECHNICAL PUBLICATION. Reports of completed research or a major significant phase of research that present the results of NASA programs and include extensive data or theoretical analysis. Includes compilations of significant scientific and technical data and information deemed to be of continuing reference value. NASA's counterpart of peer-reviewed formal professional papers but has less stringent limitations on manuscript length and extent of graphic presentations.

- TECHNICAL MEMORANDUM. Scientific and technical findings that are preliminary or of specialized interest, e.g., quick release reports, working papers, and bibliographies that contain minimal annotation. Does not contain extensive analysis.

- CONTRACTOR REPORT. Scientific and technical findings by NASA-sponsored contractors and grantees.

- CONFERENCE PUBLICATION. Collected papers from scientific and technical conferences, symposia, seminars, or other meetings sponsored or cosponsored by NASA.

- SPECIAL PUBLICATION. Scientific, technical, or historical information from NASA programs, projects, and missions, often concerned with subjects having substantial public interest.

- TECHNICAL TRANSLATION. English-language translations of foreign scientific and technical material pertinent to NASA's mission.

Specialized services that complement the STI Program Office's diverse offerings include creating custom thesauri, building customized databases, organizing and publishing research results . . . even providing videos.

For more information about the NASA STI Program Office, see the following:

- Access the NASA STI Program Home Page at ***http://www.sti.nasa.gov***

- E-mail your question via the Internet to help@sti.nasa.gov

- Fax your question to the NASA Access Help Desk at 301–621–0134

- Telephone the NASA Access Help Desk at 301–621–0390

- Write to:
  NASA Access Help Desk
  NASA Center for AeroSpace Information
  7121 Standard Drive
  Hanover, MD 21076

NASA/CR—2003-212361 91TM11

Users' Manual for Computer Code SPIRALG

Gas Lubricated Spiral Grooved Cylindrical and Face Seals

Jed A. Walowit
Jed A. Walowit, Inc., Clifton Park, New York

Prepared under Contract NAS3–25644

National Aeronautics and
Space Administration

Glenn Research Center

October 2005

Document History

The source and executable files for the CFD Seal Analysis Industrial Codes, of which this is a part, were released as LEW–16582 in 1998. This report was originally published by Mechanical Technology, Inc., in July 1992.

Document Availability Change Notice

NASA/CR—2003-212361

Users' Manual for Computer Code SPIRALG Gas Lubricated Spiral Grooved Cylindrical and Face Seals

Jed A. Walowit

This document was published in July 2003 with the restriction Export Administration Regulations (EAR). It was changed to Unclassified/Unlimited July 27, 2005, by authority of the NASA Glenn Research Center, Structures Division.

This work was sponsored by the Low Emissions Alternative Power Project of the Vehicle Systems Program at the NASA Glenn Research Center.

Available from

NASA Center for Aerospace Information
7121 Standard Drive
Hanover, MD 21076

National Technical Information Service
5285 Port Royal Road
Springfield, VA 22100

Available electronically at http://gltrs.grc.nasa.gov

Table of Contents

List of Figures

Nomenclature

$\bar{A}$	dimensionless flow control area, (area/R_0^2)
A_i	coefficients of second order linear operator defined by Eq. (44), 1 = 1,...,6
{a}	column vector of eccentricity coefficients defined by Eq. (41)
$a^k_{i,j}$	kth component of {a} evaluated at grid point (i,j)
B_{xy}	damping coefficient relating force in x direction to velocity in y direction, B_{xx}, B_{yx}, B_{yy} and B_{zz} are similarly defined
$B_{\phi\psi}$	damping coefficient relating moment about x axis to angular velocity about y axis, $B_{\phi\phi}$, $B_{\psi\phi}$ and $B_{\psi\psi}$ are similarly defined
$B_{x\phi}$	damping coefficient relating force in x direction to angular velocity about x axis, $B_{x\psi}$, $B_{y\phi}$, $B_{y\psi}$, $B_{z\phi}$ and $B_{z\psi}$ are similarly defined
$B_{\phi x}$	damping coefficient relating moment about x axis to velocity in x direction, $B_{\psi x}$, $B_{\phi y}$, $B_{\psi y}$, $B_{\phi z}$ and $B_{\psi z}$ are similarly defined
$\tilde{B}_{xy}$	dimensionless damping coefficient B_{xy}/B_0, same definitions apply to $\tilde{B}_{xx}$, $\tilde{B}_{yx}$, $\tilde{B}_{yy}$, $\tilde{B}_{zz}$
$\tilde{B}_{\phi\psi}$	dimensionless damping coefficient $B_{\phi\psi}/(B_0R_0^2)$, same definitions apply to $\tilde{B}_{\phi\phi}$, $\tilde{B}_{\psi\phi}$, $\tilde{B}_{\psi\psi}$
$\tilde{B}_{x\phi}$	dimensionless damping coefficient $B_{x\phi}/(B_0R_0)$, same definitions apply to $\tilde{B}_{x\psi}$, $\tilde{B}_{y\phi}$, $\tilde{B}_{y\psi}$, $\tilde{B}_{z\phi}$, $\tilde{B}_{z\psi}$
$\tilde{B}_{\phi x}$	dimensionless damping coefficient $B_{\phi x}/(B_0R_0)$, same definitions apply to $\tilde{B}_{\psi x}$, $\tilde{B}_{\phi y}$, $\tilde{B}_{\psi y}$, $\tilde{B}_{\phi z}$, $\tilde{B}_{\psi z}$
B_0	characteristic damping constant, $12\mu R_0^4/C^3$
$[\tilde{B}]$	dimensionless damping coefficients in matrix form
{b}	column vector of coefficients of ϵ', arising from linearization of Eq. (39)
C	clearance (cylindrical seal) or reference film thickness (face seal)
$[C^j]$	coefficient matrix used in Newton-Raphson linearization procedure, see Eq. (34)
$[\hat{C}^j]$	coefficient matrix obtained from steady state solution
$[\hat{C}^{j,k}]$	derivative of $[\hat{C}^j]$ with respect to ϵ_k
$[\bar{C}^j]$	diagonal coefficient matrix whose components are given by Eq. (51)
$[C^{*j}]$	complex coefficient matrix used in complex stiffness solution, $[\hat{C}^j] + \Im\sigma[\bar{C}^j]$
$[D^j]$	coefficient matrix used in Newton-Raphson linearization procedure, see Eq. (34)
$[\hat{D}^j]$	coefficient matrix obtained from steady state solution
$[\hat{D}^{j,k}]$	derivative of $[\hat{D}^j]$ with respect to ϵ_k
$[E^j]$	coefficient matrix used in Newton-Raphson linearization procedure, see Eq. (34)
$[\hat{E}^j]$	coefficient matrix obtained from steady state solution
$[\hat{E}^{j,k}]$	derivative of $[\hat{E}^j]$ with respect to ϵ_k
e_x,e_y	eccentricity in x,y direction (cylindrical seal)
e_z	axial displacement, (face seal)
$F_{i,j}$	residual outflow function from flow balance at grid point (i,j)
G	second order non-linear operator defined by Eq. (39)

$\hat{H}$ steady state, unperturbed, value of H_r

H_r dimensionless film thickness, h_r/C

h film thickness

h_g film thickness over grooves, see Fig. 2

h_r film thickness over ridges, see Fig. 2

i,j,k subscripts used generically as indices

$\vec{i},\vec{j}$ unit vectors in θ,s directions

$\mathfrak{I}$ unit imaginary number, $\sqrt{-1}$

K_{xy} stiffness coefficient relating force in x direction to displacement in y direction, K_{xx}, K_{yx}, K_{yy} and K_{zz} are similarly defined

$K_{\phi\psi}$ stiffness coefficient relating moment about x axis to rotation about y axis, $K_{\phi\phi}$, $K_{\psi\phi}$ and $K_{\psi\psi}$ are similarly defined

$K_{x\phi}$ stiffness coefficient relating force in x direction to rotation about x axis, $K_{x\psi}$, $K_{y\phi}$, $K_{y\psi}$, $K_{z\phi}$ and $K_{z\psi}$ are similarly defined

$K_{\phi x}$ stiffness coefficient relating moment about x axis to displacement in x direction, $K_{\psi x}$, $K_{\phi y}$, $K_{\psi y}$, $K_{\phi z}$ and $K_{\psi z}$ are similarly defined

$\tilde{K}_{xy}$ dimensionless stiffness coefficient K_{xy}/K_0, same definitions apply to $\tilde{K}_{xx}$, $\tilde{K}_{yx}$, $\tilde{K}_{yy}$, $\tilde{K}_{zz}$

$\tilde{K}_{\phi\psi}$ dimensionless stiffness coefficient $K_{\phi\psi}/(K_0R_0^2)$, same definitions apply to $\tilde{K}_{\phi\phi}$, $\tilde{K}_{\psi\phi}$, $\tilde{K}_{\psi\psi}$

$\tilde{K}_{x\phi}$ dimensionless stiffness coefficient $K_{x\phi}/(K_0R_0)$, same definitions apply to $\tilde{K}_{x\psi}$, $\tilde{K}_{y\phi}$, $\tilde{K}_{y\psi}$, $\tilde{K}_{z\phi}$, $\tilde{K}_{z\psi}$

$\tilde{K}_{\phi x}$ dimensionless stiffness coefficient $K_{\phi x}/(K_0R_0)$, same definitions apply to $\tilde{K}_{\psi x}$, $\tilde{K}_{\phi y}$, $\tilde{K}_{\psi y}$, $\tilde{K}_{\phi z}$, $\tilde{K}_{\psi z}$

K_0 characteristic stiffness constant, $p_0R_0^2/C$

$[\tilde{K}]$ dimensionless stiffnesses in matrix form

k_i spiral groove coefficient defined by Eq. (25), $i=1,2,...,8$

L seal length, see Fig. 1

$\tilde{L}$ dimensionless length, $L/(2R_0)$

l_g groove width, $r\Delta\theta_g$

l_r ridge width, $r\Delta\theta_r$

$\mathfrak{L}$ second order linear operator defined by Eq. (44)

M number of grid points in s direction

M_x,M_y applied moment about x,y axis

$\tilde{M}_x,\tilde{M}_y$ dimensionless moment, $(M_x,M_y)/(R_0^3p_0)$

N number of grid points in θ direction

N_g number of spiral grooves

$\vec{n}$ unit vector normal to $\tilde{S}$

$\vec{n}_\beta$ unit vector normal to groove

P dimensionless pressure, $(p-p_0)/p_0$

$\hat{P}$ steady state unperturbed value of P

$P_{i,j}$ dimensionless pressure, P, at grid point (i,j)

P_i dimensionless pressure, P, at point i shown in Fig. 3, i=1,...,9

P_l, P_r dimensionless boundary pressures $(p_l-p_0)/p_0$, $(p_r-p_0)/p_0$

$\{P'\}$ column vector of dimensionless pressure disturbances due to perturbation in $\{\epsilon\}$

$\{P'^k_j\}$ column vector of disturbance pressures associated with ϵ_k

$\{P^*\}$ complex amplitude of $\{P'\}$, $\{P'\} = \{P^*\}e^{\Im\sigma\bar{t}}$

$\{P^{*k}_j\}$ column vector of complex stiffness pressures associated with ϵ_k

$\{P_\Re\}$ real part of $\{P^*\}$

$\{P_\Im\}$ imaginary part of $\{P^*\}$

p global pressure in absolute units

p' local pressure in absolute units

p_0 reference pressure in absolute units, normally taken to be the minimum of the boundary pressures

p_l, p_r boundary pressures in absolute units at s_l, s_r

$\bar{Q}$ dimensionless flow vector, $12\mu R_0\bar{q}/(p_0C^3)$

Q_s, Q_θ components of dimensionless flow vector in s,θ directions

Q^+_{ij}, Q^-_{ij} dimensionless flow components shown in Fig. 3

Q_{in} dimensionless flow rate, $12\mu q_{in}/(p_0C^3)$

$\bar{q}$ global flow vector, mass flow rate per unit transverse length divided by density at pressure p_0

q_s, q_θ components of $\bar{q}$ in s,θ directions

q_A global mass flow rate per unit area displaced by rate of decrease of film, divided by density at p_0

q_{in} volumetric flow rate measured at pressure p_0

$\bar{q}'$ local flow vector, mass flow rate per unit transverse length divided by density at pressure p_0

q'_s, q'_θ components of $\bar{q}'$ in s,θ directions

q'_A local mass flow rate per unit area displaced by rate of decrease of film, divided by density at p_0

R dimensionless coordinate, r/R_0, taken as 1 for cylindrical seal

R_0 reference radius, taken as outside radius for face seal and shaft radius for cylindrical seal

R_i inside radius of face seal

$\{R^j\}$ column vector used in Newton-Raphson linearization procedure, see Eq. (34)

$\{\hat{R}^j\}$ column vector obtained from steady state solution

$\{\hat{R}^{j,k}\}$ derivative of $\{\hat{R}^j\}$ with respect to ϵ_k

$\{\bar{R}^{j,k}_i\}$ column vectors whose components are given by Eq. (52)

$\{R^{j,k}\}$ complex column vectors used complex stiffness solution $\{\hat{R}^{j,k}\} - \Im\sigma\{\bar{R}^{j,k}\}$

r radial coordinate, taken as R_0 for cylindrical seal

S dimensionless coordinate, s/R_0

S_l, S_r dimensionless boundary coordinates s_l/R_0, s_r/R_0

$\bar{S}$ dimensionless length of line surrounding flow control area (length/R_0)

s transverse coordinate, s = r for a face seal and s = z for a cylindrical seal

s_g	transverse coordinate at start of groove
s_l	left boundary coordinate, $s_l = R_i$ for face seal and $s_l = -L/2$ for cylindrical seal
s_r	right boundary coordinate, $s_r = R_0$ for face seal and $s_r = L/2$ for cylindrical seal
T	torque
$\bar{T}$	dimensionless torque, $T/(p_0 R_0^2 C)$
$\bar{T}_c$	$\bar{T}$ obtained with course grid in Romberg extrapolation example
$\bar{T}_f$	$\bar{T}$ obtained with fine grid in Romberg extrapolation example
$\bar{T}_r$	$\bar{T}$ obtained by Romberg extrapolation
t	time
$\bar{t}$	dimensionless time, $\omega t/(2\Lambda)$
$\bar{t}_\beta$	unit vector tangential to groove
$\bar{u}_1$	velocity of grooved surface
$\bar{u}_2$	velocity of smooth surface
W_x, W_y	applied loads in x,y direction (cylindrical seal)
$\bar{W}_x, \bar{W}_y$	dimensionless loads $(W_x, W_y)/(p_0 R_0^2)$
W_z	applied load in z direction (face seal)
$\bar{W}_z$	dimensionless load, $W_z/(p_0 R_0^2)$
$\{\bar{W}\}$	column vector containing dimensionless loads and moments $\{\bar{W}_x, \bar{W}_y, \bar{M}_x, \bar{M}_y\}$ for cylindrical seal, $\{\bar{W}_z, \bar{M}_x, \bar{M}_y\}$ for face seal
$\{\bar{W}\}_{old}$	$\{\bar{W}\}$ at previous iteration in eccentricity homing process
x,y	coordinate variables, see Fig. 1
Z	dimensionless axial coordinate for cylindrical seal, z/R_0
z	axial coordinate, measured from axial center for cyl. seal or from reference film, C, for face seal
α	groove to pitch ratio, $l_g/(l_g + l_r)$
α_{opt}	value of α for maximum stagnation pressure gradient in concentric cylindrical seal
β	spiral groove angle, angle between grooves and surface velocity
β_{opt}	value of β for maximum stagnation pressure gradient in concentric cylindrical seal
$\bar{\beta}$	numerical damping factor used in eccentricity homing process
Γ	film thickness ratio, h_g/h_r
$\Delta\bar{A}$	dimensionless flow control area about single grid point, shaded area in Fig. 3
$\Delta\bar{A}_i$	portion of $\Delta\bar{A}$ in quadrant containing point i, see Fig. 3
Δp	global pressure difference, see Fig. 2
$\Delta p_g'$	pressure difference across groove, see Fig. 2
$\Delta p_r'$	pressure difference across ridge, see Fig. 2
$\Delta\bar{S}^+_{ij}$	line or arc length associated with Q^+_{ij}
$\Delta\bar{S}^-_{ij}$	line or arc length associated with Q^-_{ij}
Δs	transverse length of groove-ridge pair

$\Delta\theta$	circumferential extent of groove-ridge pair, see Fig. 2; (also used generally for change in θ)
$\Delta\theta_g$	circumferential extent of groove, see Fig. 2
$\Delta\theta_r$	circumferential extent of ridge, see Fig. 2
$\tilde{\delta}$	dimensionless groove depth, $(h_g-h_r)/C$
$\tilde{\delta}_{opt}$	value of $\tilde{\delta}$ for maximum stagnation pressure gradient in concentric cylindrical seal
ϵ_x,ϵ_y	eccentricity ratio, $(e_x,e_y)/C$ (cylindrical seal)
ϵ_z	axial displacement ratio e_z/C, (face seal)
ϵ_k	kth component of eccentricity matrix
$[\epsilon]$	row matrix of eccentricity components, $[\epsilon_z,\phi,\psi]$ (face seal) and $[\epsilon_x,\epsilon_y,\phi,\psi]$ (cylindrical seal)
$\{\epsilon\}$	column vector, transpose of $[\epsilon]$
$\{\epsilon\}_{old}$	$\{\epsilon\}$ at previous iteration in homing process
ϵ'	eccentricity disturbance function (scaler)
η	small increment used in perturbations and in evaluating derivatives
θ	angular coordinate, see Fig. 1
θ	angular coordinate at start of groove
Λ	compressibility number, $6\mu\omega R_0^2/(p_0C^2)$
Λ_δ	groove compressibility number, $\Lambda\tilde{\delta}\tilde{\omega}\alpha(1-\alpha)\sin\beta$
μ	viscosity
σ	squeeze number, $2\Lambda\tilde{\Omega}$
τ	global shear stress
$\tilde{\tau}$	dimensionless shear stress, $\tau R_0/(p_0C)$
τ'	local shear stress
Φ	rotation about x axis
ϕ	reduced rotation, $\Phi R_0/C$
Ψ	rotation about y axis
ψ	reduced rotation $\Psi R_0/C$
Ω	angular velocity of disturbance
$\tilde{\Omega}$	dimensionless disturbance frequency, Ω/ω
ω	total angular velocity, $\omega_1 + \omega_2$
$\tilde{\omega}$	dimensionless angular velocity ratio, $(\omega_2-\omega_1)/\omega$
ω_1	angular velocity of grooved surface
ω_2	angular velocity of smooth surface
$\vec{\nabla}$	gradient operator, $(1/r)(\partial/\partial\theta)\vec{i} + (\partial/\partial s)\vec{j}$, on dimensional quantities and $(1/R)(\partial/\partial\theta)\vec{i} + (\partial/\partial S)\vec{j}$, on dimensionless quantities

1. Introduction

Spiral groove bearings and seals are used to provide stability, load support and pumping for both cylindrical and face seal geometries. In the case of a cylindrical seal, grooves are usually designed to pump against each other in a symmetric arrangement to provide enhanced stability. A lightly loaded cylindrical seal operating at a low compressibility number will produce a force that is nearly 90 degrees out of phase with the displacement which will tend to destabilize the rotating shaft. The introduction of spiral grooves can significantly increase the component of force in phase with the displacement and decrease the out of phase component thereby improving stability.

In the case of a face seal or thrust bearing, spiral grooves are often introduced as the primary means of load support. Since a symmetric arrangement is not possible in a radial geometry, the grooves are usually designed to pump towards an ungrooved dam region. The resistance of the dam region increases as the film thickness decreases hence the pumping pressure rise increases thereby giving rise to a positive axial stiffness. The spiral grooves can also be used to pump against an applied pressure gradient thereby resulting in either reduced or reversed leakage.

The computer codes developed here are oriented toward the prediction of performance characteristics of gas lubricated cylindrical and face seals with or without the inclusion of spiral grooves. Performance characteristics include load capacity, leakage flow, power requirements and dynamic characteristics in the form of stiffness and damping coefficients in 4 degrees of freedom for cylindrical seals and 3 degrees of freedom for face seals. These performance characteristics are computed as functions of seal and groove geometry, loads or film thicknesses, running speed, fluid viscosity, and boundary pressures.

The basic assumptions that have gone into the computer code are listed below:

1. The flow is assumed to be laminar and isothermal.

2. Inertial effects are neglected.

3. The gas is assumed to be ideal.

4. The film thickness is assumed to be small compared with seal lengths and diameters but large compared with surface roughness and the mean free path of the gas.

5. Narrow groove theory is used which characterizes the effects of grooves by a global pressure distribution without requiring computations on a groove by groove basis. This involves neglecting

edge effects and local compressibility effects associated with groove to groove pressure variations. In general, narrow groove theory is valid when there are a sufficiently large number of grooves so that $2\pi\sin\beta/N_g << 1$, where β is the groove angle and N_g is the number of grooves.

6. Transient effects are treated with the use of small perturbations on a primary steady state flow. These transient effects are characterized by stiffness and damping coefficients that are dependent on the disturbance frequencies.

7. Although displacements and misalignments are treated, machined surfaces for face seals are assumed to be flat and machined clearances for cylindrical seals are assumed to be constant.

The above assumptions still leave the code applicable to a broad range of applications. Seals generally have small clearances and gasses have low densities resulting in sufficiently low Reynolds numbers for laminar flow. Practical designs should contain a fairly large number of grooves to ensure smooth, isotropic operation. At high sealed pressure differences the flow could become sonic thereby invalidating the first two assumptions but this will usually not be the case and can readily be checked based on the predicted leakage flow. Elastic and thermal distortions as well as machining tolerances should also be estimated to validate the constant clearance assumption. The overall accuracy of the program will depend on the grid size used. Factors such as high compressibility or squeeze numbers, small values of the minimum film thickness to clearance ratio and large values of the length to diameter ratio could require either a large number of grid points or carefully selected variable grids.

A derivation of the Equations governing the performance of gas lubricated spiral groove cylindrical and face seals along with a fairly detailed description of their solution is given in the next section. This will be followed by a description of the computer codes including an input description, sample cases and comparisons with results of other codes.

2. Formulation and Method of Solution

The first formulation of the equations governing gas lubricated spiral groove bearings is generally credited to Vohr and Pan [1]*. A more concise formulation is given in a second report [2] by these authors that has been used by Smalley [3] as a starting point in his generalized numerical treatment of the performance of spiral groove gas bearings. The work performed by Smalley may be applied to both bearings and seals. A principal limitation in all of the above references relates to the fact that solutions have only been provided for one dimensional forms of the equations which have been obtained by linearizing them based on near concentric and aligned conditions. The work described here deals with the numerical solution of the nonlinear equations for gas lubricated spiral groove seals at both eccentric and misaligned conditions.

Formulation of equations governing gas lubricated spiral groove seals

For completeness, a derivation of the narrow groove equations for spiral groove gas bearings and seals along the lines of that developed in Reference 2 will be provided here. Coordinate variables will be used to make the equations applicable to both cylindrical and face seals as can be seen with the aid of Figure 1. The circumferential coordinate, θ, is as shown in Figure 1. The transverse coordinate is described by the variable, **s**, which is taken to equal the radial coordinate, **r**, for a face seal and the axial coordinate, **z**, for a cylindrical seal. The quantity **r**, when it appears will denote radial position for a face seal and should be set equal to the shaft radius, R_0 for a cylindrical seal.

The isothermal, compressible form of the "Reynolds" equation may be written as a flow balance equating the divergence of the flow vector, $\vec{q}'$, to the flow per unit area squeezed out by the time rate of decrease of the film thickness, q_A'.

$$\vec{\nabla}\cdot\vec{q}' = \frac{1}{r}\frac{\partial}{\partial s}(rq_s') + \frac{1}{r}\frac{\partial q_\theta'}{\partial \theta} = q_A' \quad , \tag{1}$$

The local flow vector $\vec{q}' = q_\theta'\vec{i} + q_s'\vec{j}$ represents the mass flow rate per unit transverse length divided by the density at a reference pressure, p_0, which may be written in vector form as

$$\vec{q}' = -\frac{h^3}{12\mu}\frac{p'}{p_0}\vec{\nabla}p' + \frac{\vec{u}_1 + \vec{u}_2}{2}\frac{p'}{p_0}h \quad .$$

Since surface motion will be in the circumferential direction, the surface velocity vectors may be written as

* Numbers in brackets refer to references given at the end of this report.

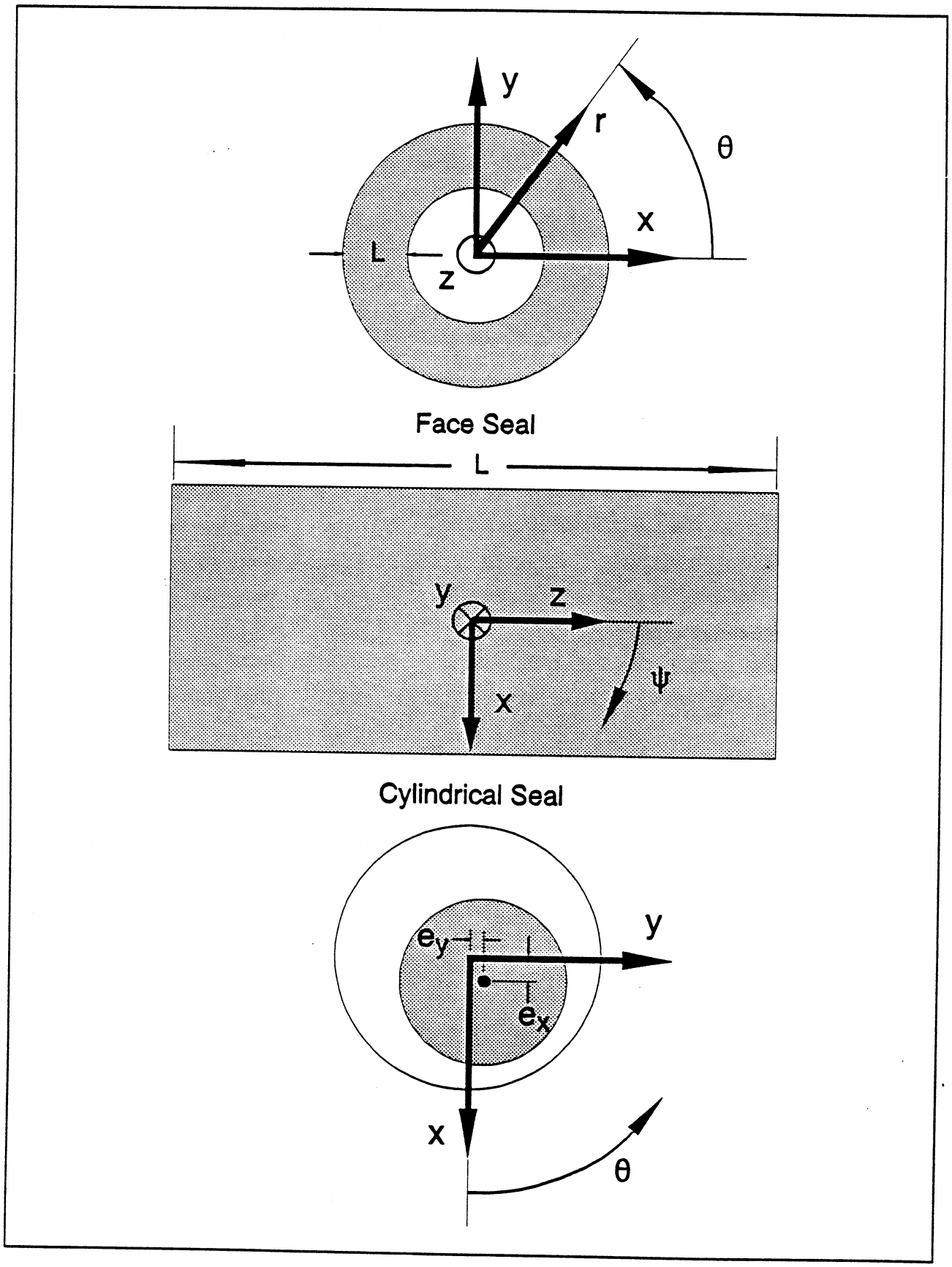

Figure 1 Coordinate system for spiral groove analysis.

$\vec{u}_1 = r\omega_1\vec{i}$ and $\vec{u}_2 = r\omega_2\vec{i}$ and the components of $\vec{q}'$ become

$$q_\theta' = -\frac{h^3}{12\mu}\frac{p'}{p_0}\frac{1}{r}\frac{\partial p'}{\partial\theta} + r\frac{\omega_1+\omega_2}{2}\frac{p'}{p_0}h \quad , \tag{2}$$

$$q_s' = -\frac{h^3}{12\mu}\frac{p'}{p_0}\frac{\partial p'}{\partial s} \quad . \tag{3}$$

The "squeeze film" term or displaced mass flow per unit area due to film motion, divided by the density at p_0 is

$$q_A' = -\frac{1}{p_0}\frac{\partial(p'h)}{\partial t} \tag{4}$$

One could substitute Equations (2) - (4) for the corresponding flow quantities in Equation (1) to obtain the usual form of the compressible Reynolds Equation which could in principle be solved, for any film thickness profile, $h(s,\theta)$ and appropriate boundary conditions, for the pressures or flow components to obtain the pressure distribution. These could in turn be integrated to obtain the various forces and moments associated with the given bearing geometry. The torque opposing the motion of say the smooth surface may be determined, once the pressure distribution is known, by integrating the shear stress relationship that arises in the development of Reynolds equation

$$\tau' = \frac{h}{2r}\frac{\partial p'}{\partial\theta} + \mu r\frac{\omega_2-\omega_1}{h} \quad . \tag{5}$$

The difficulty encountered in obtaining full numerical solutions to the above equations relates to the complexity of the grid network necessary to adequately describe the geometry of a surface containing the large number of spiral grooves usually required to provide sufficiently smooth pressure distributions to make the load characteristics independent of whether shaft displacement is over a ridge or over a groove. Narrow groove theory is generally used to circumvent this difficulty (References 1 - 3). It will be implemented here, as well and is described below.

Narrow groove theory provides the limiting form of the solution to Equations (1) - (5) as the number of grooves, N_g, becomes large, with the groove angle, β and the groove to pitch ratio, α, held constant. The discontinuities in film thickness associated with the grooves will give rise to discontinuities in the pressure gradients at the ridge-groove interfaces as illustrated schematically in Figure 2. The local pressure profile p' is shown by the sawtooth lines whose lower vertices, for purposes of illustration, are connected by the "global" pressure profile, p. The global pressure profile does not necessarily lie at the lower vertices of the

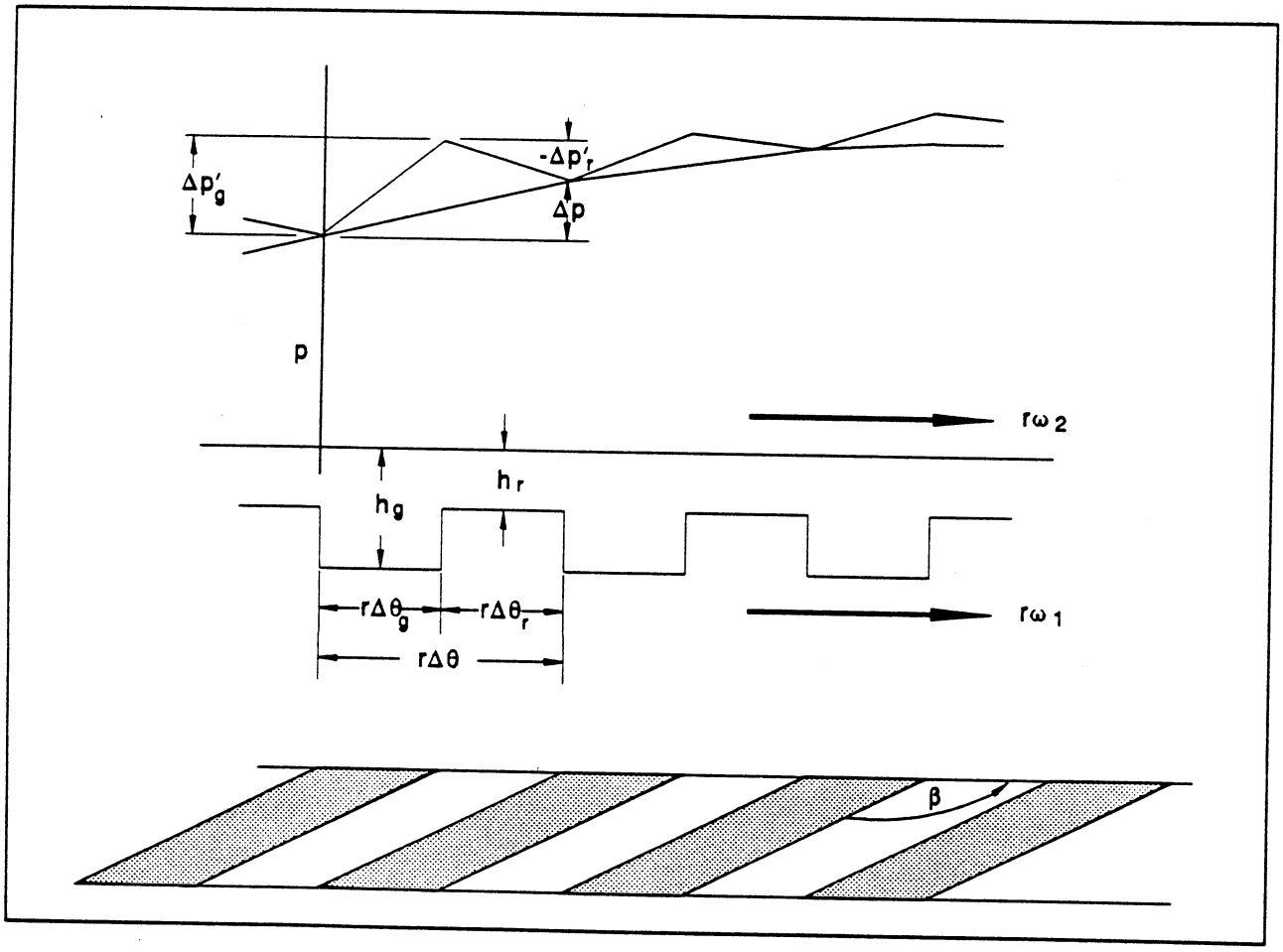

Figure 2 Schematic of spiral groove parameters, global and local pressures.

local pressure profile but could lie anywhere between the lower and upper vertices. In the limit as the number of grooves becomes large the curve connecting the upper vertices will approach the curve connecting the lower vertices. This limiting behavior is not true of $\partial p'/\partial\theta$, $\partial p'/\partial s$ or h, which will have different values over lands and grooves no matter how large the number of grooves. Narrow groove theory requires the development of expressions for the local (primed) quantities in terms of global quantities that approach single valued limits as the number of grooves becomes large. The local film thickness and pressure derivatives over the grooves will be denoted by h_g, $(\partial p'/\partial\theta)_g$ and $(\partial p'/\partial s)_g$ respectively and by h_r, $(\partial p'/\partial\theta)_r$ and $(\partial p'/\partial s)_r$ over the ridges. (The subscript r has been used here to denote ridges for consistency with References 1 - 3 and should not be confused when used in a different context later in the report to denote the right hand boundary pressure or with the radial position variable, r, which is not used as a subscript.)

When the number of grooves becomes large, the sawtooth portion of the local pressure variation may be approximated with linear representations as shown in Figure 2. Thus, equating pressures over a groove-ridge pair in the circumferential direction

$$\frac{\Delta p}{\Delta\theta} = \frac{\Delta p_g'}{\Delta\theta} + \frac{\Delta p_r'}{\Delta\theta} = \left(\frac{\partial p'}{\partial\theta}\right)_g \frac{\Delta\theta_g}{\Delta\theta} + \left(\frac{\partial p'}{\partial\theta}\right)_r \frac{\Delta\theta_r}{\Delta\theta} \quad .$$

Noting that $\Delta\theta_g/\Delta\theta = \alpha$ and $\Delta\theta_r/\Delta\theta = 1 - \alpha$ and replacing $\Delta p/\Delta\theta$ with $\partial p/\partial\theta$ as $\Delta\theta \to 0$, the above equation becomes

$$\frac{\partial p}{\partial\theta} = \alpha\left(\frac{\partial p'}{\partial\theta}\right)_g + (1-\alpha)\left(\frac{\partial p'}{\partial\theta}\right)_r \quad . \tag{6}$$

The corresponding relationship in the transverse direction,

$$\frac{\partial p}{\partial s} = \alpha\left(\frac{\partial p'}{\partial s}\right)_g + (1-\alpha)\left(\frac{\partial p'}{\partial s}\right)_r \quad , \tag{7}$$

is obtained in a similar manner.

The remaining two equations required to solve for the four local pressure derivatives are obtained from continuity considerations.

First, the pressure must be continuous at each groove-ridge interface, thus the derivative of the pressure in the direction of the interface, $\vec{\nabla}p' \cdot \vec{t}_\beta$, must also be continuous. The second requirement is for continuity of the flow normal to each groove-ridge interface as measured in a frame of reference moving with the grooves, $(\vec{q}' - r\omega_1 hp'/p_0\, \vec{i}) \cdot \vec{n}_\beta$. The unit tangent and normal vectors for a logarithmic spiral are given by

$$\vec{t}_\beta = \cos\beta\,\vec{i} + \sin\beta\,\vec{j}\,, \quad \vec{n}_\beta = \sin\beta\,\vec{i} - \cos\beta\,\vec{j} \quad .$$

The first of the above conditions requires continuity of

$$\frac{\cos\beta}{r}\frac{\partial p'}{\partial\theta} + \sin\beta\frac{\partial p'}{\partial s}$$

at each groove-ridge interface or

$$\frac{\cos\beta}{r}\left(\frac{\partial p'}{\partial\theta}\right)_g + \sin\beta\left(\frac{\partial p'}{\partial s}\right)_g = \frac{\cos\beta}{r}\left(\frac{\partial p'}{\partial\theta}\right)_r + \sin\beta\left(\frac{\partial p'}{\partial s}\right)_r \quad . \tag{8}$$

The second condition requires continuity of

$$(q_\theta' - r\omega_1 h\frac{p'}{p_0})\sin\beta - q_s'\cos\beta \quad .$$

One may substitute Equations (2) and (3) for the circumferential and transverse components of the flow vector at each groove-ridge interface, respectively to obtain

$$\begin{aligned} -\frac{h_g^3}{12\mu}\left[\frac{\sin\beta}{r}\left(\frac{\partial p'}{\partial\theta}\right)_g - \cos\beta\left(\frac{\partial p'}{\partial s}\right)_g\right] + \frac{h_g}{2}r(\omega_2-\omega_1)\sin\beta = \\ -\frac{h_r^3}{12\mu}\left[\frac{\sin\beta}{r}\left(\frac{\partial p'}{\partial\theta}\right)_r - \cos\beta\left(\frac{\partial p'}{\partial s}\right)_r\right] + \frac{h_r}{2}r(\omega_2-\omega_1)\sin\beta \quad . \end{aligned} \tag{9}$$

The density variation term, p'/p_0 is continuous at each interface and cancels out of Equation (9).

Equations (6) - (9) represent the four linear equations needed to solve for the local pressure derivatives. We may obtain the solution by first solving Equations (8) and (9) for the components of the local pressure gradient over the grooves in terms of those over the ridges. The resulting equations may be written as

$$\frac{1}{r}\left(\frac{\partial p'}{\partial \theta}\right)_g = \frac{h_g^3\cos^2\beta + h_r^3\sin^2\beta}{h_g^3}\frac{1}{r}\left(\frac{\partial p'}{\partial \theta}\right)_r + \frac{h_g^3 - h_r^3}{h_g^3}\sin\beta\cos\beta\left(\frac{\partial p'}{\partial s}\right)_r + 6\mu r(\omega_2 - \omega_1)\sin^2\beta\frac{h_g - h_r}{h_g^3}, \tag{10}$$

$$\left(\frac{\partial p'}{\partial s}\right)_g = \frac{h_g^3 - h_r^3}{h_g^3}\sin\beta\cos\beta\frac{1}{r}\left(\frac{\partial p'}{\partial \theta}\right)_r + \frac{h_g^3\sin^2\beta + h_r^3\cos^2\beta}{h_g^3}\left(\frac{\partial p'}{\partial s}\right)_r - 6\mu r(\omega_2 - \omega_1)\sin\beta\cos\beta\frac{h_g - h_r}{h_g^3}. \tag{11}$$

One may now substitute Equation (10) for $(\partial p'/\partial\theta)_g$ in Equation (6) and Equation (11) for $(\partial p'/\partial s)_g$ in Equation (7) to obtain 2 linear equations for the components of the ridge pressure gradient which may in turn be solved to yield the following expressions:

$$\frac{1}{r}\left(\frac{\partial p'}{\partial \theta}\right)_r = \frac{[h_g^3 - \alpha(h_g^3 - h_r^3\cos^2\beta)]\frac{1}{r}\frac{\partial p}{\partial \theta} - \alpha(h_g^3 - h_r^3)\sin\beta\cos\beta\frac{\partial p}{\partial s} - 6\mu r(\omega_2 - \omega_1)\alpha(h_g - h_r)\sin^2\beta}{(1-\alpha)h_g^3 + \alpha h_r^3}, \tag{12}$$

$$\frac{1}{r}\left(\frac{\partial p'}{\partial s}\right)_r = \frac{-\alpha(h_g^3 - h_r^3)\sin\beta\cos\beta\frac{1}{r}\frac{\partial p}{\partial \theta} + [h_g^3 - \alpha(h_g^3 - h_r^3\sin^2\beta)]\frac{\partial p}{\partial s} + 6\mu r(\omega_2 - \omega_1)\alpha(h_g - h_r)\sin\beta\cos\beta}{(1-\alpha)h_g^3 + \alpha h_r^3}. \tag{13}$$

The components of the local groove pressure gradient may be expressed in terms of the above ridge components by simple rearrangement of Equations (6) and (7):

$$\frac{1}{r}\left(\frac{\partial p'}{\partial \theta}\right)_g = -\frac{1-\alpha}{\alpha}\frac{1}{r}\left(\frac{\partial p'}{\partial \theta}\right)_r + \frac{1}{\alpha}\frac{1}{r}\frac{\partial p}{\partial \theta}, \tag{14}$$

$$\left(\frac{\partial p'}{\partial s}\right)_g = -\frac{1-\alpha}{\alpha}\left(\frac{\partial p'}{\partial s}\right)_r + \frac{1}{\alpha}\frac{\partial p}{\partial s}. \tag{15}$$

Now that expressions have been developed for the components of the local pressure gradients in terms of global ones, it is necessary to determine the global flow components q_s and q_θ and a global squeeze film term q_A that may be substituted for the local ones in the flow balance given by Equation (1). These global flow components are determined by matching mass flow rates over a groove-ridge pair with the mass flows obtained by integration of the local flow components over the same interval.

If θ_g is taken as the circumferential coordinate at the start of a groove, the transverse flow crossing an arc at fixed s, subtending a groove-ridge pair in the interval $\theta_g < \theta < \theta_g + \Delta\theta$ is given by the left hand term in the relationship

$$\int_{\theta_g}^{\theta_g+\Delta\theta} q_s' r d\theta \approx -\frac{h_g^3}{12\mu}\frac{p}{p_0}\left(\frac{\partial p'}{\partial s}\right)_g r\Delta\theta_g - \frac{h_r^3}{12\mu}\frac{p}{p_0}\left(\frac{\partial p'}{\partial s}\right)_r r\Delta\theta_r = q_s r\Delta\theta \quad .$$

The approximation to the integral in the above expression was obtained by dividing the integration interval, $\Delta\theta$ into sub-intervals for the groove, $\Delta\theta_g$ and ridge, $\Delta\theta_r$ and approximating q'_s, noting that as the number of grooves becomes large $\partial p'/\partial s$, will approach a constant value within each sub-interval. Since the pressure at the groove-ridge interface is continuous, the local density variation term, p'/p_0 was replaced by its global value p/p_0. The far right hand term in the above expression is based on the definition of the transverse component of the global flow rate described above. The right two equalities may be solved for q_s as

$$q_s = -\frac{h_g^3}{12\mu}\frac{p}{p_0}\alpha\left(\frac{\partial p'}{\partial s}\right)_g - \frac{h_r^3}{12\mu}\frac{p}{p_0}(1-\alpha)\left(\frac{\partial p'}{\partial s}\right)_r \quad . \tag{16}$$

One may obtain a relationship for the circumferential flow component q_θ in a similar manner by integrating q'_θ, given by Equation (3), at fixed θ, over a groove-ridge pair ($s_g < s < s_g + \Delta s$), approximating the integral over each sub-interval as above and equating the result to $q_\theta \Delta s$. The resulting expression may be written as

$$q_\theta = -\frac{h_g^3}{12\mu}\frac{p}{p_0}\alpha\frac{1}{r}\left(\frac{\partial p'}{\partial \theta}\right)_g - \frac{h_r^3}{12\mu}\frac{p}{p_0}(1-\alpha)\frac{1}{r}\left(\frac{\partial p'}{\partial \theta}\right)_r + r\frac{\omega_1+\omega_2}{2}\frac{p}{p_0}[\alpha h_g + (1-\alpha)h_r] \tag{17}$$

By integrating the squeeze film term q_A', given by Equation (4), over an area $r\Delta\theta\Delta s$, equating it to $q_A r\Delta\theta\Delta s$ and noting that the groove area fraction will be α and the ridge area fraction will be $1 - \alpha$, the following

expression is obtained:

$$q_A = -\frac{1}{p_0}\frac{\partial}{\partial t}(p[\alpha h_g + (1-\alpha)h_r]) \quad . \tag{18}$$

The global shear stress τ, may be determined by integrating the local shear stress τ', given by Equation (5), with respect to θ over the interval $\theta_g < \theta < \theta_g + \Delta\theta$, invoking the narrow groove approximations and equating the result to $\tau\Delta\theta$. The resulting expression may be written in the form

$$\tau = \frac{\alpha h_g}{2}\frac{1}{r}\left(\frac{\partial p'}{\partial\theta}\right)_g + \frac{(1-\alpha)h_r}{2}\frac{1}{r}\left(\frac{\partial p'}{\partial\theta}\right)_r + \mu r(\omega_2 - \omega_1)\left(\frac{\alpha}{h_g} + \frac{1-\alpha}{h_r}\right) \quad . \tag{19}$$

Equation (1) may now be applied directly to the global flow vector $\vec{q} = q_\theta\vec{i} + q_s\vec{j}$, as $\vec{\nabla}\cdot\vec{q} = q_A$ and by substituting Equation (18) for q_A and putting the result in dimensionless form one obtains:

$$\vec{\nabla}\cdot\vec{Q} = \frac{1}{R}\frac{\partial}{\partial S}(RQ_s) + \frac{1}{R}\frac{\partial Q_\theta}{\partial\theta} = -\frac{\partial}{\partial\tilde{t}}[(\alpha\tilde{\delta} + H_r)(1+P)] \quad . \tag{20}$$

The components of the global flow vector, q_θ and q_s are given in terms of the local pressure derivatives by Equations (16) and (17) respectively. These local derivatives are, in turn, given in terms of the global ones by Equations (12) - (15). The global flow components may be expressed completely in terms of global pressure derivatives by first substituting Equations (14) and (15) for the local pressure derivatives over the grooves and then substituting Equations (12) and (13) for the local pressure derivatives over the ridges. One may then collect terms and put the resulting two equations in dimensionless form to obtain the following expressions for the components of the dimensionless flow vector $\vec{Q} = Q_\theta\vec{i} + Q_s\vec{j}$:

$$Q_\theta = -(1+P)\left[H_r^3\left(k_2\frac{\partial}{\partial S} + \frac{k_3}{R}\frac{\partial}{\partial\theta}\right)P + \Lambda_\delta k_4 R\sin\beta - \Lambda(\alpha\tilde{\delta} + H_r)R\right] \quad , \tag{21}$$

$$Q_s = -(1+P)\left[H_r^3\left(k_1\frac{\partial}{\partial S} + \frac{k_2}{R}\frac{\partial}{\partial\theta}\right)P - \Lambda_\delta k_4 R\cos\beta\right] \quad . \tag{22}$$

The dimensionless variables associated with the above equations are

$$P = \frac{p - p_0}{p_0}\ ,\ \vec{Q} = \frac{12\mu R_0}{C^3 p_0}\vec{q}\ ,\ H_r = \frac{h_r}{C}\ ,\ S = \frac{s}{R_0}\ ,\ R = \frac{r}{R_0}\ ,\ \tilde{t} = \frac{\omega}{2\Lambda}t\ ,\ \Gamma = \frac{h_g}{h_r}\ . \qquad (23)$$

The dimensionless gage pressure P in the above equations is taken relative to the absolute pressure p_0 which will henceforth be taken as the minimum of the two boundary pressures in absolute units. The dimensionless parameters associated with the above equations are

$$\Lambda = \frac{6\mu\omega R_0^2}{p_0 C^2}\ ,\ \Lambda_\delta = \Lambda\tilde{\delta}\tilde{\omega}\alpha(1-\alpha)\sin\beta\ ,\ \tilde{\omega} = \frac{\omega_2 - \omega_1}{\omega}\ ,\ \tilde{\delta} = \frac{(h_g - h_r)}{C}\ ,\ \alpha = \frac{l_g}{l_r + l_g} \qquad (24)$$

and the column matrix containing spiral groove coefficients, $k_i(\alpha,\beta,\Gamma)$, in the above equations is

$$k = \left\{ \begin{array}{c} \dfrac{\alpha(1-\alpha)(\Gamma^3-1)^2\sin^2\beta + \Gamma^3}{(1-\alpha)\Gamma^3 + \alpha} \\ \dfrac{\alpha(1-\alpha)(\Gamma^3-1)^2\sin\beta\cos\beta}{(1-\alpha)\Gamma^3 + \alpha} \\ \dfrac{\alpha(1-\alpha)(\Gamma^3-1)^2\cos^2\beta + \Gamma^3}{(1-\alpha)\Gamma^3 + \alpha} \\ \dfrac{(\Gamma^3-1)}{(1-\alpha)\Gamma^3 + \alpha} \\ \dfrac{(1-\alpha)\Gamma + \alpha}{\Gamma} \\ \dfrac{(\Gamma-1)\sin\beta}{(1-\alpha)\Gamma^3 + \alpha} \\ \dfrac{\alpha(1-\alpha)(\Gamma^3-1)(\Gamma-1)\sin\beta\cos\beta}{(1-\alpha)\Gamma^3 + \alpha} \\ \dfrac{\alpha(1-\alpha)(\Gamma^3-1)(\Gamma-1)\cos^2\beta + \alpha\Gamma + (1-\alpha)\Gamma^3}{(1-\alpha)\Gamma^3 + \alpha} \end{array} \right\}\ . \qquad (25)$$

Only the first 4 components of k are used in Equations (21) - (22). The remaining components are used in evaluating the shear stress. The relationships for k_i, i=1,2,3,4 derived here are consistent with Equation (3.27) of Reference 2.

The global shear stress is obtained by substituting Equation (14) for $(\partial p'/\partial\theta)_g/r$ in Equation (19) then substituting Equation (12) for $(\partial p'/\partial\theta)_r/r$ in the resulting expression. The latter result may be expressed in dimensionless form as

$$\bar{\tau} = \frac{1}{2}\left[k_5\frac{\Lambda}{3}\frac{\tilde{\omega}R}{H_r} + k_6\Lambda_\delta\frac{R}{H_r^2} + k_7H_r\frac{\partial P}{\partial S} + k_8\frac{H_r}{R}\frac{\partial P}{\partial\theta}\right] , \qquad (26)$$

which is consistent with Equation (3.88) of Reference 2.

The equations presented thus far are directly applicable to either a cylindrical seal or a face seal. As mentioned earlier, a face seal is represented in the above equations by setting the transverse coordinate **s** equal to the radial coordinate **r**. This is equivalent to setting **S = R** in dimensionless form. A cylindrical seal is represented in dimensionless form by setting **S = Z** and **R = 1**.

The quantities required to characterize the groove dimensions are shown in Figure 2. If by convention ω is taken to be positive (surface motion in the direction of increasing θ), then the groove angle, β, will be the angle measured from the groove to the direction of surface motion associated with ω. A positive acute value of β will tend to pump in the positive S direction if the grooves are on the stator and in the negative S direction for grooves on the rotor. By setting the groove depth parameter $\tilde{\delta} = 0$, Γ becomes 1 and Equations (20) - (26) reduce to those for ungrooved seals. By treating **k** and $\tilde{\delta}$ as sectionally continuous functions of **S**, these equations may be applied to composite smooth and grooved geometries with Q_s and **P** held continuous at all transition boundaries.

The film thickness relationship for H_r, which may be applied to either a cylindrical seal or a face seal is

$$H_r = 1 - \epsilon_z - (\epsilon_x + \psi S)\cos\theta - (\epsilon_y - \phi S)\sin\theta \qquad (27)$$

with $\epsilon_z = 0$ for a cylindrical seal and $\epsilon_x = \epsilon_y = 0$ for a face seal.

The boundary pressures will be taken to be p_i and p_r at the inside and outside radii respectively for a face seal or at the two ends ($z = -L/2$ and $Z = L/2$) for a cylindrical seal. This is expressed in dimensionless form

$$P = P_i \text{ at } S = S_i , \quad P = P_r \text{ at } S = S_r . \qquad (28)$$

The remaining boundary condition relates to periodicity with respect to θ which requires **P** and Q_θ to have

the same values at $\theta = 0$ as they do at $\theta = 2\pi$:

$$P|_{\theta=0} = P|_{\theta=2\pi} \quad \text{and} \quad Q_\theta|_{\theta=0} = Q_\theta|_{\theta=2\pi} \ . \tag{29}$$

The above treatment is intended to represent a complete statement of the mathematical problem for determining the pressures and surface shear stresses in plain or spiral groove face or cylindrical seals. The rest of this section will deal with the numerical determination of the pressure distribution and the computation of related quantities such as loads, leakage, power loss, stiffness and damping.

Discretization of pressure equations

Discretization will be carried out with the use of the cell method [4] which involves the performance of a flow balance about each interior grid point. One may integrate Equation (20) over an arbitrary control area within a seal

$$\int_{\bar{A}} \vec{\nabla}\cdot\vec{Q}\, d\bar{A} + \int_{\bar{A}} \frac{\partial}{\partial \bar{t}}[(\alpha\bar{\delta} + H_r)(1 + P)]\, d\bar{A} = 0$$

and apply the divergence theorem to the first integral on the left to obtain the relationship

$$\oint_{\bar{S}} \vec{Q}\cdot\vec{n}\, d\bar{S} + \int_{\bar{A}} \frac{\partial}{\partial \bar{t}}[(\alpha\bar{\delta} + H_r)(1 + P)]\, d\bar{A} = 0 \ , \tag{30}$$

which will be used as a starting point in the discretization process.

A grid network may be set up along with flow control areas about each grid point as shown in Figure 3. The grid will contain **M** lines in the **S** direction including boundaries and **N** lines in the θ direction from $\theta = 0$ to $\theta = 2\pi$, inclusive. The grid points at the intersections of these lines are noted by the solid circles. Flow control areas to be used in evaluation of the integrals in Equation (30) are set up about each grid point as shown by the shaded area in Figure 3. The corners of the flow control area denoted by the shaded points marked **1**,**2**,**3**, and **4** are located at the geometric centers of the rectangles formed by the grid lines and will be referred to as half grid points. The flow components labeled Q^{+}_{12} etc., represent the components of the flow vector in the positive coordinate directions as indicated by the arrows. The subscripts (**12** etc.) refer to the line connecting points **1** and **2**, and the superscripts (+,-) refer to the positive or negative side of the

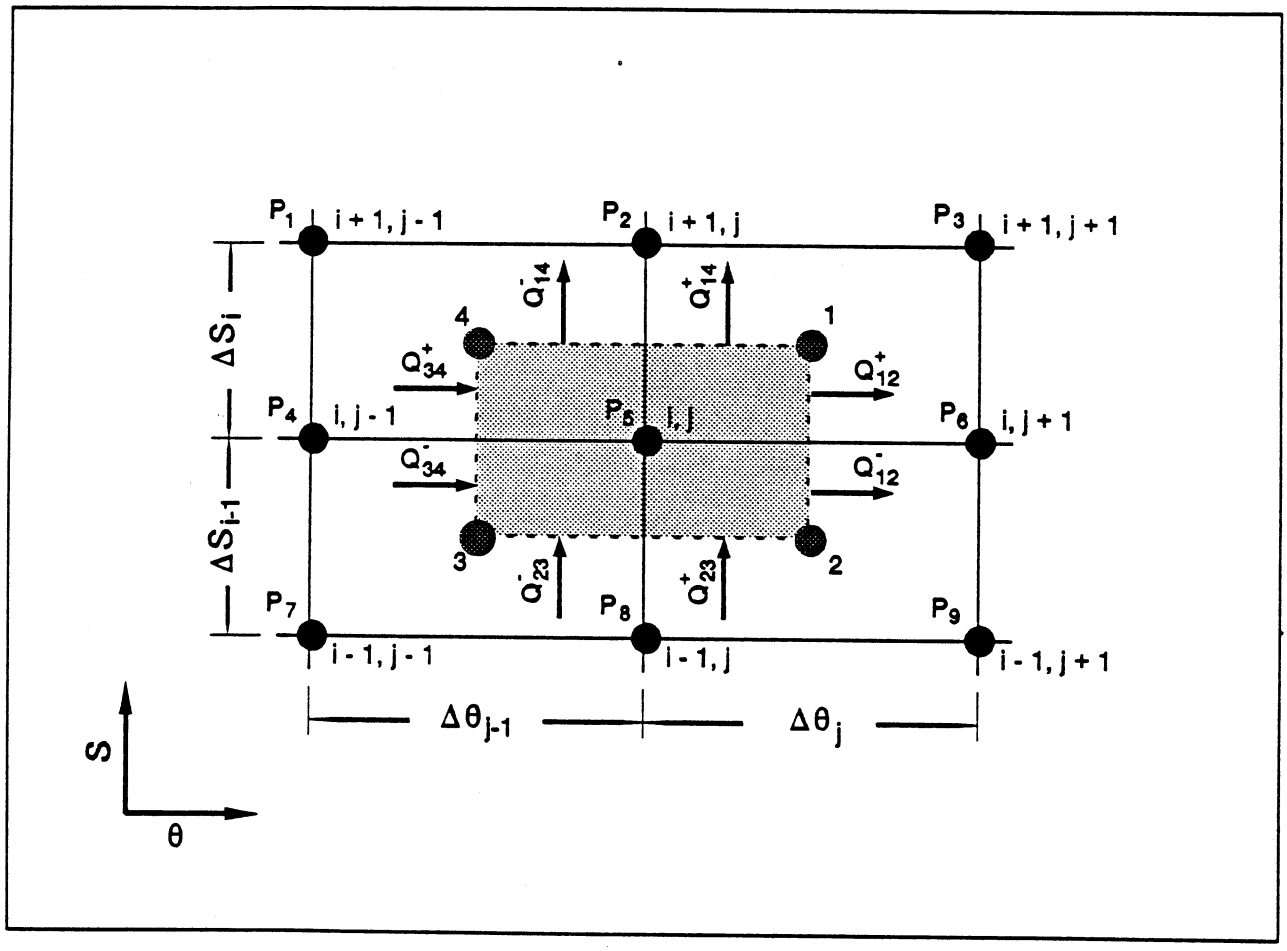

Figure 3 Schematic of grid network and flow control area for discretization process

point of intersection with the grid line.

We will adopt the convention that the subscripts i,j refer to grid points and subscripts such as $i+\frac{1}{2},j+\frac{1}{2}$ refer to half grid points. The value of the radius R at half grid point 2 would thus be $R_{i-\frac{1}{2}}$. The differential control length, $d\bar{S}$, in Equation (30) will be approximated by the lengths of the various lines or arcs bounding the flow control area thus $\Delta\bar{S}^{+}_{12}$ refers to the length of the line associated with Q^{+}_{12} described above which for this example would be $\Delta S_i/2$. Similarly the arc length associated with Q^{-}_{14} would be $\Delta\bar{S}^{-}_{14} = R_{i+\frac{1}{2}}\Delta\theta_{j-1}/2$.

The area element $d\bar{A}$ will be made up of the parts of the flow control area in each of the four quadrants about the center point (i,j) and numbered based on the shaded half grid point that each contains. Thus $\Delta\bar{A}_1 = (R_i+R_{i+\frac{1}{2}})\Delta\theta_j\Delta S_i/8$, etc. and the discretized form of Equation (30) may be written as:

$$Q^{-}_{12}\Delta\bar{S}^{-}_{12} + Q^{+}_{12}\Delta\bar{S}^{+}_{12} + Q^{+}_{14}\Delta\bar{S}^{+}_{14} + Q^{-}_{14}\Delta\bar{S}^{-}_{14} - Q^{+}_{34}\Delta\bar{S}^{+}_{34} - Q^{-}_{34}\Delta\bar{S}^{-}_{34} - Q^{-}_{23}\Delta\bar{S}^{-}_{23} - Q^{+}_{23}\Delta\bar{S}^{+}_{23} =$$
$$-\frac{\partial}{\partial\bar{t}}\left\{(1+P_{ij})\left[(\alpha\bar{\delta}+H_r)_{i+\frac{1}{2},j+\frac{1}{2}}\Delta\bar{A}_1 + (\alpha\bar{\delta}+H_r)_{i+\frac{1}{2},j-\frac{1}{2}}\Delta\bar{A}_4 + (\alpha\bar{\delta}+H_r)_{i-\frac{1}{2},j-\frac{1}{2}}\Delta\bar{A}_3 + (\alpha\bar{\delta}+H_r)_{i-\frac{1}{2},j+\frac{1}{2}}\Delta\bar{A}_2\right]\right\} . \quad (31)$$

The flow components on the left hand side of Equation (31) are obtained from discretization of Equations (21) and (22). A numbering system for the 9 pressures at the grid point (i,j) and the 8 surrounding points is shown in Figure 3, where $P_1 = P_{i+1,j-1}$, $P_5 = P_{i,j}$ etc. The determination of the flows out of the sub-area containing the half grid point labeled 1 is discussed here as an example. The flow component Q^{+}_{12}, is determined from Equation (21). The derivative of the pressure normal to the line connecting points 1 and 2 is evaluated at the intersection of the line with the grid line. The tangential derivative is evaluated at the half grid point, 1 as the average of the difference between P_3 and P_6 with that between P_2 and P_5, divided by ΔS_i. Thus,

$$\frac{1}{R}\frac{\partial P}{\partial\theta} \approx \frac{P_6 - P_5}{R_i\Delta\theta_j}, \quad \frac{\partial P}{\partial S} \approx \frac{(P_3 - P_6) + (P_2 - P_5)}{2\Delta S_i} \quad (\text{for } Q^{+}_{12}) .$$

The flow component Q^{+}_{14} is determined in a similar manner from Equation (22). The normal derivative is approximated as the difference between P_2 and P_5 divided by ΔS_i and the tangential derivative is approximated as the average of the differences between P_3 and P_2, and P_6 and P_5, divided by $R_{i+\frac{1}{2}}\Delta\theta_j$.

$$\frac{\partial P}{\partial S} \approx \frac{P_2 - P_5}{\Delta S_i}, \quad \frac{1}{R}\frac{\partial P}{\partial\theta} \approx \frac{(P_3 - P_2) + (P_6 - P_5)}{2R_{i+\frac{1}{2}}\Delta\theta_j} \quad (\text{for } Q^{+}_{14}) .$$

For both of the above flow components the pressure in the $(1+P)$ term appearing in Equations (21) and (22) is evaluated at the half grid point by averaging the four surrounding pressures $(P_2+P_3+P_5+P_6)/4$. All of the remaining quantities (R, H_r, k_1, k_2, k_3, k_4, α, β and $\tilde{\delta}$) are evaluated directly at the half grid point.

The flow balances over the other quadrants are performed in a similar manner. For steady state conditions, the right hand side of Equation (31) will be 0 and the flow balance about any interior grid point (i,j) may be written in the form

$$F_{ij}(H_r, P_1, P_2, P_3, P_4, P_5, P_6, P_7, P_8, P_9) = 0 \quad . \tag{32}$$

The definition of F_{ij} may be extended to make Equation (32) applicable to the ends of the seal as well as the interior points by applying Equation (28) at the endpoints as follows:

$$F_{1j} = P_5 - P_l \quad (i = 1) \quad \text{and} \quad F_{Mj} = P_5 - P_r \quad (i = M) \quad .$$

The solution to Equation (32) may be used to provide all of the steady state quantities such as pressures, forces, moments, flow rate and power loss. The inclusion of the right hand side of Equation (31) will be necessary for determination of frequency dependent stiffness and damping coefficients which will be discussed later.

Newton-Raphson linearization procedure

The Newton-Raphson [5] procedure is perhaps the most widely used method for obtaining solutions to non-linear systems of algebraic equations and is described in many textbooks on numerical methods such as Reference 5. A procedure similar to that used here is described in a paper by Artiles, Walowit and Shapiro [6].

The procedure is started with an initial pressure distribution that satisfies the end conditions given by Equation (28). A new set of approximations to the pressures in Equation (32), P_k^{new} may be obtained by linearizing F_{ij} about a previously established set of approximations P_k as follows:

$$F_{ij} + \sum_{k=1}^{9} \frac{\partial F_{ij}}{\partial P_k}\left(P_k^{new} - P_k\right) = 0 \tag{33}$$

where a forward difference

$$\frac{\partial F_{ij}}{\partial P_k} = \frac{F_{ij}(H_r, P_1, \ldots, P_k + \eta, \ldots, P_9) - F_{ij}(H_r, P_1, \ldots, P_9)}{\eta}$$

may be used to numerically evaluate the partial derivatives.

Pressures without the superscript **new** relate to the previous or "old" approximation. It should be noted that the function F_{ij} will not be 0 unless the pressures comprising its arguments are exact. If we go back to using grid notation for P ($P_{i,j}$ in place of P_5 etc.) and introduce the column vector $\{P_j^{new}\}$ as the M new pressures at the jth column of grid points, Equation (33) may be written in the following form:

$$[C^j]\{P_j^{new}\} + [E^j]\{P_{j-1}^{new}\} + [D^j]\{P_{j+1}^{new}\} = \{R^j\} \quad , \tag{34}$$

where $[C^j]$, $[E^j]$ and $[D^j]$ are tri-diagonal matrices whose interior elements, from Equation (33), are

$$C^j_{i,i+k} = \frac{\partial F_{ij}}{\partial P_{i+k,j}} \quad , \quad E^j_{i,i+k} = \frac{\partial F_{ij}}{\partial P_{i+k,j-1}} \quad , \quad D^j_{i,i+k} = \frac{\partial F_{ij}}{\partial P_{i+k,j+1}} \quad , \quad k = -1,0,1 \; ; \; i = 2,\ldots,M-1 \; .$$

The interior elements of the column vector $\{R^j\}$ are

$$R_i^j = \sum_{k=-1}^{1} \left(C^j_{i,i+k} P_{i+k,j} + E^j_{i,i+k} P_{i+k,j-1} + D^j_{i,i+k} P_{i+k,j+1} \right) - F_{ij} \quad .$$

The above equations may also be applied to the corner elements to produce the result

$$C^j_{1,1} = C^j_{M,M} = 1 \; , \quad E^j_{1,1} = E^j_{M,M} = D^j_{1,1} = D^j_{M,M} = 0 \; , \quad R^j_1 = P_l \; , \quad R^j_M = P_r \quad .$$

Equation (34) represents a linear system of simultaneous equations that may be solved by various matrix inversion procedures. The method used here is the column or transfer matrix method, which is described in References 4 and 7. It has been used extensively in solving finite difference problems associated with various forms of the lubrication equations and produces accurate results in a fairly efficient manner. Convergence of the Newton-Raphson procedure is generally obtained within 3 - 6 iterations depending on degree of non-linearity and the accuracy required.

Determination of loads, moments, torque and leakage

The dimensionless loads and moments may be obtained by integrating the pressure distribution over the seal area as shown below:

$$\tilde{W}_x = \int_0^{2\pi}\int_{S_i}^{S_r} P\cos\theta R\,dS\,d\theta\,,\quad \tilde{W}_y = \int_0^{2\pi}\int_{S_i}^{S_r} P\sin\theta R\,dS\,d\theta\,,\quad \tilde{W}_z = \int_0^{2\pi}\int_{S_i}^{S_r} PR\,dS\,d\theta\,,$$
$$\tilde{M}_x = -\int_0^{2\pi}\int_{S_i}^{S_r} P\sin\theta RS\,dS\,d\theta\,,\quad \tilde{M}_y = \int_0^{2\pi}\int_{S_i}^{S_r} P\cos\theta RS\,dS\,d\theta\,. \tag{35}$$

The dimensionless torque is obtained from integration of the shear stress given by Equation (26) over the seal area:

$$\tilde{T} = \text{sign}(\tilde{\omega})\int_0^{2\pi}\int_{S_i}^{S_r} \tilde{\tau} R\,dS\,d\theta\,. \tag{36}$$

The **sign**($\tilde{\omega}$) term has been added to make the torque positive when it opposes the net surface motion regardless of which surface (smooth or grooved) is moving.

Finally, the dimensionless leakage flow, Q_{in} going into the seal at $S = S_i$ may be obtained from integration of Q_θ, given by Equation (21), over the circumference of the seal:

$$Q_{in} = \int_0^{2\pi} Q_\theta R\,d\theta\,. \tag{37}$$

The integrand in the above expression is evaluated by summing the flow components to the right of the first θ grid line in the same manner as that used in developing Equation (31). It should be noted that any value of S can be used since Q_{in} is independent of S.

The physical quantities corresponding to the dimensionless ones given above are

$$W_{\{x,y,z\}} = R_0^2 p_0 \tilde{W}_{\{x,y,z\}} \ , \quad M_{\{x,y\}} = R_0^3 p_0 \tilde{M}_{\{x,y\}} \ , \quad q_{in} = \frac{C^3 p_0}{12\mu} Q_{in} \ , \quad T = R_0^2 p_0 C \tilde{T} \ . \quad (38)$$

In the above equations the loads W_x and W_y apply only to a cylindrical seal and W_z applies only to a face seal. The leakage flow q_{in} is the volumetric flow rate going into the seal measured at pressure p_0.

Determination of stiffness and damping coefficients

Equation (20) with flow components Q_θ and Q_s given by Equations (21) and (22) represents a second order non-linear partial differential equation that may be used to define a second order non-linear operator **G**, such that

$$G(P,H_r) = -\frac{\partial}{\partial \bar{t}}[(\alpha\bar{\delta} + H_r)(1 + P)] \quad . \tag{39}$$

The determination of **P** under steady state conditions, where the right hand side of Equation (39) is **0**, was described earlier in this section. These steady state pressures will now be referred to as $\hat{P}$. The various eccentricities and rotations used in determining H_r from Equation (27) may, for convenience, be put in the form of a row matrix as

$$[\epsilon] = \begin{cases} [\epsilon_z, \phi, \psi] \ , & \text{(face seal)} \\ [\epsilon_x, \epsilon_y, \phi, \psi] \ , & \text{(shaft seal)} \end{cases} \tag{40}$$

and Equation (27) may be written as

$$H_r = 1 + [\epsilon]\{a\} \quad , \tag{41}$$

where the column vector **{a}**is given by

$$\{a\} = \begin{cases} \{-1, S\sin\theta, -S\cos\theta\} \ , & \text{(face seal)} \\ \{-\cos\theta, -\sin\theta, S\sin\theta, -S\cos\theta\} \ , & \text{(shaft seal)} \end{cases} \quad . \tag{42}$$

One could develop a perturbation analysis for prediction of stiffness and damping coefficients with the following procedure: (a) perturb say the ith component of the eccentricity matrix in Equation (40) by $\eta\epsilon'$, where η is a small parameter and ϵ' is time dependent; (b) express H_r in the form $H_r = \hat{H} + \eta\epsilon'\{a\}$ and the corresponding pressures as $P = \hat{P} + \eta\{P'\}$; (c) substitute the above expressions for **P** and H_r in Equation (39); (d) expand the resulting expression neglecting terms of order η^2 and higher; (e) collect terms of order η. The resulting expression could be written in the form:

$$\mathcal{L}\{P'\} + \{b\}\epsilon' = -(\alpha\bar{\delta} + \hat{H})\frac{\partial\{P'\}}{\partial\bar{t}} - (1 + \hat{P})\{a\}\frac{\partial\epsilon'}{\partial\bar{t}} \quad , \tag{43}$$

where $\mathcal{L}$ is a second order linear operator given by

$$\mathcal{L} = A_1\frac{\partial^2}{\partial S^2} + A_2\frac{\partial^2}{\partial S\,\partial\theta} + A_3\frac{\partial^2}{\partial\theta^2} + A_4\frac{\partial}{\partial S} + A_5\frac{\partial}{\partial\theta} + A_6 \quad . \tag{44}$$

The coefficients in the above equations (A_1, A_2, {b} etc.) will depend on the coordinate variables as well as $\hat{P}$, $\hat{H}$ and their various derivatives. Only the form of the above equations is important to the numerical procedure under development and the significant amount of algebraic manipulation required to determine these coefficients will be shown to be unnecessary.

If the time dependence of the eccentricity is restricted to oscillatory disturbances one may set $\epsilon' = e^{\Im\sigma\tilde{t}}$ and look for solutions in the form $\{P'\} = \{P^*\}e^{\Im\sigma\tilde{t}}$, where $\{P^*\}$ is complex but independent of time. When this transformation is introduced into Equation (43), the result is

$$\mathcal{L}\{P^*\} + \{b\} = -\Im\sigma\left[(\alpha\tilde{\delta} + \hat{H})\{P^*\} + (1 + \hat{P})\{a\}\right] \quad . \tag{45}$$

The representation of $\{P^*\}$ and the eccentricity coefficients {a} as column vectors relates to the fact that each of the eccentricities must be perturbed to obtain the complete stiffness matrix but Equation (45) is solved independently for each perturbation. The periodic boundary conditions given by Equation (29) also apply to Equation (39) (continuity of $\{P^*\}$ and $\partial\{P^*\}/\partial\theta$ is sufficient when H_r and the spiral groove coefficients $k_1,\ldots,k_4$ are continuous functions of θ as they are here). The end boundary conditions given by Equation (28) become $\{P^*\} = 0$ at $S = S_l$ and $S = S_r$.

If Equation (45) were solved for $\{P^*\}$ subject to the above boundary conditions, all of the dimensionless stiffness and damping coefficients could be obtained by substituting $\{P^*\}$ for P in Equation (35). The real parts of the computed forces and moments would be in phase with the eccentricity perturbations and constitute the dimensionless stiffness coefficients. Thus $\tilde{K}_{yx}$ would correspond to the real part of $\tilde{W}_y$ computed from the component of $\{P^*\}$ associated with the perturbation in ϵ_x and $\tilde{K}_{\phi y}$ would correspond to the real part of $\tilde{M}_x$ computed from the component of $\{P^*\}$ associated with the perturbation in ϵ_y etc. In a similar manner, the dimensionless damping coefficients which are 90° out of phase with the eccentricity perturbations would be obtained by dividing the imaginary parts of the forces and moments computed in the manner described above by σ.

The parameter σ, is a dimensionless disturbance frequency referred to as the "squeeze number" and is given by $\sigma = 2\Lambda\Omega/\omega$ where Ω is the angular velocity of the disturbance. The limiting form of the stiffness and damping coefficients as $\sigma \to 0$, is of interest as it applies to incompressible flow, and the limiting stiffnesses

are used in the homing procedure that has been implemented for determining eccentricities from given loads which will be described later. This limiting form may be obtained by expressing Equation (45) in terms of its real and imaginary parts as

$$\mathcal{L}\{P_{\mathcal{R}}\} + \{b\} = \sigma^2(\alpha\tilde{\delta} + \hat{H})\{P_{\mathcal{I}}\} \quad , \tag{46}$$

$$\mathcal{L}\{P_{\mathcal{I}}\} = -(\alpha\tilde{\delta} + \hat{H})\{P_{\mathcal{R}}\} - (1 + \hat{P})\{a\} \quad , \tag{47}$$

where

$$\{P^*\} = \{P_{\mathcal{R}}\} + \mathcal{I}\sigma\{P_{\mathcal{I}}\} \quad . \tag{48}$$

The column vectors $\{P_{\mathcal{R}}\}$ and $\{P_{\mathcal{I}}\}$ are the "stiffness" and "damping" pressures respectively. If one formally sets $\sigma = 0$ in Equation (46) it decouples from Equation (47) and may be solved directly. Since the right hand side of Equation (46) becomes 0, the stiffness pressures are the same as those that would be obtained by computing the steady state pressures at a perturbed eccentricity, subtracting the unperturbed pressures and dividing by the eccentricity perturbation. This latter method is frequently used for computing steady state stiffnesses in incompressible flow and has been implemented here for the computation of "stiffnesses at 0 frequency" used in the above mentioned homing procedure. The 0 frequency damping pressures may be obtained by solving Equation (47) with $\{P_{\mathcal{R}}\}$ as determined from the solution to Equation (46).

The above discussion assumed that the perturbation coefficients in Equations (40) - (42) were determined prior to setting up the finite discretized equations for their solution. Identical results can be achieved by direct numerical perturbation of the difference equations. This approach, which has been implemented here and is described below, avoids algebraic error in determining the perturbation coefficients and may be used in complex situations where analytical determination of the perturbation coefficients is not feasible.

After desired convergence of the Newton-Raphson process has been achieved under steady (unperturbed) conditions one may denote the resulting steady state pressure vectors as $\{\hat{P}_j\}$ and the coefficient matrices as $[\hat{C}^j]$, etc. and Equation (34) may be written as

$$[\hat{C}^j]\{\hat{P}_j\} + [\hat{E}^j]\{\hat{P}_{j-1}\} + [\hat{D}^j]\{\hat{P}_{j+1}\} = \{\hat{R}^j\} \quad . \tag{49}$$

One may now perturb the kth component of the eccentricity vector by an amount η, recalculate $[\hat{C}^j]$ at the new film thickness (but old pressure distribution, $\hat{P}$) then subtract $[\hat{C}^j]$ at the old film thickness and divide the difference by η to numerically obtain the derivative of $[\hat{C}^j]$ with respect to ϵ_k which will be denoted by

$[\hat{C}^{j,k}]$. Thus

$$[\hat{C}^{j,k}] = \frac{[\hat{C}^{j}]|_{\epsilon_k+\eta} - [\hat{C}^{j}]|_{\epsilon_k}}{\eta} \quad .$$

The matrices $[\hat{E}^{j,k}]$, $[\hat{D}^{j,k}]$ and $\{\hat{R}^{j,k}\}$ are obtained in a similar manner from the other coefficient matrices. If we introduce a disturbance to ϵ_k of magnitude $\epsilon'\eta$, as was done in deriving Equation (43), then the change in the coefficient matrix $[\hat{C}^j]$ would be $\epsilon'\eta[\hat{C}^{j,k}]$ with corresponding changes in the other coefficient matrices. If we disturb Equation (49) by replacing $\{\hat{P}_j\}$ with $\{\hat{P}_j\} + \eta\{P'^{k}_j\}$, $[\hat{C}_j]$ with $[\hat{C}^j] + \epsilon'\eta[\hat{C}^{j,k}]$, etc. and collect terms of order η, the following expression is obtained:

$$[\hat{C}^{j}]\{P'^{k}_{j}\} + [\hat{E}^{j}]\{P'^{k}_{j-1}\} + [\hat{D}^{j}]\{P'^{k}_{j+1}\} = \left(\{\hat{R}^{j,k}\} - [\hat{C}^{j,k}]\{\hat{P}_j\} - [\hat{E}^{j,k}]\{\hat{P}_{j-1}\} - [\hat{D}^{j,k}]\{\hat{P}_{j+1}\}\right)\epsilon' \quad . \qquad (50)$$

If we set ϵ' to unity in Equation (50) then $\{P'^{k}_j\}$ will become the 0 frequency stiffness pressure (the change in steady state pressure per unit change in eccentricity). It should be noted that the coefficients of the 0 frequency stiffness pressures in Equation (50) are the same as those for the steady state pressures in Equation (49); only the right hand side has changed. Equation (50) thus represents the construction of the discretized form of Equation (43) when $\sigma = 0$. In order to complete the process for $\sigma \neq 0$, one may introduce the same disturbances to the right hand side of Equation (31), with $\mathbf{H}_r = \hat{H} + \epsilon'\eta\{\mathbf{a}\}$ and add the terms of order η to the right hand side of Equation (50). The terms to be added are $-\partial([\bar{C}^j]\{P'^{k}_j\} + \{\bar{R}^{j,k}\}\epsilon')/\partial\tilde{t}$, where $[\bar{C}^j]$ are diagonal matrices whose components are

$$\bar{C}^{j}_{ii} = (\alpha\tilde{\delta} + \hat{H})_{i+\frac{1}{2},j+\frac{1}{2}}\Delta\bar{A}_1 + (\alpha\tilde{\delta} + \hat{H})_{i+\frac{1}{2},j-\frac{1}{2}}\Delta\bar{A}_4 + (\alpha\tilde{\delta} + \hat{H})_{i-\frac{1}{2},j-\frac{1}{2}}\Delta\bar{A}_3 + (\alpha\tilde{\delta} + \hat{H})_{i-\frac{1}{2},j+\frac{1}{2}}\Delta\bar{A}_2 \quad (51)$$

and $\{\bar{R}^{j,k}\}$ are column vectors whose components are

$$\bar{R}^{j,k}_i = (1 + \hat{P}_{ij})\left(a^{k}_{i+\frac{1}{2},j+\frac{1}{2}}\Delta\bar{A}_1 + a^{k}_{i+\frac{1}{2},j-\frac{1}{2}}\Delta\bar{A}_4 + a^{k}_{i-\frac{1}{2},j-\frac{1}{2}}\Delta\bar{A}_3 + a^{k}_{i-\frac{1}{2},j+\frac{1}{2}}\Delta\bar{A}_2\right) \approx (1 + \hat{P}_{ij})\,a^{k}_{i,j}\Delta\bar{A} \quad . \qquad (52)$$

The far right side of Equation (52) is a quadradically equivalent representation that was used in the computer program described in Section 3. One may now set $\epsilon' = e^{\Im\sigma\tilde{t}}$ in Equation (50) and look for solutions in the form $\{P'^{k}_j\} = \{P^{*k}_j\}e^{\Im\sigma\tilde{t}}$, by introducing these substitutions into Equation (50) and combining terms to obtain the final set of linear difference equations for the complex stiffness pressures $\{P^{*k}_j\}$:

$$[C^{*j}]\{P_j^{*k}\} + [\hat{E}^j]\{P_{j-1}^{*k}\} + [\hat{D}^j]\{P_{j+1}^{*k}\} = \{R^{j,k}\} - [\hat{C}^{j,k}]\{\hat{P}_j\} - [\hat{E}^{j,k}]\{\hat{P}_{j-1}\} - [\hat{D}^{j,k}]\{\hat{P}_{j+1}\} , \quad (53)$$

where $[C^{*j}] = [\hat{C}^j] + \Im\sigma[\bar{C}^j]$ and $\{R^{j,k}\} = \{\hat{R}^{j,k}\} - \Im\sigma\{\bar{R}^{j,k}\}$.

The system of equations given by Equation (53) has been solved by the column method in a directly analogous manner to that used in solving Equation (34). The principal difference lies in the fact that all of the matrix operations were performed using complex arithmetic. The dimensionless, frequency dependent stiffness and damping coefficients were computed from the complex stiffness pressures in the previously described manner. Relationships of the following type may be used to calculate the physical stiffness and damping coefficients from the dimensionless ones:

$$K_{xx} = K_0\tilde{K}_{xx} , \quad K_{\phi\phi} = K_0R_0^2\tilde{K}_{\phi\phi} , \quad K_{x\phi} = K_0R_0\tilde{K}_{x\phi} \quad (54)$$

and

$$B_{xx} = B_0\tilde{B}_{xx} , \quad B_{\phi\phi} = B_0R_0^2\tilde{B}_{\phi\phi} , \quad B_{x\phi} = B_0R_0\tilde{B}_{x\phi} , \quad (55)$$

where $K_0 = p_0R_0^2/C$ and $B_0 = 12\mu R_0^4/C^3$.

Optimization of groove parameters for maximum stagnation pressure in a concentric cylindrical seal

Since spiral grooves are solely responsible for the axial stiffness of an aligned, gas lubricated face seal with parallel surfaces under steady state conditions, it is often desirable to optimize groove parameters for maximum axial stiffness. An optimization procedure for doing this has been implemented in the computer code SPIRALP described in Reference 8. The analogous situation is not as evident in a concentric gas lubricated cylindrical seal which will have considerable, if not maximum stiffness without spiral grooves. A large portion of the stiffness in the absence of spiral grooves will be cross coupled, particularly at low values of Λ, thus giving rise to stability problems which may be alleviated with the use of spiral grooves. The criteria for optimizing groove geometry from a dynamic standpoint would thus depend on both the desired load capacity and the various other elements in the system affecting rotordynamic performance.

An alternate approach for developing a stand alone criterion for optimizing groove geometry in a cylindrical seal is to maximize the pressure gradient that the grooves can generate at stagnation. If the grooves are being used to pump against a pressure gradient, the maximum stagnation pressure gradient would represent the maximum pressure gradient that the grooves could pump against without allowing any net flow to go through. It would also represent the maximum axial pressure gradient that the grooves could generate in

an aligned, symmetric herringbone bearing in the absence of an imposed pressure gradient. In any event, the stagnation pressure gradient is a strong measure of spiral groove performance and even though optimizing it is not a precise criterion for optimizing dynamic performance, computations obtained with geometries optimized in this manner should provide a strong indication of the maximum benefits obtainable with the use of spiral grooves.

The stagnation pressure gradient for a cylindrical seal under concentric conditions may be obtained from Equation (22) by setting $Q_s = 0$ (stagnation), $\partial P/\partial\theta = 0$, $H_r = 1$ (concentric), $S = Z$ and $R = 1$ (cylindrical seal). The resulting equation may be solved for $\Delta P/\Delta Z$ making use of the definition of Λ_δ given by Equation (24) and the definitions of k_1 and k_4 given by Equation (25) to obtain the following relationship

$$\frac{\partial P}{\partial Z} = \Lambda\tilde{\omega}\,\frac{\tilde{\delta}\,\alpha\,(1-\alpha)\sin\beta\cos\beta\,(\Gamma^3-1)}{\alpha\,(1-\alpha)\,(\Gamma^3-1)^2\sin^2\beta+\Gamma^3}\,.$$

The right hand side of the above equation may be treated as a function of α, β and $\tilde{\delta}$ ($\Gamma = 1 + \tilde{\delta}$) and has a maximum value of $\partial P/\partial Z = 0.09118\,\Lambda\tilde{\omega}$ at $\alpha_{opt} = 0.5$, $\beta_{opt} = 0.2736$ (15.68°) and $\tilde{\delta} = 2.653$.

The variation of the pressure gradient near the optimum point is shown in Figure 4. The curve marked α was obtained by holding β and $\tilde{\delta}$ at their optimum values and varying α. The other curves were obtained in an analogous manner. The curves show the sensitivity of the optimum pressure gradient to the various parameters and verify the existence of a relative maximum at the optimum point.

Other approaches to the optimization problem are given in Reference 2 for spiral groove bearings and Reference 9 for spiral groove viscous pumps.

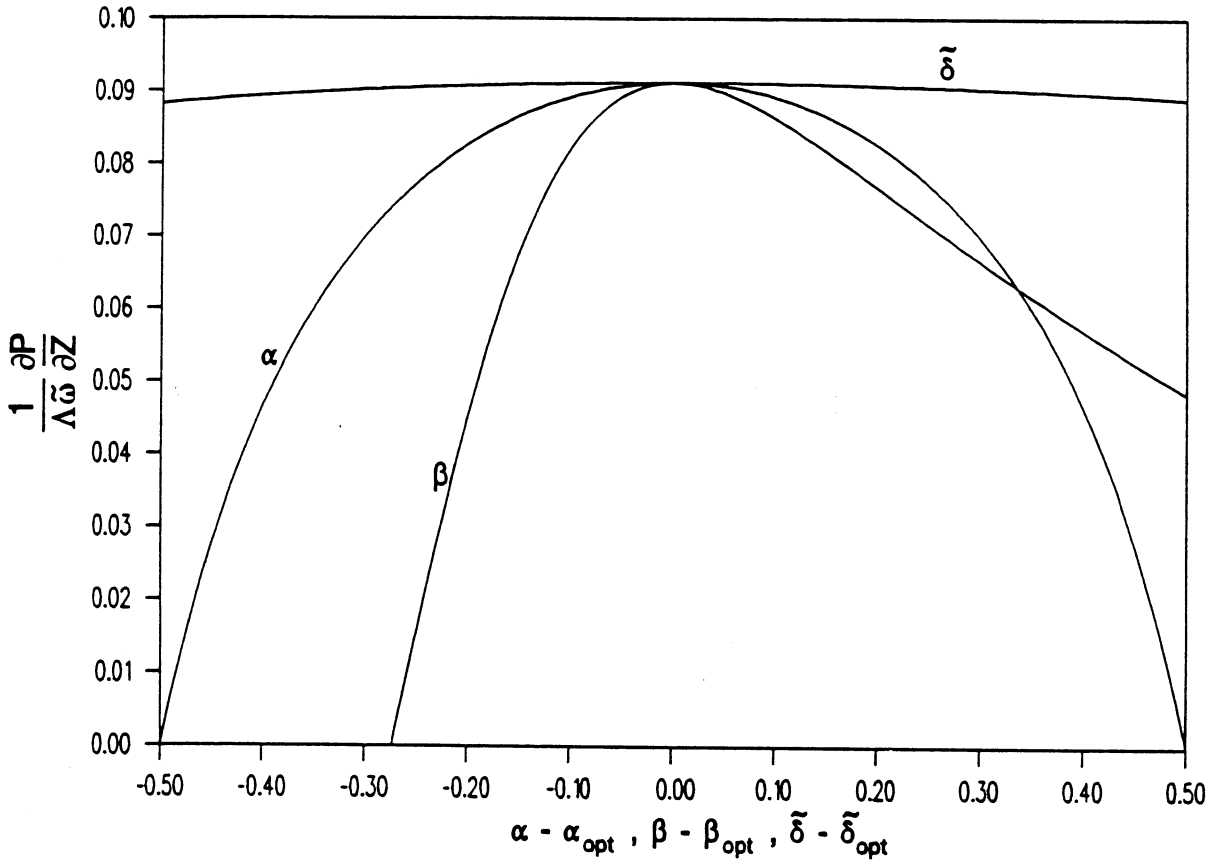

Figure 4 The variation of the stagnation pressure gradient about the optimum point

3. Description of Computer Code SPIRALG and Subroutine SPIRAL

A FORTRAN subroutine, SPIRAL, has been written to implement the analysis developed under Section 2 in dimensionless form. The analysis has been programmed in this form to permit easy incorporation into the knowledge base system currently under development. SPIRAL and its associated sub-programs (listed in Appendix A) constitute a self contained system that has no input-output and is thus independent of the operating system. SPIRAL has been compiled, in its present form with Version 5.0 of the Microsoft® Fortran Compiler and should work with many other compilers with relatively little modification. SPIRAL uses one feature that is supported by a wide variety of compilers that are extensions to FORTRAN 77. This extension relates to the implementation of complex double precision variables to compute frequency dependent stiffness and damping values. Users with compilers that do not support complex double precision may still use the program to calculate "zero frequency" stiffness and damping values by first deleting the subroutine DCLOAD and all subroutines listed in Appendix A that start with the letter C, with the exception of COLP; then deleting the calls to these routines; then finally setting the variable OMEG=0.D0 in the main program prior to calling SPIRAL. It should be noted that the above extension is part of both IBM Systems Application Architecture and VAX extensions to FORTRAN 77.

The main program, SPIRALG, which calls SPIRAL, is listed in Appendix B, along with its supporting subroutines. SPIRALG primarily processes input and output and performs conversions between dimensional quantities contained in the input and output files and the dimensionless ones used by SPIRAL. The main program is system dependent in that it opens files and allows placement of file names on the command line. It also uses NAMELIST for input which is another widely supported FORTRAN 77 extension. The supporting routines either write to the standard output unit or take FORTRAN supported logical unit numbers as input, hence should not require significant modification with any FORTRAN 77 compiler. SPIRAL communicates it's status through a subroutine called OUTSCR(MSG,NUM) which is one of the routines included with SPIRALG in Appendix B. MSG is a variable length character string containing status messages and NUM is an integer. This routine presently sends all messages to the standard output unit but may be readily modified to disregard the messages or to process them in another manner.

The analytical procedure contained in Section 2 has been oriented toward determining pressure distribution, load, flow, torque, stiffness and damping for a given film thickness distribution. In practice it is often desirable to determine the equilibrium film thickness or eccentricities from prescribed loads and possibly moments. SPIRAL provides a homing option for determining the eccentricities based on the steady state bearing stiffnesses. This homing option is controlled by the input flag IHOME and is based on the procedure described below.

If one were to write the dimensionless load and eccentricity as column vectors $\{\tilde{W}\}$ and $\{\epsilon\}$ (transpose row

matrix $[\epsilon]$) and take the previous estimate (or initial guess) of $\{\epsilon\}$ as $\{\epsilon\}_{old}$ and the load vector computed from $\{\epsilon\}_{old}$ as $\{\bar{W}\}_{old}$, the steady state stiffness matrix $[\bar{K}]$ could be used to arrive at a new approximation for $\{\epsilon\}$. The method for doing this is shown by first writing the equation for the change in load as $\{\bar{W}\} - \{\bar{W}\}_{old} = [\bar{K}](\{\epsilon\} - \{\epsilon\}_{old})$. The new approximation to $\{\epsilon\}$ is obtained by inverting the stiffness matrix and solving for $\{\epsilon\}$ as $\{\epsilon\} = \{\epsilon\}_{old} + [\bar{K}]^{-1}(\{\bar{W}\} - \{\bar{W}\}_{old})$. This approach is in effect the application of the Newton-Raphson method for determining the eccentricities.

While the above approach can be very effective it can also diverge if the initial guesses are bad. This divergence is usually accompanied by the generation of negative film thicknesses in the course of the iteration process. In order to attempt to correct this problem, an optional numerical damping algorithm has been implemented which replaces $\{\epsilon\}$ with $\{\epsilon\} = \{\epsilon\}_{old} + \bar{\beta}\,[\bar{K}]^{-1}(\{\bar{W}\} - \{\bar{W}\}_{old})$ when the originally calculated value of $\{\epsilon\}$ would result in a negative film thickness. The numerical damping factor $\bar{\beta}$ is determined by the program based on the value of the input parameter NUMDMP described in the input description.

The cell method of discretization is designed to obtain quadratic accuracy. Numerical testing indicates that this has apparently been achieved. One may make use of this property to obtain greater accuracy, (or the same degree of accuracy with coarser grids and ensuing reductions in computer time) with the use of Romberg extrapolation. Suppose for example we computed the dimensionless torque $\bar{T}$ with a coarse grid and denoted it by $\bar{T}_c$ then halved the grid spacing in both directions and recomputed $\bar{T}$ denoting it as $\bar{T}_f$ (subscript denotes fine grid). If the truncation error were to approach 0 as the square of the grid spacing and $\bar{T}_r$ were the true solution then $(\bar{T}_f - \bar{T}_r) = (\bar{T}_c - \bar{T}_r)/4$, or $\bar{T}_r = (4\bar{T}_f - \bar{T}_c)/3$. The above extrapolation can, in principal, increase the rate of convergence from quadratic to cubic. The subroutine SPIRAL, provides the option of implementing Romberg extrapolation for all of the outputs by setting the flag IACC as explained in the input description.

The logic used in SPIRAL for performing the pressure iterations, computing stiffness and damping coefficients, homing in on eccentricities and implementing Romberg extrapolation is shown in Figure 5. It can be seen there that when the homing process is implemented, it is completed for both coarse grid and fine grid solutions prior to performing the Romberg extrapolation. The extrapolation is thus performed with solutions obtained at two different displacements. When the displacements are specified (IHOME=0) extrapolations are performed with solutions obtained at the same displacement, which is believed to be a more accurate approach. If one were to compute displacements for a given loading and then recompute the loading from the displacements using Romberg extrapolation for both computations the computed loading would thus differ slightly from the input loading even though all tolerances were met. The degree of this difference will depend on the grid size and caution should be exercised in using Romberg extrapolation when homing in on the displacements with very coarse grids.

The program SPIRALG may be run in its present form by entering the command

SPIRAL1

The Input filename must be "SPIRAL.INP". The filename of the output file is a namelist variable (OUTFIL) in the input file. No file extension should be given to this variable as the program automatically gives the extension ".OUT" to the output file.

The remainder of this section contains descriptions of the input and output to SPIRALG along with a separate description of the arguments to SPIRAL. Sample cases and verification data will be given in succeeding sections.

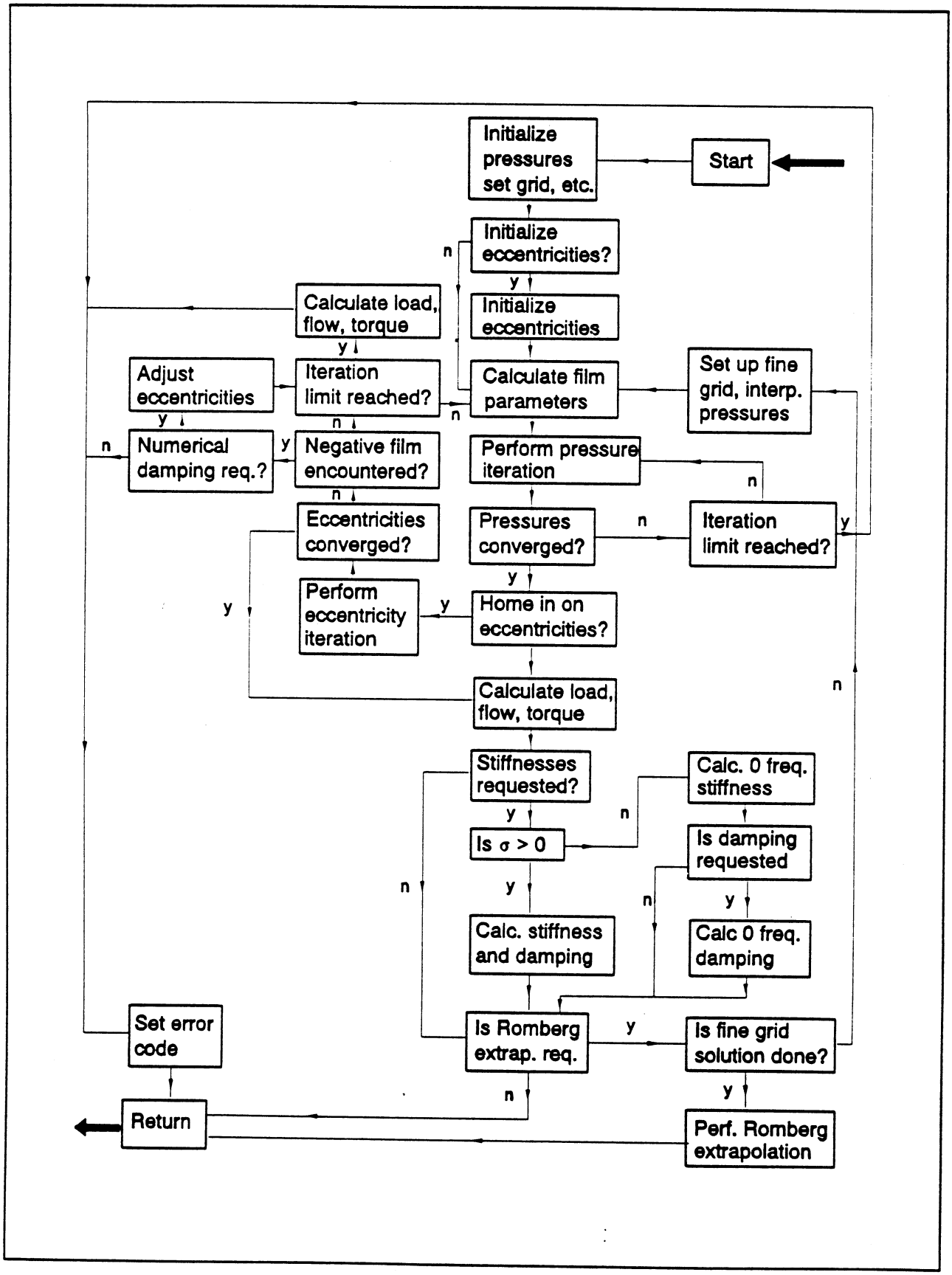

Figure 5 Flow diagram for logic used in SUBROUTINE SPIRAL

Input description for SPIRALG

SPIRALG requires its input in NAMELIST form. The NAMELIST variables will be given below in the order that they are listed in the output (see Section 4). Units for dimensional inputs will be given in English units as required when ISIUN=0, followed by SI units required when ISIUN=1 in parentheses, where applicable. The relationship between the NAMELIST variables and symbols appearing in the nomenclature will be given wherever possible.

OUTFIL	Filename of output file (no extension).
TITLE	Any character string enclosed in quotes containing up to 64 characters.
IFACE	0 for cylindrical seal, 1 for face seal
ISIUN	0 for English units, 1 for SI units
IACC	0 for input grid, 1 for Romberg extrapolation. When set to 1, computations are performed for input grid which should be coarse. The grid spacing is then halved in each direction (size limitations permitting) and a fine grid solution is obtained. Romberg extrapolation is used to obtain a more accurate solution. Final pressures etc. are returned at coarse grid mesh points. If dimension statements don't permit halving the grid, the process is aborted immediately. The fine grid solution will not be run if a non-zero error code is encountered in the coarse grid solution. If an error is encountered during the fine grid solution the process is aborted and the coarse grid solution is returned.
R0	R_0, radius of cylindrical seal (IFACE=0) or outside radius of face seal (IFACE=1), in. (M).
EL	L, length of cylindrical seal (IFACE=0) or land width of face seal (IFACE=1) as shown in Figure 1, in. (M)
C	C, radial clearance of cylindrical seal (IFACE=0) or reference film thickness for face seal (IFACE=1), in. (M)
IGROT	groove rotation flag, set to 1, if the rotating surface is grooved or 0, if smooth
RPM	angular speed of rotating surface converted to revolutions per minute
RPMD	Ω, angular speed of disturbance converted to revolutions per minute
PLEA	p_i, absolute pressure at the start of the seal (IFACE=0) or at the inside radius (IFACE=1), psi (Pa)
PRIA	p_r, absolute pressure at the end of the seal (IFACE=0) or at the outside radius (IFACE=1), psi (Pa)
VISC	μ, gas viscosity, psi-sec (Pa-sec)
ISTIF	Stiffness flag. Set it to 1 to calculate stiffness or 0 for no stiffness calculation.
IDAMP	Damping flag. Set it to 1 to calculate damping or 0 for no damping calculation. If OMEG > 0 and ISTIFF = 1, damping is always calculated and IDAMP is ignored.
MOM	Moment flag. Set it to 1 to calculate moments, 0 for no moment calculation.

ICONT If set to 1 eccentricities from previous case are used. If set to 0 user provided eccentricities (EX,EY, etc) are used as starting values. ICONT must be 0 for initial run.

IHOME Flag to calculate eccentricities from supplied forces and moments. Set it to 0 to bypass calculation and use input eccentricities. Set flag to 1 to find translational eccentricities that correspond to input forces (but not moments) preserving input rotational eccentricities. Set flag to 2 to home in on forces and moments.

NUMDMP A numerical damping algorithm has been provided for homing in on forces and moments when a poor set of initial guesses have been used and negative film thicknesses are encountered during the homing process. If NUMDMP = 0, the algorithm will not be used and the subroutine will be aborted returning a non zero error code to the user. If NUMDMP = 1, a damping factor, $\tilde{\beta}$, will be introduced which drops the minimum film thickness to half its previous non-negative value. If NUMDMP = 2 greater damping will be introduced so that the minimum film thickness for the next iteration is reduced by only 25%. A value of 3 reduces it by 12.5% and so on. NUMDMP is not used if IHOME = 0.

EZD e_z, displacement in z direction, used only if IFACE = 1, in (M)

EXD e_x, eccentricity in x direction, used only if IFACE = 0, in (M)

EYD e_y, eccentricity in y direction, used only if IFACE = 0, in (M)

PHIR Φ, rotation about x axis, radians

PSIR Ψ, rotation about y axis, radians

FZD W_z, applied load in z direction, used only if IHOME > 0 and IFACE = 1, lb. (N). (It should be noted that the ambient pressure, p_0, does not contribute to the applied load and should be subtracted form all pressures when determining pressure induced loading.

FXD W_x, applied load in x direction, used only if IHOME > 0 and IFACE = 0, lb. (N)

FYD W_y, applied load in y direction, used only if IHOME > 0 and IFACE = 0, lb. (N)

EMXD M_x, applied moment about x axis, used only if IHOME = 2, in-lb. (N-M)

EMYD M_y, applied moment about y axis, used only if IHOME = 2, in-lb. (N-M)

NIT Maximum number of iterations to be used in pressure computations.

DPRE Dimensionless differential increment, η, used in pressure computations.

TOLP Maximum allowable relative error in dimensionless pressures, P. An error code is returned if this tolerance is not met in NIT iterations.

NITF Maximum number of iterations to be used in eccentricity computations (used only if IHOME > 0.

DECC Dimensionless differential increment, η, used in eccentricity ratio computations (used only if IHOME > 0).

TOLE Maximum allowable absolute error in eccentricity ratios (used only if IHOME > 0). An error code is returned if this tolerance is not met in NITF iterations.

N Number of grid points in θ (including both 0 and 2π).

NREG Number of regions in axial direction (IFACE=0) or radial direction (IFACE=1).

NRSUB Vector of length NREG containing number of sub-intervals in each of the NREG regions.

ELFR Vector of length NREG containing fractional extent of each of the NREG regions (length of region divided by L, must add up to 1).

ALPI Vector of length NREG containing groove to pitch ratio, α, for each of the NREG regions. Set α = 0 in ungrooved regions.

BETI Vector of length NREG containing groove angle, β (degrees), for each of the NREG regions. Set to 0 in ungrooved region.

DELT Vector of length NREG containing groove depth, δ, for each of the NREG regions, in (M). Set to zero in ungrooved regions. Regions are assumed to be ungrooved if either α, β, or δ are 0.

DZIN Vector of length $\sum_{i=1}^{NREG}$ NRSUB(I) containing axial (IFACE = 0) or radial (IFACE = 1) grid spacing intervals. The grid is input in a fractional manner for each region so that the sum of the DZIN values for each of the NREG regions must add up to 1. This method permits changing the ELFR values without having to change the DZIN array. If DZIN(1) = 0, a fixed grid is assumed and DZIN is ignored.

DTHIN Vector of length N-1 containing circumferential grid spacing intervals in form $\Delta\theta_i/(2\pi)$, 1=1,2,..,N-1. The sum of the DTHIN values, if used must add up to 1. If DTHIN(1) = 0, a fixed grid is assumed and DTHIN is ignored.

The default values of the NAMELIST variables are given in Figure 6. These values correspond to a smooth, unloaded shaft seal with a uniform grid and inputs in English units. The default case cannot be run until non-zero values are, at least, provided for R0, EL, C, PLEA, PRIA and VISC.

Description of output from SPIRALG

Listings of output files generated by SPIRALG are given in Section 4 under sample prpblems. The first line for each case consists of a case number generated by the program followed by the contents of the input string TITLE. This is followed by a listing of the NAMELIST variables in a form suitable for extraction as an input file. The next 5 lines provide a brief description of the seal type, geometry and operating as readily calculated from the input data.

If IHOME > 0, the lines following the viscosity and ambient pressure will provide the error code and number of iterations required to home in on the prescribed loading, along with the calculated values of the displacements (and rotations if requested) and the number of iterations in the last pressure calculation. If IHOME = 0, only the error code and number of iterations in the last pressure calculation are given. An error code of 0 indicates that convergence within the prescribed tolerances without exceeding the prescribed maximum number of iterations. The interpretation of non-zero error codes is given in Section 7.

```
&INPUTS
   OUTFIL =  'SPIRAL'
   TITLE  =  ' '
   IFACE  =  0              ISIUN  =  0              IACC   =  0
   RO     =  0.0000E+00     EL     =  0.0000E+00     C      =  0.0000E+00
   IGROT  =  0              RPM    =  0.0000E+00     RPMD   =  0.0000E+00
   PLEA   =  0.0000E+00     PRIA   =  0.0000E+00     VISC   =  0.0000E+00
   ISTIF  =  0              IDAMP  =  0              MOM    =  0
   ICONT  =  0              IHOME  =  0              NUMDMP =  0
   EZD    =  0.0000E+00     EXD    =  0.0000E+00     EYD    =  0.0000E+00
   PHIR   =  0.0000E+00     PSIR   =  0.0000E+00
   FZD    =  0.0000E+00     FXD    =  0.0000E+00     FYD    =  0.0000E+00
   EMXD   =  0.0000E+00     EMYD   =  0.0000E+00
   NIT    =  8              DPRE   =  1.0000E-06     TOLP   =  1.0000E-04
   NITF   =  8              DECC   =  1.0000E-06     TOLE   =  1.0000E-03
   N      =  21             NREG   =  1              NRSUB  =  10
   ELFR   =  1.0000E+00
   ALPI   =  0.0000E+00
   BETI   =  0.0000E+00
   DELT   =  0.0000E+00
   DZIN   =  0.0000E+00
   DTHIN  =  0.0000E+00
/
```

Figure 6 Namelist defaults

The calculated force (and moment if requested) data which follows, should agree closely with the input values if IHOME > 0. Again, it is noted that the ambient pressure, p_0, does not contribute to the force. The force data are followed by the minimum value of the film thickness, h_r, the flow rate, q_{in}, the torque, T and corresponding power loss, the compressibility number, Λ, the squeeze number, σ and finally the stiffness and damping values, if requested.

The stiffness and damping values are printed as a matrix where the column corresponds to the displacement or rotation and the row corresponds to the force or moment. The units for any given stiffness or damping value will be the force unit given at the end of its row divided by the displacement unit given at the top of its column.

The optional dump file, if requested on the command line, will contain a binary dump of the quantities M,N,ZT,THG,P, and H, where M and N are the number of grid points in the transverse and circumferential directions respectively and the other quantities are defined under output arguments from SUBROUTINE SPIRAL. These outputs as written with the FORTRAN statement

```
      WRITE(3)M,N,(ZT(I),I=1,M),(THG(I),I=1,N),
     +((P(I,J),I=1,M),J=1,N),((H(I,J),I=1,M,M-1),J=1,N)
```

and are intended for use in subsequent post-processing procedures for pressure plots, etc.

Input arguments for SUBROUTINE SPIRAL

All of the arguments to SPIRAL are dimensionless. The reader will be referred back to the input description for SPIRALG for definitions of arguments that are the same as NAMELIST variables in SPIRALG.

ICASE	case number used as a reference when passing status messages
IFACE	see SPIRALG
IACC	see SPIRALG
XL	Λ, gas bearing compressibility number
ELT	$L/(2R_0)$, where L is the seal length (IFACE=0) or land width (IFACE=1)
OMT	$\tilde{\omega}$, angular velocity ratio
OMEG	σ, squeeze number
PLEFT	P_l, dimensionless gage pressure at the inside radius (IFACE=1), or at z = -L/2 (IFACE=0)
PRIGHT	P_r, dimensionless gage pressure at the outside radius (IFACE=1), or at z = L/2 (IFACE=0)
ISTIF	see SPIRALG

IDAMP	see SPIRALG
MOM	see SPIRALG
IHOME	see SPIRALG
ICONT	see SPIRALG
NUMDMP	see SPIRALG
EZ	ϵ_z, eccentricity ratio, used only if IFACE = 1
EX	ϵ_x, eccentricity ratio, used only if IFACE = 0
EY	ϵ_y, eccentricity ratio, used only if IFACE = 0
PHI	ϕ, reduced rotation about x axis
PSI	ψ, reduced rotation about y axis
FZ	$\tilde{W}_z$, applied load, used only if IHOME > 0 and IFACE = 1
FX	$\tilde{W}_x$, applied load, used only if IHOME > 0 and IFACE = 0
FY	$\tilde{W}_y$, applied load, used only if IHOME > 0 and IFACE = 0
EMX	$\tilde{M}_x$, applied moment about x axis, used only if IHOME = 2
EMY	$\tilde{M}_y$, applied moment about y axis, used only if IHOME = 2
NIT	see SPIRALG
DPRE	see SPIRALG
TOLP	see SPIRALG
NITF	see SPIRALG
DECC	see SPIRALG
TOLE	see SPIRALG
N	see SPIRALG
NREG	see SPIRALG
NRSUB	see SPIRALG
ELFR	see SPIRALG
ALPI	see SPIRALG
BETI	see SPIRALG
DELTI	Vector of length NREG containing groove depth, $\tilde{\delta}$, for each of the NREG regions. Set to zero in ungrooved regions. Regions are assumed to be ungrooved if either α, β, or $\tilde{\delta}$ are 0.
DZIN	see SPIRALG
DTHIN	see SPIRALG

Output arguments from SUBROUTINE SPIRAL

M	number of grid points in z direction
ZT	array of M grid points in z direction
THG	array of N grid point in θ direction
H	film thickness array for H_r, (M×N)
P	pressure array, P, (M×N)
F	Computed force vector, contains $\bar{W}_x$, and $\bar{W}_y$ if IFACE = 0, or $\bar{W}_z$ if IFACE = 1. Forces are followed by $\bar{M}_x$ and $\bar{M}_y$ when MOM=1.
EC	Computed eccentricity vector when IHOME>0. Contains ϵ_x, and ϵ_y if IFACE = 0, or ϵ_z if IFACE = 1. These are followed by computed values of ϕ and ψ when IHOME = 2.
CK	Stiffness matrix, $[\bar{K}]$. If IFACE = 0 it is a 4×4 matrix with subscripts 1 - 4 referring to x,y,ϕ,ψ. If IFACE = 1 it is a 3×3 matrix with subscripts 1 - 3 referring to z,ϕ,ψ. If MOM = 0, ϕ and ψ terms are not calculated and the order of the matrices are reduced by 2.
CB	Damping matrix, $[\bar{B}]$. Same rules apply here as for CK.
TOR	dimensionless torque, $\bar{T}$
QIN	dimensionless flow rate, Q_{in}
HMIN	minimum value of H_r
ITER	number of iterations required for convergence of pressures used in last load computation
ITERH	number of iterations for convergence of eccentricity homing process when IHOME > 0
IER	Error code will be 0 if no errors encountered. Definitions of non-zero error codes are given in Section 7.

4. Sample Problems

A number of sample problems have been prepared to demonstrate the behavior and various features of the computer program. They are intended primarily for illustration and do not necessarily represent recommended seal designs. Separate input files are not given since the complete input NAMELIST is included in the output file for each case.

Cases 1 - 3 serve to show the improvement in accuracy that can be obtained with the use of Romberg extrapolation (IACC=1) for a concentric, asymmetric cylindrical seal. The seal is divided into two regions of equal length as shown in Figure 7. The stationary surface in the first region has a groove geometry optimized for maximum stagnation pressure as described at the end of Section 2. The grooves are oriented to produce a pumping component in the positive axial direction to partially offset the larger negative one caused by the imposed pressure gradient. The second region is smooth. The case 1 results were obtained without the use of Romberg extrapolation. Romberg extrapolation was used in Case 2 with coarse grid solution obtained for the same grid geometry as used in Case 1. Since the grid spacing is halved in each direction when obtaining the fine grid solution, Case 2 should represent a much more accurate solution than Case 1. It also took approximately 11 times as long to run. Romberg extrapolation was used in Case 3 with twice the grid spacing as that used in Case 2 and took only 25% longer to run than Case 1. The direct stiffness coefficients, K_{xx}, calculated for Cases 1 - 3 are 54684, 57622 and 57342 lb/in, respectively. Using Case 2 as a standard, the error in the Case 1 stiffness is 5.1% while the error in the Case 3 stiffness is only .5%.

A symmetric "herringbone groove" pattern is used in Case 4 with the same overall geometry as that used in Cases 1 - 3. The groove pattern on the stator in region 2 is the same as that for region 1 with the exception of the sign of the groove angle. The grid geometry is the same as that used in Case 1 but the operating conditions differ in that there is no imposed pressure gradient and the shaft is displaced in the x direction and tilted about the y axis. It can be seen that the imposed displacement and tilt produces non-zero values for the calculated forces and moments. The results of Case 5 were obtained by setting IHOME = 2 and prescribing the forces and moments computed for Case 4. The initial guess for the shaft displacement for Case 5 was taken to be somewhat larger than prescribed for Case 4 and initial guess for the tilt was taken as 0. The displacements calculated for Case 5 are essentially the same as those imposed in Case 4. Case 6 differs from Case 4 only in that ISIUN = 1 and is presented to illustrate the use of the program with SI units.

The remaining 2 cases correspond to a mechanical face seal under a very high imposed pressure gradient with spiral grooves on the outside surface of the stator oriented to pump inward with the pressure gradient. The stator geometry is shown schematically in Figure 8, with the land width somewhat enlarged for clarity.

The inward pumping is induced by the counterclockwise motion of the rotor. Solutions to this problem will be approximate in nature in that choking is likely to occur (not treated hear as a result of assumed isothermal flow with negligible inertia) which will raise the effective film pressure at the inside radius to a value somewhat higher than that prescribed. These cases are provided to illustrate the use of the program with a face seal and the evaluation of the internal accuracy of the program. Case 8 was obtained by halving the grid spacing used in Case 7, in both directions. This procedure provides a test for truncation error, which is small in this case, that is recommended for frequent use in determining appropriate grid spacing.

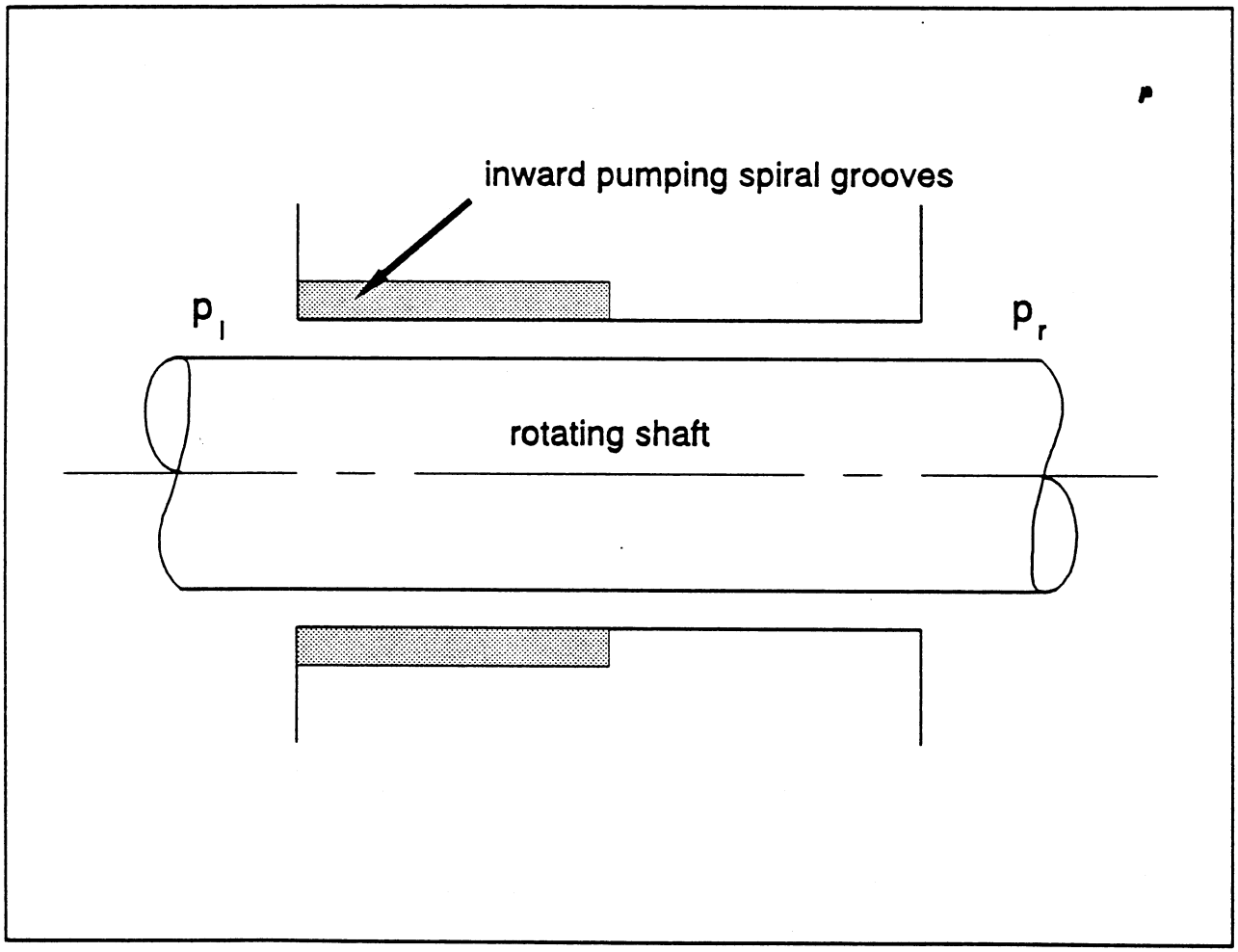

Figure 7 Schematic of shaft seal for Cases 1 - 3

(CASE 1) Asymmetric cyl. seal with grooves pumping against pres. grad.

```
&INPUTS
   TITLE  =  'Asymmetric cyl. seal with grooves pumping against pres. grad.'
   IFACE  =  0              ISIUN  =  0              IACC   =  0
   RO     =  1.0000E+00     EL     =  2.0000E+00     C      =  5.0000E-04
   IGROT  =  0              RPM    =  1.0000E+04     RPMD   =  1.0000E+04
   PLEA   =  1.4700E+01     PRIA   =  6.4700E+01     VISC   =  2.9000E-09
   ISTIF  =  1              IDAMP  =  1              MOM    =  1
   ICONT  =  0              IHOME  =  0              NUMDMP =  0
   EZD    =  0.0000E+00     EXD    =  0.0000E+00     EYD    =  0.0000E+00
   PHIR   =  0.0000E+00     PSIR   =  0.0000E+00
   FZD    =  0.0000E+00     FXD    =  0.0000E+00     FYD    =  0.0000E+00
   EMXD   =  0.0000E+00     EMYD   =  0.0000E+00
   NIT    =  8              DPRE   =  1.0000E-06     TOLP   =  1.0000E-04
   NITF   =  8              DECC   =  1.0000E-06     TOLE   =  1.0000E-03
   N      =  17             NREG   =  2              NRSUB  =  4  4
   ELFR   =  5.0000E-01  5.0000E-01
   ALPI   =  5.0000E-01  0.0000E+00
   BETI   =  1.5680E+01  0.0000E+00
   DELT   =  1.3265E-03  0.0000E+00
   DZIN   =  0.0000E+00
   DTHIN  =  0.0000E+00
/
```

SPIRAL GROOVE SHAFT SEAL, ROTATING SURFACE IS SMOOTH

LENGTH, DIAMETER, CLEARANCE = 2.0000E+00, 2.0000E+00, 5.0000E-04 (IN)

ROTATION SPEED, DISTURBANCE SPEED = 1.0000E+04, 1.0000E+04 (RPM)

PRESSURE AT START, END AXIAL BOUNDARIES = 1.4700E+01, 6.4700E+01 (PSI)

VISCOSITY = 2.9000E-09 (PSI-SEC), AMBIENT PRESSURE = 1.4700E+01 (PSI)

ITERATIONS AND ERROR CODE IN LAST PRESSURE CALCULATION = 3 0

CALCULATED FORCES IN X,Y DIRECTIONS = -2.1540E-14, 1.2544E-13 (LB)
CALCULATED MOMENTS ABOUT X,Y AXES = -8.6002E-15, -2.2927E-14 (IN-LB)

MINIMUM FILM THICKNESS = 5.0000E-04 (IN)

FLOW = -2.1757E+00 (IN**3/SEC) MEASURED AT 1.4700E+01 (PSI)

TORQUE = 7.4543E-02 (IN-LB), FILM POWER LOSS = 1.1827E-02 (HP)

COMPRESSIBILITY NUMBER = 4.9582E+00, SQUEEZE NUMBER = 9.9163E+00

DYNAMIC COEFFICIENTS (FORCE UNIT / DISP. UNIT)

DISP.	x (IN)	y (IN)	phi (RAD)	psi (RAD)	FORCE UNIT
Kx	5.4684E+04	3.0916E+04	-2.7046E+04	-6.0468E+04	LB
Ky	-3.0916E+04	5.4684E+04	6.0468E+04	-2.7046E+04	LB
Kphi	7.8082E+03	-8.1693E+03	-3.4030E+03	1.0593E+04	IN-LB
Kpsi	8.1693E+03	7.8082E+03	-1.0593E+04	-3.4030E+03	IN-LB
Bx	1.1158E+02	-2.9219E+01	1.8107E+01	6.2395E+01	LB-SEC
By	2.9219E+01	1.1158E+02	-6.2395E+01	1.8107E+01	LB-SEC
Bphi	-1.0745E+01	-1.7276E+01	1.7903E+01	-7.7389E+00	IN-LB-SEC
Bpsi	1.7276E+01	-1.0745E+01	7.7389E+00	1.7903E+01	IN-LB-SEC

(CASE 2) Romberg extrapolation with coarse grid the same as Case 1

```
&INPUTS
   TITLE  =  'Romberg extrapolation with coarse grid the same as Case 1'
   IFACE  =  0              ISIUN  =  0              IACC   =  1
   RO     =  1.0000E+00     EL     =  2.0000E+00     C      =  5.0000E-04
   IGROT  =  0              RPM    =  1.0000E+04     RPMD   =  1.0000E+04
   PLEA   =  1.4700E+01     PRIA   =  6.4700E+01     VISC   =  2.9000E-09
   ISTIF  =  1              IDAMP  =  1              MOM    =  1
   ICONT  =  0              IHOME  =  0              NUMDMP =  0
   EZD    =  0.0000E+00     EXD    =  0.0000E+00     EYD    =  0.0000E+00
   PHIR   =  0.0000E+00     PSIR   =  0.0000E+00
   FZD    =  0.0000E+00     FXD    =  0.0000E+00     FYD    =  0.0000E+00
   EMXD   =  0.0000E+00     EMYD   =  0.0000E+00
   NIT    =  8              DPRE   =  1.0000E-06     TOLP   =  1.0000E-04
   NITF   =  8              DECC   =  1.0000E-06     TOLE   =  1.0000E-03
   N      =  17             NREG   =  2              NRSUB  =  4  4
   ELFR   =  5.0000E-01  5.0000E-01
   ALPI   =  5.0000E-01  0.0000E+00
   BETI   =  1.5680E+01  0.0000E+00
   DELT   =  1.3265E-03  0.0000E+00
   DZIN   =  0.0000E+00
   DTHIN  =  0.0000E+00
/
```

SPIRAL GROOVE SHAFT SEAL, ROTATING SURFACE IS SMOOTH

LENGTH, DIAMETER, CLEARANCE = 2.0000E+00, 2.0000E+00, 5.0000E-04 (IN)

ROTATION SPEED, DISTURBANCE SPEED = 1.0000E+04, 1.0000E+04 (RPM)

PRESSURE AT START, END AXIAL BOUNDARIES = 1.4700E+01, 6.4700E+01 (PSI)

VISCOSITY = 2.9000E-09 (PSI-SEC), AMBIENT PRESSURE = 1.4700E+01 (PSI)

ITERATIONS AND ERROR CODE IN LAST PRESSURE CALCULATION = 3 0

CALCULATED FORCES IN X,Y DIRECTIONS = 3.0897E-13, 1.7781E-13 (LB)
CALCULATED MOMENTS ABOUT X,Y AXES = -9.7768E-14, 1.3279E-13 (IN-LB)

MINIMUM FILM THICKNESS = 5.0000E-04 (IN)

FLOW = -2.1749E+00 (IN**3/SEC) MEASURED AT 1.4700E+01 (PSI)

TORQUE = 7.4550E-02 (IN-LB), FILM POWER LOSS = 1.1829E-02 (HP)

COMPRESSIBILITY NUMBER = 4.9582E+00, SQUEEZE NUMBER = 9.9163E+00

DYNAMIC COEFFICIENTS (FORCE UNIT / DISP. UNIT)

DISP.	x (IN)	y (IN)	phi (RAD)	psi (RAD)	FORCE UNIT
Kx	5.7622E+04	3.2577E+04	-2.9332E+04	-6.4855E+04	LB
Ky	-3.2577E+04	5.7622E+04	6.4855E+04	-2.9332E+04	LB
Kphi	8.1664E+03	-8.4866E+03	-3.6583E+03	1.2003E+04	IN-LB
Kpsi	8.4866E+03	8.1664E+03	-1.2003E+04	-3.6583E+03	IN-LB
Bx	1.1837E+02	-3.1897E+01	2.0183E+01	6.7544E+01	LB-SEC
By	3.1897E+01	1.1837E+02	-6.7544E+01	2.0183E+01	LB-SEC
Bphi	-1.2229E+01	-1.8217E+01	1.9551E+01	-9.0828E+00	IN-LB-SEC
Bpsi	1.8217E+01	-1.2229E+01	9.0828E+00	1.9551E+01	IN-LB-SEC

(CASE 3) Romberg extrapolation with fine grid the same as Case 1

```
&INPUTS
   TITLE  =  'Romberg extrapolation with fine grid the same as Case 1'
   IFACE  =  0              ISIUN  =  0              IACC   =  1
   RO     =  1.0000E+00     EL     =  2.0000E+00     C      =  5.0000E-04
   IGROT  =  0              RPM    =  1.0000E+04     RPMD   =  1.0000E+04
   PLEA   =  1.4700E+01     PRIA   =  6.4700E+01     VISC   =  2.9000E-09
   ISTIF  =  1              IDAMP  =  1              MOM    =  1
   ICONT  =  0              IHOME  =  0              NUMDMP =  0
   EZD    =  0.0000E+00     EXD    =  0.0000E+00     EYD    =  0.0000E+00
   PHIR   =  0.0000E+00     PSIR   =  0.0000E+00
   FZD    =  0.0000E+00     FXD    =  0.0000E+00     FYD    =  0.0000E+00
   EMXD   =  0.0000E+00     EMYD   =  0.0000E+00
   NIT    =  8              DPRE   =  1.0000E-06     TOLP   =  1.0000E-04
   NITF   =  8              DECC   =  1.0000E-06     TOLE   =  1.0000E-03
   N      =  9              NREG   =  2              NRSUB  =  2  2
   ELFR   =  5.0000E-01  5.0000E-01
   ALPI   =  5.0000E-01  0.0000E+00
   BETI   =  1.5680E+01  0.0000E+00
   DELT   =  1.3265E-03  0.0000E+00
   DZIN   =  0.0000E+00
   DTHIN  =  0.0000E+00
/
```

SPIRAL GROOVE SHAFT SEAL, ROTATING SURFACE IS SMOOTH

LENGTH, DIAMETER, CLEARANCE = 2.0000E+00, 2.0000E+00, 5.0000E-04 (IN)

ROTATION SPEED, DISTURBANCE SPEED = 1.0000E+04, 1.0000E+04 (RPM)

PRESSURE AT START, END AXIAL BOUNDARIES = 1.4700E+01, 6.4700E+01 (PSI)

VISCOSITY = 2.9000E-09 (PSI-SEC), AMBIENT PRESSURE = 1.4700E+01 (PSI)

ITERATIONS AND ERROR CODE IN LAST PRESSURE CALCULATION = 3 0

CALCULATED FORCES IN X,Y DIRECTIONS = -2.5045E-14, 8.0461E-14 (LB)
CALCULATED MOMENTS ABOUT X,Y AXES = -3.2816E-14, -1.0084E-14 (IN-LB)

MINIMUM FILM THICKNESS = 5.0000E-04 (IN)

FLOW = -2.1750E+00 (IN**3/SEC) MEASURED AT 1.4700E+01 (PSI)

TORQUE = 7.4549E-02 (IN-LB), FILM POWER LOSS = 1.1828E-02 (HP)

COMPRESSIBILITY NUMBER = 4.9582E+00, SQUEEZE NUMBER = 9.9163E+00

DYNAMIC COEFFICIENTS (FORCE UNIT / DISP. UNIT)

DISP.	x (IN)	y (IN)	phi (RAD)	psi (RAD)	FORCE UNIT
Kx	5.7342E+04	3.2559E+04	-2.9001E+04	-6.4238E+04	LB
Ky	-3.2559E+04	5.7342E+04	6.4238E+04	-2.9001E+04	LB
Kphi	8.2990E+03	-8.5936E+03	-3.7301E+03	1.1766E+04	IN-LB
Kpsi	8.5936E+03	8.2990E+03	-1.1766E+04	-3.7301E+03	IN-LB
Bx	1.1766E+02	-3.1507E+01	1.9728E+01	6.6992E+01	LB-SEC
By	3.1507E+01	1.1766E+02	-6.6992E+01	1.9728E+01	LB-SEC
Bphi	-1.1932E+01	-1.8433E+01	1.9494E+01	-8.7410E+00	IN-LB-SEC
Bpsi	1.8433E+01	-1.1932E+01	8.7410E+00	1.9494E+01	IN-LB-SEC

(CASE 4) Displaced and tilted symmetric cyl. seal, no pres. grad.

```
&INPUTS
   TITLE  =  'Displaced and tilted symmetric cyl. seal, no pres. grad.'
   IFACE  =  0              ISIUN  =  0              IACC   =  0
   RO     =  1.0000E+00     EL     =  2.0000E+00     C      =  5.0000E-04
   IGROT  =  0              RPM    =  1.0000E+04     RPMD   =  1.0000E+04
   PLEA   =  1.4700E+01     PRIA   =  1.4700E+01     VISC   =  2.9000E-09
   ISTIF  =  1              IDAMP  =  1              MOM    =  1
   ICONT  =  0              IHOME  =  0              NUMDMP =  0
   EZD    =  0.0000E+00     EXD    =  1.2500E-04     EYD    =  0.0000E+00
   PHIR   =  0.0000E+00     PSIR   =  1.2500E-04
   FZD    =  0.0000E+00     FXD    =  0.0000E+00     FYD    =  0.0000E+00
   EMXD   =  0.0000E+00     EMYD   =  0.0000E+00
   NIT    =  8              DPRE   =  1.0000E-06     TOLP   =  1.0000E-04
   NITF   =  8              DECC   =  1.0000E-06     TOLE   =  1.0000E-03
   N      =  17             NREG   =  2              NRSUB  =  4  4
   ELFR   =  5.0000E-01  5.0000E-01
   ALPI   =  5.0000E-01  5.0000E-01
   BETI   =  1.5680E+01 -1.5680E+01
   DELT   =  1.3265E-03  1.3265E-03
   DZIN   =  0.0000E+00
   DTHIN  =  0.0000E+00
/

SPIRAL GROOVE SHAFT SEAL,  ROTATING SURFACE IS SMOOTH

LENGTH, DIAMETER, CLEARANCE =  2.0000E+00,  2.0000E+00,  5.0000E-04  (IN)

ROTATION SPEED, DISTURBANCE SPEED =  1.0000E+04,  1.0000E+04  (RPM)

PRESSURE AT START, END AXIAL BOUNDARIES =  1.4700E+01,  1.4700E+01  (PSI)

VISCOSITY =  2.9000E-09  (PSI-SEC),   AMBIENT PRESSURE =  1.4700E+01  (PSI)

ITERATIONS AND ERROR CODE IN LAST PRESSURE CALCULATION =  4  0

CALCULATED FORCES IN  X,Y DIRECTIONS =  3.3938E+00, -3.0660E+00  (LB)
CALCULATED MOMENTS ABOUT X,Y AXES =  2.6476E-01,  3.6468E-01  (IN-LB)

MINIMUM FILM THICKNESS =  2.5000E-04  (IN)

FLOW =  2.0302E-02  (IN**3/SEC) MEASURED AT  1.4700E+01  (PSI)

TORQUE =  5.8726E-02  (IN-LB),   FILM POWER LOSS =  9.3178E-03  (HP)

COMPRESSIBILITY NUMBER =  4.9582E+00,   SQUEEZE NUMBER =  9.9163E+00

        DYNAMIC COEFFICIENTS  ( FORCE UNIT / DISP. UNIT )

DISP.      x (IN)       y (IN)     phi (RAD)    psi (RAD)    FORCE UNIT
Kx       4.0657E+04  9.7405E+03 -8.3206E+01 -2.8523E+02   LB
Ky      -9.4351E+03  4.0515E+04  2.5345E+02  1.2957E+02   LB
Kphi    -2.9470E+01  2.1556E+02  4.8420E+03  1.5075E+03   IN-LB
Kpsi    -1.2690E+02  7.3977E+01 -1.4889E+03  4.8095E+03   IN-LB
Bx       2.3280E+01 -1.3471E+01  1.0865E-01  6.3426E-01   LB-SEC
By       1.3609E+01  2.2299E+01 -1.3412E-01  2.1028E-01   LB-SEC
Bphi    -7.2952E-02 -1.0697E-01  4.5324E+00 -1.0203E+00   IN-LB-SEC
Bpsi     4.7944E-01 -7.1164E-02  9.5944E-01  4.8461E+00   IN-LB-SEC
```

(CASE 5) Same seal as Case 4 with applied forces instead of displ.

```
&INPUTS
   TITLE  =  'Same seal as Case 4 with applied forces instead of displ.'
   IFACE  =  0              ISIUN  =  0              IACC   =  0
   RO     =  1.0000E+00     EL     =  2.0000E+00     C      =  5.0000E-04
   IGROT  =  0              RPM    =  1.0000E+04     RPMD   =  1.0000E+04
   PLEA   =  1.4700E+01     PRIA   =  1.4700E+01     VISC   =  2.9000E-09
   ISTIF  =  1              IDAMP  =  1              MOM    =  1
   ICONT  =  0              IHOME  =  2              NUMDMP =  0
   EZD    =  0.0000E+00     EXD    =  2.0000E-04     EYD    =  0.0000E+00
   PHIR   =  0.0000E+00     PSIR   =  0.0000E+00
   FZD    =  0.0000E+00     FXD    =  3.3938E+00     FYD    = -3.0660E+00
   EMXD   =  2.6476E-01     EMYD   =  3.6468E-01
   NIT    =  8              DPRE   =  1.0000E-06     TOLP   =  1.0000E-04
   NITF   =  8              DECC   =  1.0000E-06     TOLE   =  1.0000E-03
   N  .   =  17             NREG   =  2              NRSUB  =  4  4
   ELFR   =  5.0000E-01  5.0000E-01
   ALPI   =  5.0000E-01  5.0000E-01
   BETI   =  1.5680E+01 -1.5680E+01
   DELT   =  1.3265E-03  1.3265E-03
   DZIN   =  0.0000E+00
   DTHIN  =  0.0000E+00
/
```

SPIRAL GROOVE SHAFT SEAL, ROTATING SURFACE IS SMOOTH

LENGTH, DIAMETER, CLEARANCE = 2.0000E+00, 2.0000E+00, 5.0000E-04 (IN)

ROTATION SPEED, DISTURBANCE SPEED = 1.0000E+04, 1.0000E+04 (RPM)

PRESSURE AT START, END AXIAL BOUNDARIES = 1.4700E+01, 1.4700E+01 (PSI)

VISCOSITY = 2.9000E-09 (PSI-SEC), AMBIENT PRESSURE = 1.4700E+01 (PSI)

ERROR CODE = 0, ITERATIONS IN HOMING PROCESS = 3

CALCULATED DISPLACEMENTS IN X,Y DIRECTIONS = 1.2500E-04, -1.1010E-09 (IN)
CALCULATED TILTS ABOUT X,Y AXES = 9.8499E-10, 1.2500E-04 (RAD)

ITERATIONS IN LAST PRESSURE CALCULATION = 1

CALCULATED FORCES IN X,Y DIRECTIONS = 3.3938E+00, -3.0660E+00 (LB)
CALCULATED MOMENTS ABOUT X,Y AXES = 2.6476E-01, 3.6468E-01 (IN-LB)

MINIMUM FILM THICKNESS = 2.5000E-04 (IN)

FLOW = 2.0301E-02 (IN**3/SEC) MEASURED AT 1.4700E+01 (PSI)

TORQUE = 5.8726E-02 (IN-LB), FILM POWER LOSS = 9.3178E-03 (HP)

COMPRESSIBILITY NUMBER = 4.9582E+00, SQUEEZE NUMBER = 9.9163E+00

DYNAMIC COEFFICIENTS (FORCE UNIT / DISP. UNIT)

DISP.	x (IN)	y (IN)	phi (RAD)	psi (RAD)	FORCE UNIT
Kx	4.0657E+04	9.7405E+03	-8.3205E+01	-2.8523E+02	LB
Ky	-9.4351E+03	4.0515E+04	2.5345E+02	1.2957E+02	LB
Kphi	-2.9469E+01	2.1556E+02	4.8420E+03	1.5075E+03	IN-LB
Kpsi	-1.2690E+02	7.3975E+01	-1.4889E+03	4.8095E+03	IN-LB
Bx	2.3280E+01	-1.3471E+01	1.0865E-01	6.3425E-01	LB-SEC
By	1.3609E+01	2.2299E+01	-1.3412E-01	2.1028E-01	LB-SEC
Bphi	-7.2948E-02	-1.0696E-01	4.5324E+00	-1.0203E+00	IN-LB-SEC
Bpsi	4.7943E-01	-7.1166E-02	9.5944E-01	4.8461E+00	IN-LB-SEC

(CASE 6) Same as Case 4 with SI units

```
&INPUTS
   TITLE  =  'Same as Case 4 with SI units'
   IFACE  =  0              ISIUN  =  1              IACC   =  0
   RO     =  2.5400E-02     EL     =  5.0800E-02     C      =  1.2700E-05
   IGROT  =  0              RPM    =  1.0000E+04     RPMD   =  1.0000E+04
   PLEA   =  1.0135E+05     PRIA   =  1.0135E+05     VISC   =  1.9995E-05
   ISTIF  =  1              IDAMP  =  1              MOM    =  1
   ICONT  =  0              IHOME  =  0              NUMDMP =  0
   EZD    =  0.0000E+00     EXD    =  3.1750E-06     EYD    =  0.0000E+00
   PHIR   =  0.0000E+00     PSIR   =  1.2500E-04
   FZD    =  0.0000E+00     FXD    =  3.3938E+00     FYD    = -3.0660E+00
   EMXD   =  2.6476E-01     EMYD   =  3.6468E-01
   NIT    =  8              DPRE   =  1.0000E-06     TOLP   =  1.0000E-04
   NITF   =  8              DECC   =  1.0000E-06     TOLE   =  1.0000E-03
   N      =  17             NREG   =  2              NRSUB  =  4  4
   ELFR   =  5.0000E-01  5.0000E-01
   ALPI   =  5.0000E-01  5.0000E-01
   BETI   =  1.5680E+01 -1.5680E+01
   DELT   =  3.3693E-05  3.3693E-05
   DZIN   =  0.0000E+00
   DTHIN  =  0.0000E+00
/
```

SPIRAL GROOVE SHAFT SEAL, ROTATING SURFACE IS SMOOTH

LENGTH, DIAMETER, CLEARANCE = 5.0800E-02, 5.0800E-02, 1.2700E-05 (m)

ROTATION SPEED, DISTURBANCE SPEED = 1.0000E+04, 1.0000E+04 (RPM)

PRESSURE AT START, END AXIAL BOUNDARIES = 1.0135E+05, 1.0135E+05 (Pa)

VISCOSITY = 1.9995E-05 (Pa-SEC), AMBIENT PRESSURE = 1.0135E+05 (Pa)

ITERATIONS AND ERROR CODE IN LAST PRESSURE CALCULATION = 4 0

CALCULATED FORCES IN X,Y DIRECTIONS = 1.5097E+01, -1.3638E+01 (N)
CALCULATED MOMENTS ABOUT X,Y AXES = 2.9914E-02, 4.1204E-02 (N-m)

MINIMUM FILM THICKNESS = 6.3500E-06 (m)

FLOW = 3.3268E-07 (m**3/SEC) MEASURED AT 1.0135E+05 (Pa)

TORQUE = 6.6352E-03 (N-m), FILM POWER LOSS = 6.9483E+00 (WATT)

COMPRESSIBILITY NUMBER = 4.9584E+00, SQUEEZE NUMBER = 9.9167E+00

DYNAMIC COEFFICIENTS (FORCE UNIT / DISP. UNIT)

DISP.	x (m)	y (m)	phi (RAD)	psi (RAD)	FORCE UNIT
Kx	7.1202E+06	1.7058E+06	-3.7010E+02	-1.2688E+03	N
Ky	-1.6523E+06	7.0953E+06	1.1274E+03	5.7639E+02	N
Kphi	-1.3110E+02	9.5888E+02	5.4708E+02	1.7032E+02	N-m
Kpsi	-5.6446E+02	3.2904E+02	-1.6822E+02	5.4341E+02	N-m
Bx	4.0768E+03	-2.3592E+03	4.8331E-01	2.8213E+00	N-SEC
By	2.3833E+03	3.9051E+03	-5.9660E-01	9.3536E-01	N-SEC
Bphi	-3.2450E-01	-4.7582E-01	5.1209E-01	-1.1528E-01	N-m-SEC
Bpsi	2.1326E+00	-3.1658E-01	1.0841E-01	5.4754E-01	N-m-SEC

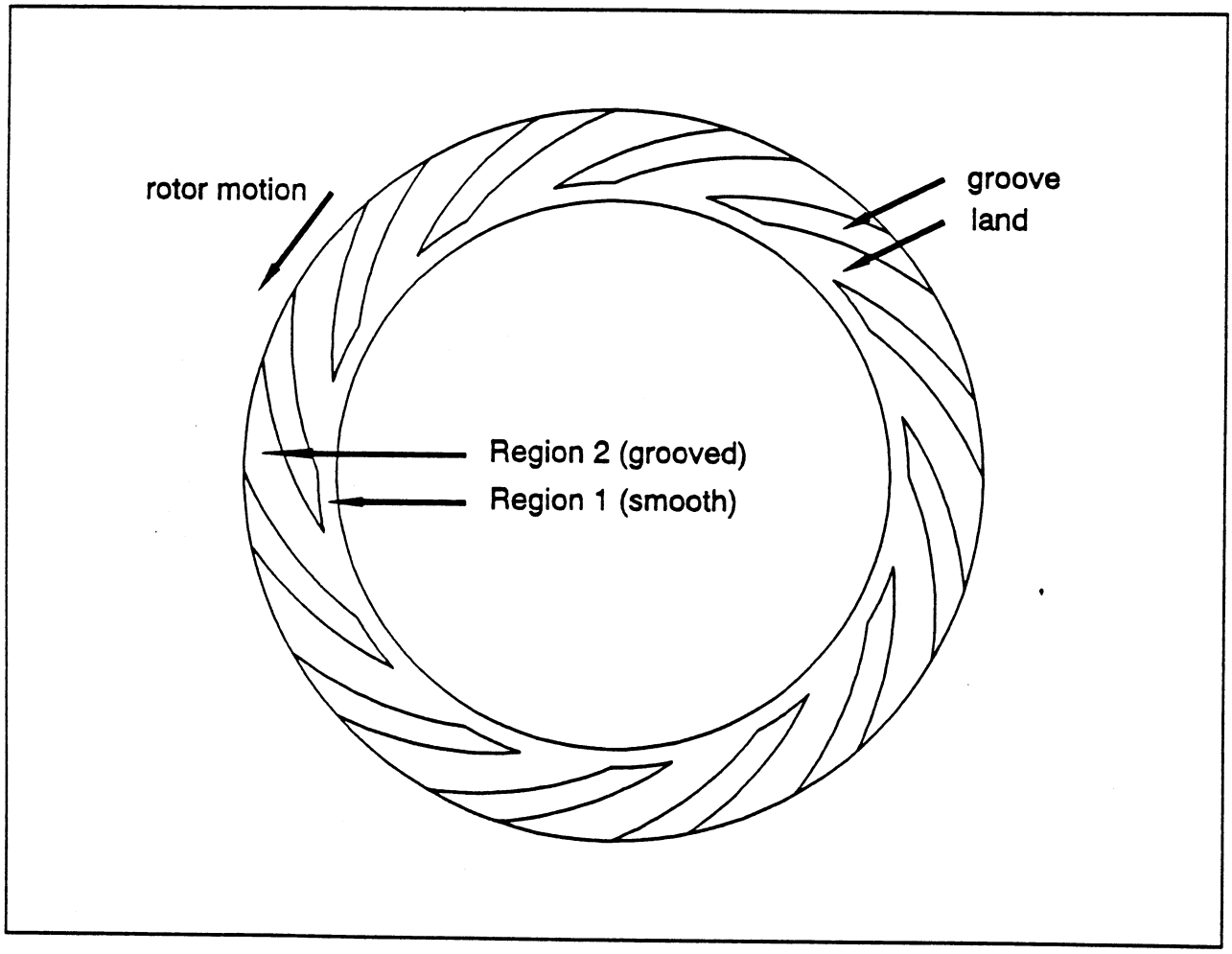

Figure 8 Stator with inward pumping grooves for Cases 7 and 8

```
( CASE  7 )  Face seal for pipe line compressor

&INPUTS
   TITLE  =  'Face seal for pipe line compressor'
   IFACE  =  1              ISIUN  =  0              IACC   =  1
   R0     =  2.2525E+00     EL     =  3.5600E-01     C      =  1.0000E-04
   IGROT  =  0              RPM    =  1.4500E+04     RPMD   =  1.4500E+04
   PLEA   =  1.4700E+01     PRIA   =  9.1470E+02     VISC   =  1.7500E-09
   ISTIF  =  1              IDAMP  =  1              MOM    =  1
   ICONT  =  0              IHOME  =  0              NUMDMP =  0
   EZD    =  0.0000E+00     EXD    =  0.0000E+00     EYD    =  0.0000E+00
   PHIR   =  0.0000E+00     PSIR   =  0.0000E+00
   FZD    =  0.0000E+00     FXD    =  0.0000E+00     FYD    =  0.0000E+00
   EMXD   =  0.0000E+00     EMYD   =  0.0000E+00
   NIT    =  8              DPRE   =  1.0000E-06     TOLP   =  1.0000E-04
   NITF   =  8              DECC   =  1.0000E-06     TOLE   =  1.0000E-03
   N      =  9              NREG   =  2              NRSUB  =  2  4
   ELFR   =  2.1048E-01  7.8952E-01
   ALPI   =  0.0000E+00  4.2290E-01
   BETI   =  0.0000E+00 -2.2844E+01
   DELT   =  0.0000E+00  2.1824E-04
   DZIN   =  0.0000E+00
   DTHIN  =  0.0000E+00
/

SPIRAL GROOVE FACE SEAL,  ROTATING SURFACE IS SMOOTH

ID, OD, REFERENCE FILM THICKNESS =  3.7930E+00,  4.5050E+00,  1.0000E-04  (IN)

ROTATION SPEED, DISTURBANCE SPEED =  1.4500E+04,  1.4500E+04  (RPM)

INSIDE, OUTSIDE PRESSURE =  1.4700E+01,  9.1470E+02  (PSI)

VISCOSITY =  1.7500E-09  (PSI-SEC),   AMBIENT PRESSURE =  1.4700E+01  (PSI)

ITERATIONS AND ERROR CODE IN LAST PRESSURE CALCULATION =  4  0

CALCULATED FORCE IN  Z DIRECTION =  3.4246E+03  (LB)
CALCULATED MOMENTS ABOUT X,Y AXES = -1.0069E-12, -5.7018E-12  (IN-LB)

MINIMUM FILM THICKNESS =  1.0000E-04  (IN)

FLOW = -1.3026E+02  (IN**3/SEC) MEASURED AT  1.4700E+01  (PSI)

TORQUE =  3.2695E-01  (IN-LB),   FILM POWER LOSS =  7.5219E-02  (HP)

COMPRESSIBILITY NUMBER =  5.5030E+02,   SQUEEZE NUMBER =  1.1006E+03

        DYNAMIC COEFFICIENTS  ( FORCE UNIT / DISP. UNIT )

DISP.      z (IN)     phi (RAD)    psi (RAD)     FORCE UNIT
Kz       7.0137E+06 -5.7802E+00 -5.7791E+00   LB
Kphi    -6.0544E-03  1.2466E+07  1.6134E+06   IN-LB
Kpsi     2.0659E-02 -1.6134E+06  1.2466E+07   IN-LB
Bz       2.8634E+02  1.7180E-04  1.7161E-04   LB-SEC
Bphi    -2.2269E-07  6.6669E+02 -7.0380E+01   IN-LB-SEC
Bpsi    -1.0207E-06  7.0380E+01  6.6669E+02   IN-LB-SEC
```

(CASE 8) Same as case 7 with half the grid spacing in each direction

```
&INPUTS
   TITLE  =  'Same as case 7 with half the grid spacing in each direction'
   IFACE  =  1              ISIUN  =  0              IACC   =  1
   RO     =  2.2525E+00     EL     =  3.5600E-01     C      =  1.0000E-04
   IGROT  =  0              RPM    =  1.4500E+04     RPMD   =  1.4500E+04
   PLEA   =  1.4700E+01     PRIA   =  9.1470E+02     VISC   =  1.7500E-09
   ISTIF  =  1              IDAMP  =  1              MOM    =  1
   ICONT  =  0              IHOME  =  0              NUMDMP =  0
   EZD    =  0.0000E+00     EXD    =  0.0000E+00     EYD    =  0.0000E+00
   PHIR   =  0.0000E+00     PSIR   =  0.0000E+00
   FZD    =  0.0000E+00     FXD    =  0.0000E+00     FYD    =  0.0000E+00
   EMXD   =  0.0000E+00     EMYD   =  0.0000E+00
   NIT    =  8              DPRE   =  1.0000E-06     TOLP   =  1.0000E-04
   NITF   =  8              DECC   =  1.0000E-06     TOLE   =  1.0000E-03
   N      =  17             NREG   =  2              NRSUB  =  4  8
   ELFR   =  2.1048E-01  7.8952E-01
   ALPI   =  0.0000E+00  4.2290E-01
   BETI   =  0.0000E+00 -2.2844E+01
   DELT   =  0.0000E+00  2.1824E-04
   DZIN   =  0.0000E+00
   DTHIN  =  0.0000E+00
/
```

SPIRAL GROOVE FACE SEAL, ROTATING SURFACE IS SMOOTH

ID, OD, REFERENCE FILM THICKNESS = 3.7930E+00, 4.5050E+00, 1.0000E-04 (IN)

ROTATION SPEED, DISTURBANCE SPEED = 1.4500E+04, 1.4500E+04 (RPM)

INSIDE, OUTSIDE PRESSURE = 1.4700E+01, 9.1470E+02 (PSI)

VISCOSITY = 1.7500E-09 (PSI-SEC), AMBIENT PRESSURE = 1.4700E+01 (PSI)

ITERATIONS AND ERROR CODE IN LAST PRESSURE CALCULATION = 4 0

CALCULATED FORCE IN Z DIRECTION = 3.4282E+03 (LB)
CALCULATED MOMENTS ABOUT X,Y AXES = 5.0522E-12, 2.5739E-12 (IN-LB)

MINIMUM FILM THICKNESS = 1.0000E-04 (IN)

FLOW = -1.3026E+02 (IN**3/SEC) MEASURED AT 1.4700E+01 (PSI)

TORQUE = 3.2695E-01 (IN-LB), FILM POWER LOSS = 7.5219E-02 (HP)

COMPRESSIBILITY NUMBER = 5.5030E+02, SQUEEZE NUMBER = 1.1006E+03

DYNAMIC COEFFICIENTS (FORCE UNIT / DISP. UNIT)

DISP.	z (IN)	phi (RAD)	psi (RAD)	FORCE UNIT
Kz	7.0318E+06	-5.8003E+00	-5.8209E+00	LB
Kphi	-4.1461E-02	1.2507E+07	1.6209E+06	IN-LB
Kpsi	-1.4393E-02	-1.6209E+06	1.2507E+07	IN-LB
Bz	2.8690E+02	1.7193E-04	1.7350E-04	LB-SEC
Bphi	6.6840E-07	6.6815E+02	-7.0687E+01	IN-LB-SEC
Bpsi	7.0000E-07	7.0687E+01	6.6815E+02	IN-LB-SEC

5. Verification

SPIRALG has been compared with the results of two computer codes. The first of these is MTI Computer Code PN471 which is fully described in Reference 3. The program is based on perturbation analyses and is only applicable to bearings and seals operating in the concentric, aligned position ($\epsilon_x = \epsilon_y = \phi = \psi = 0$). The program does not predict loads and moments that would occur at finite displacements but it does predict stiffness and damping values as well as flow, torque, and power loss for spiral groove bearings as well as cylindrical and face seals. Since the program solves ordinary rather than partial differential equations it can be made to rapidly produce highly accurate results for evaluating the accuracy of SPIRALG. The second MTI computer code, named GASBEAR, is used to verify SPIRALG under displaced and misaligned conditions. GASBEAR was written for use in conjunction with plane journal bearings and cylindrical seals. It does not treat spiral grooves or face seals. Since SPIRALG does not contain and special instructions for treating concentric behavior and has relatively few instructions for distinguishing between face and cylindrical seals, the above two programs should provide reasonable verification. Since the treatment of the effects of spiral grooves under eccentric and misaligned conditions is believed to be new, terms that become significant only under those conditions remain unverified.

The results of 7 verification tests are reported on the following pages. A SPIRALG output listing followed by the relevant output from the verification code, converted to equivalent units and format, is given for each case. The somewhat strange looking input values (unit ambient pressure, high RPM but low viscosity etc.) were selected to simplify the conversion process between dimensional quantities and the dimensionless ones that were used throughout the development of the code. The compressibility number of $\Lambda = 10$ used for all cases and the seal pressure ratio of 2 used for imposed pressure gradients should be typical of many practical applications under fairly compressible conditions.

Cases 1 - 6 show comparisons between SPIRALG and PN471. Romberg extrapolation was used for each of these cases, with 21 grid points in the circumferential direction and 5 sub-intervals in each of the two regions in the transverse direction for the coarse grid solution. The fine grid solutions thus use 41 circumferential points and 10 sub-intervals per region in the transverse direction. These represent numbers close to the resource limits of the OS2 version of the code as given in Section 6.

The first case verifies stiffness and damping values for a synchronous disturbance acting on a cylindrical seal with a herringbone groove pattern and an imposed pressure gradient. Cases 2 and 3 verify the differences in stiffness and damping values predicted to occur for a cylindrical seal when grooves are placed on the rotor (with groove angles reversed) rather than on the stator. The static quantities (flow, torque and power loss) remain unchanged. Cases 4 - 6 show comparisons between SPIRALG and PN471 for a spiral groove face seal with an imposed pressure gradient at three different disturbance frequencies; zero (case

4), synchronous (case 5) and ten times synchronous (case 6).

Case 7 shows a comparison between SPIRALG and GASBEAR for and eccentric, tilted cylindrical seal with an imposed pressure gradient. The grid size was chosen to match the maximum size allowable for the available version of GASBEAR. A separate program was written to perform Romberg extrapolations with the results of GASBEAR. The agreement between the two programs is good. The apparent discrepancy between the moments about the y axis is a result of the fact that component is very small. The relative error obtained by dividing the discrepancy by the absolute magnitude of the moment vector is 0.33%.

```
( CASE  1 )  Concentric cyl. seal with pres. grad. lamda=10, sigma=20

&INPUTS
   TITLE  =  'Concentric cyl. seal with pres. grad. lamda=10, sigma=20'
   IFACE  =  0              ISIUN  =  0              IACC   =  1
   RO     =  1.0000E+00     EL     =  2.0000E+00     C      =  1.0000E-03
   IGROT  =  0              RPM    =  1.9099E+05     RPMD   =  1.9099E+05
   PLEA   =  2.0000E+00     PRIA   =  1.0000E+00     VISC   =  8.3333E-11
   ISTIF  =  1              IDAMP  =  1              MOM    =  1
   ICONT  =  0              IHOME  =  0              NUMDMP =  0
   EZD    =  0.0000E+00     EXD    =  0.0000E+00     EYD    =  0.0000E+00
   PHIR   =  0.0000E+00     PSIR   =  0.0000E+00
   FZD    =  0.0000E+00     FXD    =  0.0000E+00     FYD    =  0.0000E+00
   EMXD   =  0.0000E+00     EMYD   =  0.0000E+00
   NIT    =  8              DPRE   =  1.0000E-06     TOLP   =  1.0000E-04
   NITF   =  8              DECC   =  1.0000E-06     TOLE   =  1.0000E-03
   N      =  21             NREG   =  2              NRSUB  =  5  5
   ELFR   =  5.0000E-01  5.0000E-01
   ALPI   =  5.0000E-01  5.0000E-01
   BETI   =  2.5000E+01  1.5500E+02
   DELT   =  1.0000E-03  1.0000E-03
   DZIN   =  0.0000E+00
   DTHIN  =  0.0000E+00
/

SPIRAL GROOVE SHAFT SEAL,  ROTATING SURFACE IS SMOOTH

LENGTH, DIAMETER, CLEARANCE =  2.0000E+00,  2.0000E+00,  1.0000E-03  (IN)

ROTATION SPEED, DISTURBANCE SPEED =  1.9099E+05,  1.9099E+05  (RPM)

PRESSURE AT START, END AXIAL BOUNDARIES =  2.0000E+00,  1.0000E+00  (PSI)

VISCOSITY =  8.3333E-11  (PSI-SEC),   AMBIENT PRESSURE =  1.0000E+00  (PSI)

ITERATIONS AND ERROR CODE IN LAST PRESSURE CALCULATION =  2  0

CALCULATED FORCES IN  X,Y DIRECTIONS = -1.0902E-15, -8.1153E-16  (LB)
CALCULATED MOMENTS ABOUT X,Y AXES = -9.3565E-16, -2.4405E-16  (IN-LB)

MINIMUM FILM THICKNESS =  1.0000E-03  (IN)

FLOW =  1.2816E+01  (IN**3/SEC) MEASURED AT  1.0000E+00  (PSI)

TORQUE =  1.7015E-02  (IN-LB),   FILM POWER LOSS =  5.1562E-02  (HP)

COMPRESSIBILITY NUMBER =  1.0000E+01,   SQUEEZE NUMBER =  2.0000E+01

        DYNAMIC COEFFICIENTS  ( FORCE UNIT / DISP. UNIT )

DISP.      x (IN)       y (IN)     phi (RAD)    psi (RAD)    FORCE UNIT
Kx       5.4607E+03  9.0379E+01 -6.8886E+01  2.6847E+02   LB
Ky      -9.0379E+01  5.4607E+03 -2.6847E+02 -6.8886E+01   LB
Kphi    -1.0824E+02 -1.7773E+01  7.0561E+02  1.9521E+02   IN-LB
Kpsi     1.7773E+01 -1.0824E+02 -1.9521E+02  7.0561E+02   IN-LB
Bx       7.3200E-02 -5.5832E-02 -1.5172E-02 -2.9538E-02   LB-SEC
By       5.5832E-02  7.3200E-02  2.9538E-02 -1.5172E-02   LB-SEC
Bphi     1.9442E-03  6.9321E-03  2.7091E-02 -1.1690E-02   IN-LB-SEC
Bpsi    -6.9321E-03  1.9442E-03  1.1690E-02  2.7091E-02   IN-LB-SEC
```

COMPARISON OF CASE 1 WITH PN471

FLOW = 1.282E+01 (IN**3/SEC) MEASURED AT 1.0000E+00 (PSI)

TORQUE = 1.701E-02 (IN-LB), FILM POWER LOSS = 5.156E-02 (HP)

DYNAMIC COEFFICIENTS (FORCE UNIT / DISP. UNIT)

DISP.	x (IN)	y (IN)	phi (RAD)	psi (RAD)	FORCE UNIT
Kx	5.4608E+03	9.0292E+01	-6.8846E+01	2.6823E+02	LB
Ky	-9.0292E+01	5.4608E+03	-2.6823E+02	-6.8846E+01	LB
Kphi	-1.0809E+02	-1.7525E+01	7.0356E+02	1.9537E+02	IN-LB
Kpsi	1.7525E+01	-1.0809E+02	-1.9537E+02	7.0356E+02	IN-LB
Bx	7.3215E-02	-5.5805E-02	-1.5192E-02	-2.9534E-02	LB-SEC
By	5.5805E-02	7.3215E-02	2.9534E-02	-1.5192E-02	LB-SEC
Bphi	1.9403E-03	6.9195E-03	2.7097E-02	-1.1667E-02	IN-LB-SEC
Bpsi	-6.9195E-03	1.9403E-03	1.1667E-02	2.7097E-02	IN-LB-SEC

```
( CASE  2 )  Concentric asymmetric cyl. seal, lamda=10, sigma=0

&INPUTS
   TITLE  =  'Concentric asymmetric cyl. seal, lamda=10, sigma=0'
   IFACE  =  0              ISIUN  =  0              IACC   =  1
   RO     =  1.0000E+00     EL     =  2.0000E+00     C      =  1.0000E-03
   IGROT  =  0              RPM    =  1.9099E+05     RPMD   =  0.0000E+00
   PLEA   =  1.0000E+00     PRIA   =  1.0000E+00     VISC   =  8.3333E-11
   ISTIF  =  1              IDAMP  =  1              MOM    =  1
   ICONT  =  0              IHOME  =  0              NUMDMP =  0
   EZD    =  0.0000E+00     EXD    =  0.0000E+00     EYD    =  0.0000E+00
   PHIR   =  0.0000E+00     PSIR   =  0.0000E+00
   FZD    =  0.0000E+00     FXD    =  0.0000E+00     FYD    =  0.0000E+00
   EMXD   =  0.0000E+00     EMYD   =  0.0000E+00
   NIT    =  8              DPRE   =  1.0000E-06     TOLP   =  1.0000E-04
   NITF   =  8              DECC   =  1.0000E-06     TOLE   =  1.0000E-03
   N      =  21             NREG   =  2              NRSUB  =  5  5
   ELFR   =  5.0000E-01  5.0000E-01
   ALPI   =  5.0000E-01  0.0000E+00
   BETI   =  2.5000E+01  0.0000E+00
   DELT   =  1.0000E-03  0.0000E+00
   DZIN   =  0.0000E+00
   DTHIN  =  0.0000E+00
/

SPIRAL GROOVE SHAFT SEAL,  ROTATING SURFACE IS SMOOTH

LENGTH, DIAMETER, CLEARANCE =  2.0000E+00,  2.0000E+00,  1.0000E-03  (IN)

ROTATION SPEED, DISTURBANCE SPEED =  1.9099E+05,  0.0000E+00  (RPM)

PRESSURE AT START, END AXIAL BOUNDARIES =  1.0000E+00,  1.0000E+00  (PSI)

VISCOSITY =  8.3333E-11  (PSI-SEC),   AMBIENT PRESSURE =  1.0000E+00  (PSI)

ITERATIONS AND ERROR CODE IN LAST PRESSURE CALCULATION =  2  0

CALCULATED FORCES IN  X,Y DIRECTIONS = -2.8151E-15, -1.6233E-15  (LB)
CALCULATED MOMENTS ABOUT X,Y AXES =  2.7524E-16, -5.2158E-17  (IN-LB)

MINIMUM FILM THICKNESS =  1.0000E-03  (IN)

FLOW =  3.5000E+00  (IN**3/SEC) MEASURED AT  1.0000E+00  (PSI)

TORQUE =  1.8850E-02  (IN-LB),   FILM POWER LOSS =  5.7122E-02  (HP)

COMPRESSIBILITY NUMBER =  1.0000E+01,   SQUEEZE NUMBER =  0.0000E+00

        DYNAMIC COEFFICIENTS  ( FORCE UNIT / DISP. UNIT )

DISP.      x (IN)       y (IN)     phi (RAD)    psi (RAD)    FORCE UNIT
Kx       4.9657E+03   1.5689E+03 -4.9960E+02   2.6673E+02   LB
Ky      -1.5689E+03   4.9657E+03 -2.6673E+02  -4.9960E+02   LB
Kphi     5.3012E+01  -3.6877E+02  6.0778E+02   5.3984E+02   IN-LB
Kpsi     3.6877E+02   5.3012E+01 -5.3984E+02   6.0778E+02   IN-LB
Bx      -6.9953E-02  -1.1123E-01  4.3933E-02  -1.2462E-02   LB-SEC
By       1.1123E-01  -6.9953E-02  1.2462E-02   4.3933E-02   LB-SEC
Bphi    -8.3037E-03  -4.4522E-03  2.2471E-02  -4.3624E-02   IN-LB-SEC
Bpsi     4.4522E-03  -8.3037E-03  4.3624E-02   2.2471E-02   IN-LB-SEC
```

COMPARISON OF CASE 2 WITH PN471

FLOW = 3.500E+00 (IN**3/SEC) MEASURED AT 1.0000E+00 (PSI)

TORQUE = 1.885E-02 (IN-LB), FILM POWER LOSS = 5.712E-02 (HP)

DYNAMIC COEFFICIENTS (FORCE UNIT / DISP. UNIT)

DISP.	x (IN)	y (IN)	phi (RAD)	psi (RAD)	FORCE UNIT
Kx	4.9648E+03	1.5692E+03	-4.9982E+02	2.6552E+02	LB
Ky	-1.5692E+03	4.9648E+03	-2.6552E+02	-4.9982E+02	LB
Kphi	5.3156E+01	-3.6793E+02	6.0602E+02	5.3900E+02	IN-LB
Kpsi	3.6793E+02	5.3156E+01	-5.3900E+02	6.0602E+02	IN-LB
Bx	-6.9955E-02	-1.1143E-01	4.3975E-02	-1.2344E-02	LB-SEC
By	1.1143E-01	-6.9955E-02	1.2344E-02	4.3975E-02	LB-SEC
Bphi	-8.3373E-03	-4.4940E-03	2.2617E-02	-4.3536E-02	IN-LB-SEC
Bpsi	4.4940E-03	-8.3373E-03	4.3536E-02	2.2617E-02	IN-LB-SEC

(CASE 3) Same case with grooves on moving surf., groove angle rev.

```
&INPUTS
   TITLE  =  'Same case with grooves on moving surf., groove angle rev.'
   IFACE  =  0              ISIUN  =  0              IACC   =  1
   RO     =  1.0000E+00     EL     =  2.0000E+00     C      =  1.0000E-03
   IGROT  =  1              RPM    =  1.9099E+05     RPMD   =  0.0000E+00
   PLEA   =  1.0000E+00     PRIA   =  1.0000E+00     VISC   =  8.3333E-11
   ISTIF  =  1              IDAMP  =  1              MOM    =  1
   ICONT  =  0              IHOME  =  0              NUMDMP =  0
   EZD    =  0.0000E+00     EXD    =  0.0000E+00     EYD    =  0.0000E+00
   PHIR   =  0.0000E+00     PSIR   =  0.0000E+00
   FZD    =  0.0000E+00     FXD    =  0.0000E+00     FYD    =  0.0000E+00
   EMXD   =  0.0000E+00     EMYD   =  0.0000E+00
   NIT    =  8              DPRE   =  1.0000E-06     TOLP   =  1.0000E-04
   NITF   =  8              DECC   =  1.0000E-06     TOLE   =  1.0000E-03
   N      =  21             NREG   =  2              NRSUB  =  5  5
   ELFR   =  5.0000E-01  5.0000E-01
   ALPI   =  5.0000E-01  0.0000E+00
   BETI   = -2.5000E+01  0.0000E+00
   DELT   =  1.0000E-03  0.0000E+00
   DZIN   =  0.0000E+00
   DTHIN  =  0.0000E+00
/
```

SPIRAL GROOVE SHAFT SEAL, ROTATING SURFACE IS GROOVED

LENGTH, DIAMETER, CLEARANCE = 2.0000E+00, 2.0000E+00, 1.0000E-03 (IN)

ROTATION SPEED, DISTURBANCE SPEED = 1.9099E+05, 0.0000E+00 (RPM)

PRESSURE AT START, END AXIAL BOUNDARIES = 1.0000E+00, 1.0000E+00 (PSI)

VISCOSITY = 8.3333E-11 (PSI-SEC), AMBIENT PRESSURE = 1.0000E+00 (PSI)

ITERATIONS AND ERROR CODE IN LAST PRESSURE CALCULATION = 2 0

CALCULATED FORCES IN X,Y DIRECTIONS = -3.4729E-16, -1.2658E-15 (LB)
CALCULATED MOMENTS ABOUT X,Y AXES = 1.6213E-16, 6.2386E-17 (IN-LB)

MINIMUM FILM THICKNESS = 1.0000E-03 (IN)

FLOW = 3.5000E+00 (IN**3/SEC) MEASURED AT 1.0000E+00 (PSI)

TORQUE = 1.8850E-02 (IN-LB), FILM POWER LOSS = 5.7122E-02 (HP)

COMPRESSIBILITY NUMBER = 1.0000E+01, SQUEEZE NUMBER = 0.0000E+00

DYNAMIC COEFFICIENTS (FORCE UNIT / DISP. UNIT)

DISP.	x (IN)	y (IN)	phi (RAD)	psi (RAD)	FORCE UNIT
Kx	4.5241E+03	1.2933E+03	-3.6977E+02	2.1989E+02	LB
Ky	-1.2933E+03	4.5241E+03	-2.1989E+02	-3.6977E+02	LB
Kphi	3.4694E+02	-4.7068E+02	5.9016E+02	5.1362E+02	IN-LB
Kpsi	4.7068E+02	3.4694E+02	-5.1362E+02	5.9016E+02	IN-LB
Bx	-2.3432E-02	-1.2667E-01	3.4823E-02	-5.9373E-03	LB-SEC
By	1.2667E-01	-2.3432E-02	5.9373E-03	3.4823E-02	LB-SEC
Bphi	-2.7769E-02	6.0874E-03	2.3559E-02	-4.4038E-02	IN-LB-SEC
Bpsi	-6.0874E-03	-2.7769E-02	4.4038E-02	2.3559E-02	IN-LB-SEC

COMPARISON OF CASE 3 WITH PN471

FLOW = 3.500E+00 (IN**3/SEC) MEASURED AT 1.0000E+00 (PSI)

TORQUE = 1.885E-02 (IN-LB), FILM POWER LOSS = 5.712E-02 (HP)

DYNAMIC COEFFICIENTS (FORCE UNIT / DISP. UNIT)

DISP.	x (IN)	y (IN)	phi (RAD)	psi (RAD)	FORCE UNIT
Kx	4.5236E+03	1.2934E+03	-3.6992E+02	2.1883E+02	LB
Ky	-1.2934E+03	4.5236E+03	-2.1883E+02	-3.6992E+02	LB
Kphi	3.4697E+02	-4.6939E+02	5.8843E+02	5.1292E+02	IN-LB
Kpsi	4.6939E+02	3.4697E+02	-5.1292E+02	5.8843E+02	IN-LB
Bx	-2.3471E-02	-1.2673E-01	3.4849E-02	-5.8520E-03	LB-SEC
By	1.2673E-01	-2.3471E-02	5.8520E-03	3.4849E-02	LB-SEC
Bphi	-2.7798E-02	5.9155E-03	2.3693E-02	-4.3962E-02	IN-LB-SEC
Bpsi	-5.9155E-03	-2.7798E-02	4.3962E-02	2.3693E-02	IN-LB-SEC

```
( CASE  4 )  Face seal, no tilt, with pres. grad., lamda=10, sigma=0

&INPUTS
   TITLE  =  'Face seal, no tilt, with pres. grad., lamda=10, sigma=0'
   IFACE  =  1              ISIUN  =  0              IACC   =  1
   RO     =  1.0000E+00     EL     =  5.0000E-01     C      =  1.0000E-03
   IGROT  =  0              RPM    =  1.9099E+05     RPMD   =  0.0000E+00
   PLEA   =  2.0000E+00     PRIA   =  1.0000E+00     VISC   =  8.3333E-11
   ISTIF  =  1              IDAMP  =  1              MOM    =  1
   ICONT  =  0              IHOME  =  0              NUMDMP =  0
   EZD    =  0.0000E+00     EXD    =  0.0000E+00     EYD    =  0.0000E+00
   PHIR   =  0.0000E+00     PSIR   =  0.0000E+00
   FZD    =  0.0000E+00     FXD    =  0.0000E+00     FYD    =  0.0000E+00
   EMXD   =  0.0000E+00     EMYD   =  0.0000E+00
   NIT    =  8              DPRE   =  1.0000E-06     TOLP   =  1.0000E-04
   NITF   =  8              DECC   =  1.0000E-06     TOLE   =  1.0000E-03
   N      =  21             NREG   =  2              NRSUB  =  5  5
   ELFR   =  5.0000E-01  5.0000E-01
   ALPI   =  5.0000E-01  0.0000E+00
   BETI   =  2.5000E+01  0.0000E+00
   DELT   =  1.0000E-03  0.0000E+00
   DZIN   =  0.0000E+00
   DTHIN  =  0.0000E+00
/

SPIRAL GROOVE FACE SEAL,  ROTATING SURFACE IS SMOOTH

ID, OD, REFERENCE FILM THICKNESS =  1.0000E+00,  2.0000E+00,  1.0000E-03  (IN)

ROTATION SPEED, DISTURBANCE SPEED =  1.9099E+05,  0.0000E+00  (RPM)

INSIDE, OUTSIDE PRESSURE =  2.0000E+00,  1.0000E+00  (PSI)

VISCOSITY =  8.3333E-11  (PSI-SEC),   AMBIENT PRESSURE =  1.0000E+00  (PSI)

ITERATIONS AND ERROR CODE IN LAST PRESSURE CALCULATION =  2  0

CALCULATED FORCE IN  Z DIRECTION =  1.3612E+00  (LB)
CALCULATED MOMENTS ABOUT X,Y AXES = -3.0782E-16,  1.1794E-15  (IN-LB)

MINIMUM FILM THICKNESS =  1.0000E-03  (IN)

FLOW =  2.2763E+01  (IN**3/SEC) MEASURED AT  1.0000E+00  (PSI)

TORQUE =  2.2645E-03  (IN-LB),   FILM POWER LOSS =  6.8621E-03  (HP)

COMPRESSIBILITY NUMBER =  1.0000E+01,   SQUEEZE NUMBER =  0.0000E+00

        DYNAMIC COEFFICIENTS  ( FORCE UNIT / DISP. UNIT )

DISP.       z (IN)     phi (RAD)    psi (RAD)     FORCE UNIT
Kz       3.9524E+02 -4.8585E-04 -4.8576E-04   LB
Kphi    -6.1349E-07  2.0998E+02  8.2256E+01   IN-LB
Kpsi    -3.0546E-07 -8.2256E+01  2.0998E+02   IN-LB
Bz       2.9491E-02 -7.3530E-07 -7.3551E-07   LB-SEC
Bphi    -1.1280E-09  7.0914E-03 -1.8082E-03   IN-LB-SEC
Bpsi    -2.3148E-09  1.8082E-03  7.0914E-03   IN-LB-SEC
```

COMPARISON OF CASE 4 WITH PN471

CALCULATED FORCE IN Z DIRECTION = 1.3612E+00 (LB)

FLOW = 2.2763E+01 (IN**3/SEC) MEASURED AT 1.0000E+00 (PSI)

TORQUE = 2.2644E-03 (IN-LB), FILM POWER LOSS = 6.8620E-03 (HP)

DYNAMIC COEFFICIENTS (FORCE UNIT / DISP. UNIT)

DISP.	z (IN)	phi (RAD)	psi (RAD)	FORCE UNIT
Kz	3.9524E+02			LB
Kphi		2.0998E+02	8.2240E+01	IN-LB
Kpsi		-8.2240E+01	2.0998E+02	IN-LB
Bz	2.9485E-02			LB-SEC
Bphi		7.0901E-03	-1.8058E-03	IN-LB-SEC
Bpsi		1.8058E-03	7.0901E-03	IN-LB-SEC

```
( CASE  5 )  Face seal, no tilt, with pres. grad., lamda=10, sigma=20

&INPUTS
   TITLE  =  'Face seal, no tilt, with pres. grad., lamda=10, sigma=20'
   IFACE  =  1              ISIUN  =  0              IACC   =  1
   RO     =  1.0000E+00     EL     =  5.0000E-01     C      =  1.0000E-03
   IGROT  =  0              RPM    =  1.9099E+05     RPMD   =  1.9099E+05
   PLEA   =  2.0000E+00     PRIA   =  1.0000E+00     VISC   =  8.3333E-11
   ISTIF  =  1              IDAMP  =  1              MOM    =  1
   ICONT  =  0              IHOME  =  0              NUMDMP =  0
   EZD    =  0.0000E+00     EXD    =  0.0000E+00     EYD    =  0.0000E+00
   PHIR   =  0.0000E+00     PSIR   =  0.0000E+00
   FZD    =  0.0000E+00     FXD    =  0.0000E+00     FYD    =  0.0000E+00
   EMXD   =  0.0000E+00     EMYD   =  0.0000E+00
   NIT    =  8              DPRE   =  1.0000E-06     TOLP   =  1.0000E-04
   NITF   =  8              DECC   =  1.0000E-06     TOLE   =  1.0000E-03
   N      =  21             NREG   =  2              NRSUB  =  5  5
   ELFR   =  5.0000E-01  5.0000E-01
   ALPI   =  5.0000E-01  0.0000E+00
   BETI   =  2.5000E+01  0.0000E+00
   DELT   =  1.0000E-03  0.0000E+00
   DZIN   =  0.0000E+00
   DTHIN  =  0.0000E+00
/

SPIRAL GROOVE FACE SEAL,  ROTATING SURFACE IS SMOOTH

ID, OD, REFERENCE FILM THICKNESS =  1.0000E+00,  2.0000E+00,  1.0000E-03  (IN)

ROTATION SPEED, DISTURBANCE SPEED =  1.9099E+05,  1.9099E+05  (RPM)

INSIDE, OUTSIDE PRESSURE =  2.0000E+00,  1.0000E+00  (PSI)

VISCOSITY =  8.3333E-11  (PSI-SEC),   AMBIENT PRESSURE =  1.0000E+00  (PSI)

ITERATIONS AND ERROR CODE IN LAST PRESSURE CALCULATION =  2  0

CALCULATED FORCE IN  Z DIRECTION =  1.3612E+00  (LB)
CALCULATED MOMENTS ABOUT X,Y AXES = -3.0782E-16,  1.1794E-15  (IN-LB)

MINIMUM FILM THICKNESS =  1.0000E-03  (IN)

FLOW =  2.2763E+01  (IN**3/SEC) MEASURED AT  1.0000E+00  (PSI)

TORQUE =  2.2645E-03  (IN-LB),   FILM POWER LOSS =  6.8621E-03  (HP)

COMPRESSIBILITY NUMBER =  1.0000E+01,   SQUEEZE NUMBER =  2.0000E+01

        DYNAMIC COEFFICIENTS  ( FORCE UNIT / DISP. UNIT )

DISP.       z (IN)     phi (RAD)    psi (RAD)    FORCE UNIT
Kz       5.3566E+02 -2.9756E-04 -2.9746E-04   LB
Kphi    -2.1294E-07  2.4013E+02  7.0968E+01   IN-LB
Kpsi     2.5103E-07 -7.0968E+01  2.4013E+02   IN-LB
Bz       2.7697E-02  3.8068E-09  3.8070E-09   LB-SEC
Bphi     2.2173E-12  6.7533E-03 -1.6346E-03   IN-LB-SEC
Bpsi    -2.0783E-12  1.6346E-03  6.7533E-03   IN-LB-SEC
```

COMPARISON OF CASE 5 WITH PN471

CALCULATED FORCE IN Z DIRECTION = 1.3612E+00 (LB)

FLOW = 2.2763E+01 (IN**3/SEC) MEASURED AT 1.0000E+00 (PSI)

TORQUE = 2.2644E-03 (IN-LB), FILM POWER LOSS = 6.8620E-03 (HP)

DYNAMIC COEFFICIENTS (FORCE UNIT / DISP. UNIT)

DISP.	z (IN)	phi (RAD)	psi (RAD)	FORCE UNIT
Kz	5.3557E+02			LB
Kphi		2.4011E+02	7.0959E+01	IN-LB
Kpsi		-7.0959E+01	2.4011E+02	IN-LB
Bz	2.7692E-02			LB-SEC
Bphi		6.7528E-03	-1.6341E-03	IN-LB-SEC
Bpsi		1.6341E-03	6.7528E-03	IN-LB-SEC

```
( CASE  6 )  Face seal, no tilt, with pres. grad., lamda=10, sigma=200

&INPUTS
   TITLE  =  'Face seal, no tilt, with pres. grad., lamda=10, sigma=200'
   IFACE  =  1              ISIUN  =  0              IACC   =  1
   RO     =  1.0000E+00     EL     =  5.0000E-01     C      =  1.0000E-03
   IGROT  =  0              RPM    =  1.9099E+05     RPMD   =  1.9099E+06
   PLEA   =  2.0000E+00     PRIA   =  1.0000E+00     VISC   =  8.3333E-11
   ISTIF  =  1              IDAMP  =  1              MOM    =  1
   ICONT  =  0              IHOME  =  0              NUMDMP =  0
   EZD    =  0.0000E+00     EXD    =  0.0000E+00     EYD    =  0.0000E+00
   PHIR   =  0.0000E+00     PSIR   =  0.0000E+00
   FZD    =  0.0000E+00     FXD    =  0.0000E+00     FYD    =  0.0000E+00
   EMXD   =  0.0000E+00     EMYD   =  0.0000E+00
   NIT    =  8              DPRE   =  1.0000E-06     TOLP   =  1.0000E-04
   NITF   =  8              DECC   =  1.0000E-06     TOLE   =  1.0000E-03
   N      =  21             NREG   =  2              NRSUB  =  5  5
   ELFR   =  5.0000E-01  5.0000E-01
   ALPI   =  5.0000E-01  0.0000E+00
   BETI   =  2.5000E+01  0.0000E+00
   DELT   =  1.0000E-03  0.0000E+00
   DZIN   =  0.0000E+00
   DTHIN  =  0.0000E+00
/

SPIRAL GROOVE FACE SEAL,  ROTATING SURFACE IS SMOOTH

ID, OD, REFERENCE FILM THICKNESS =  1.0000E+00,  2.0000E+00,  1.0000E-03  (IN)

ROTATION SPEED, DISTURBANCE SPEED =  1.9099E+05,  1.9099E+06  (RPM)

INSIDE, OUTSIDE PRESSURE =  2.0000E+00,  1.0000E+00  (PSI)

VISCOSITY =  8.3333E-11  (PSI-SEC),   AMBIENT PRESSURE =  1.0000E+00  (PSI)

ITERATIONS AND ERROR CODE IN LAST PRESSURE CALCULATION =  2  0

CALCULATED FORCE IN  Z DIRECTION =  1.3612E+00  (LB)
CALCULATED MOMENTS ABOUT X,Y AXES = -3.0782E-16,  1.1794E-15  (IN-LB)

MINIMUM FILM THICKNESS =  1.0000E-03  (IN)

FLOW =  2.2763E+01  (IN**3/SEC) MEASURED AT  1.0000E+00  (PSI)

TORQUE =  2.2645E-03  (IN-LB),   FILM POWER LOSS =  6.8621E-03  (HP)

COMPRESSIBILITY NUMBER =  1.0000E+01,   SQUEEZE NUMBER =  2.0000E+02

        DYNAMIC COEFFICIENTS  ( FORCE UNIT / DISP. UNIT )

DISP.      z (IN)     phi (RAD)    psi (RAD)    FORCE UNIT
Kz      2.3872E+03 -4.1732E-05 -4.1685E-05   LB
Kphi   -2.5267E-08  7.2912E+02 -7.4833E+00   IN-LB
Kpsi    5.8389E-08  7.4833E+00  7.2912E+02   IN-LB
Bz      4.1358E-03  5.3850E-10  5.3818E-10   LB-SEC
Bphi    4.2377E-13  1.2426E-03 -5.8922E-05   IN-LB-SEC
Bpsi   -5.5928E-13  5.8922E-05  1.2426E-03   IN-LB-SEC
```

COMPARISON OF CASE 6 WITH PN471

CALCULATED FORCE IN Z DIRECTION = 1.3612E+00 (LB)

FLOW = 2.2763E+01 (IN**3/SEC) MEASURED AT 1.0000E+00 (PSI)

TORQUE = 2.2644E-03 (IN-LB), FILM POWER LOSS = 6.8620E-03 (HP)

DYNAMIC COEFFICIENTS (FORCE UNIT / DISP. UNIT)

DISP.	z (IN)	phi (RAD)	psi (RAD)	FORCE UNIT
Kz	2.3870E+03			LB
Kphi		7.2907E+02	-7.4987E+00	IN-LB
Kpsi		7.4987E+00	7.2907E+02	IN-LB
Bz	4.1383E-03			LB-SEC
Bphi		1.2438E-03	-5.8939E-05	IN-LB-SEC
Bpsi		5.8939E-05	1.2438E-03	IN-LB-SEC

(CASE 7) Misaligned shaft seal with pres. grad. to comp. w/ GASBEAR

```
&INPUTS
   TITLE  =  'Misaligned shaft seal with pres. grad. to comp. w/ GASBEAR'
   IFACE  =  0              ISIUN  =  0              IACC   =  1
   RO     =  1.0000E+00     EL     =  2.0000E+00     C      =  1.0000E-03
   IGROT  =  0              RPM    =  1.9099E+05     RPMD   =  0.0000E+00
   PLEA   =  2.0000E+00     PRIA   =  1.0000E+00     VISC   =  8.3333E-11
   ISTIF  =  1              IDAMP  =  1              MOM    =  1
   ICONT  =  0              IHOME  =  0              NUMDMP =  0
   EZD    =  0.0000E+00     EXD    =  2.5000E-04     EYD    =  2.5000E-04
   PHIR   =  2.5000E-04     PSIR   =  2.5000E-04
   FZD    =  0.0000E+00     FXD    =  0.0000E+00     FYD    =  0.0000E+00
   EMXD   =  0.0000E+00     EMYD   =  0.0000E+00
   NIT    =  8              DPRE   =  1.0000E-06     TOLP   =  1.0000E-04
   NITF   =  8              DECC   =  1.0000E-06     TOLE   =  1.0000E-03
   N      =  17             NREG   =  1              NRSUB  =  8
   ELFR   =  1.0000E+00
   ALPI   =  0.0000E+00
   BETI   =  0.0000E+00
   DELT   =  0.0000E+00
   DZIN   =  0.0000E+00
   DTHIN  =  0.0000E+00
/
```

SPIRAL GROOVE SHAFT SEAL, ROTATING SURFACE IS SMOOTH

LENGTH, DIAMETER, CLEARANCE = 2.0000E+00, 2.0000E+00, 1.0000E-03 (IN)

ROTATION SPEED, DISTURBANCE SPEED = 1.9099E+05, 0.0000E+00 (RPM)

PRESSURE AT START, END AXIAL BOUNDARIES = 2.0000E+00, 1.0000E+00 (PSI)

VISCOSITY = 8.3333E-11 (PSI-SEC), AMBIENT PRESSURE = 1.0000E+00 (PSI)

ITERATIONS AND ERROR CODE IN LAST PRESSURE CALCULATION = 3 0

CALCULATED FORCES IN X,Y DIRECTIONS = 3.1535E+00, 1.2350E+00 (LB)
CALCULATED MOMENTS ABOUT X,Y AXES = 3.7793E-01, -1.9883E-03 (IN-LB)

MINIMUM FILM THICKNESS = 5.0000E-04 (IN)

FLOW = 4.7315E+00 (IN**3/SEC) MEASURED AT 1.0000E+00 (PSI)

TORQUE = 2.3248E-02 (IN-LB), FILM POWER LOSS = 7.0448E-02 (HP)

COMPRESSIBILITY NUMBER = 1.0000E+01, SQUEEZE NUMBER = 0.0000E+00

DYNAMIC COEFFICIENTS (FORCE UNIT / DISP. UNIT)

DISP.	x (IN)	y (IN)	phi (RAD)	psi (RAD)	FORCE UNIT
Kx	9.2287E+03	4.8183E+03	1.1084E+03	5.7870E+02	LB
Ky	-2.6167E+03	9.5964E+03	4.7033E+02	8.7124E+02	LB
Kphi	-9.8594E+01	6.5068E+02	1.5189E+03	7.7760E+02	IN-LB
Kpsi	7.1674E+02	-9.7210E+01	-1.0491E+03	1.2765E+03	IN-LB
Bx	-2.0553E-01	-4.5816E-01	-1.0900E-01	6.2037E-02	LB-SEC
By	2.5253E-01	-2.9852E-01	-6.7612E-02	-7.7454E-02	LB-SEC
Bphi	2.3869E-02	1.4706E-02	3.7737E-02	-8.3553E-02	IN-LB-SEC
Bpsi	-7.4893E-02	-5.8155E-02	5.7003E-02	6.7719E-02	IN-LB-SEC

COMPARISON OF CASE 7 WITH GASBEAR USING SAME GRID AND ROMBERG EXTRAPOLATION

CALCULATED FORCES IN X,Y DIRECTIONS = 3.1529E+00, 1.2362E+00 (LB)
CALCULATED MOMENTS ABOUT X,Y AXES = 3.7751E-01, -7.3904E-04 (IN-LB)

DYNAMIC COEFFICIENTS (FORCE UNIT / DISP. UNIT)

DISP.	x (IN)	y (IN)	phi (RAD)	psi (RAD)	FORCE UNIT
Kx	9.2287E+03	4.8097E+03	1.1044E+03	5.7867E+02	LB
Ky	-2.6113E+03	9.5993E+03	4.7249E+02	8.7343E+02	LB
Kphi	-1.0249E+02	6.5339E+02	1.5237E+03	7.7076E+02	IN-LB
Kpsi	7.1455E+02	-9.4976E+01	-1.0403E+03	1.2793E+03	IN-LB
Bx	-2.0561E-01	-4.5802E-01	-1.0909E-01	6.1715E-02	LB-SEC
By	2.5292E-01	-2.9885E-01	-6.7494E-02	-7.7535E-02	LB-SEC
Bphi	2.3875E-02	1.4639E-02	3.7502E-02	-8.3706E-02	IN-LB-SEC
Bpsi	-7.4561E-02	-5.7965E-02	5.6982E-02	6.7347E-02	IN-LB-SEC

6. Operating Environment

The computer code SPIRALG and especially the main subroutine SPIRAL have been written to run under a variety of operating environments with very little modification. The extensions to ANSI Standard FORTRAN 77 that have been used are discussed at the start of Section 2. Executable versions of SPIRALG have been compiled with Version 5.0 of the Microsoft FORTRAN compiler and tested for use on IBM PC compatible computers with 80x87 floating point coprocessors. The two files constituting the source program listed in Appendices A and B have been compiled with the command:

```
fl /AH /Gt /c /4I2 SPIRALG.FOR SPIRALGS.FOR
```

and linked as follows with the appropriate large model, floating point libraries provided by Microsoft to run under either DOS or OS2 operating systems.

```
fl /Lp SPIRALG SPIRALGS /link <path>\llibf7p <path>\DOScalls, SPIRAL1.def.
Rename SPIRALG.EXE, SPIRAL1.EXE.
```

The executable file is renamed to be consistent with the CFD Executive program. A program definition file is required when running this program in order to define the program as a PM text window compatible (VIO) program. The following file named "SPIRAL1.DEF" must be used:

```
NAME            SPIRAL1  WINDOWCOMPAT
DESCRIPTION     'SPIRAL1 Analysis Program'
STUB            'OS2STUB.EXE'
DATA            MULTIPLE
STACKSIZE       8192
HEAPSIZE        8192
PROTMODE
EXPORTS
```

The memory required to run the program is controlled by the values of the parameters NDT and NDZ at the time of compilation. The program has been compiled and tested under DOS with the following statement

```
PARAMETER (NDT=21,NDZ=13,NDREG=3)
```

where NDT and NDZ represent the maximum allowable number of grid points in the circumferential and transverse directions respectively. It requires less that 350k of available memory.

The program has been compiled and tested under OS2 with the following statement

```
PARAMETER (NDT=41,NDZ=25,NDREG=3)
```

which permits doubling the grid in both directions. This OS2 uses approximately 1500k of memory.

The DOS version of the program should run on any IBM PC or compatible with a math coprocessor, sufficient memory and DOS 3.0 or higher. Mass storage requirements are minimal (a 360k diskette drive should be sufficient). The OS2 version will require sufficient additional resources to run OS2 (version 1.2 or higher) and the 1500k program loading.

7. Error Messages

1 Pressures did not converge in final load calculation.

Occurs when the Newton-Raphson iteration procedure for finding the pressures does not converge to within a relative error of TOLP in NIT iterations. Check to see if reasonable values are given for these quantities. If so, try using a finer grid.

2 Eccentricities did not converge in homing process.

This error occurs when IHOME>0 and the homing process failed to converge within a relative error of TOLH in NITF iterations. Modify initial displacements. Try increasing them if possible as this error is more likely to occur if initial guesses ar too low. A good set of initial displacements can often be found relatively easily by trial and error with IHOME=0.

3 Homing process and final load calculation both diverged.

This is a combination of errors 1 and 2. Pressures converged during the homing process which in turn diverged. The final load calculation also diverged.

4 Pressures did not converge during homing process.

This error occurs when IHOME>0 and the pressures fail to converge during the homing process. When this occurs the homing process is aborted. Possible remedies are given under message (1).

5 Negative film thickness encountered numerical damping not requested.

This error will occur when IHOME>0 and a bad guess is given for initial displacements, or excessive truncation error occurs. If the grid is believed to be fine enough, try either modifying initial displacements or setting NUMDMP>0.

6 Computation of numerical damping coefficient diverged.

This error should not normally occur. If it does, check to see if inputs are correct and if necessary set IHOME=0 and try to find a better set or starting displacements.

7 Matrix inversion error encountered in updating eccentricities.

This error would occur in the event that a singular stiffness matrix was encountered during the homing process. The most likely cause for this would be an attempt to impose a load on a seal that has no load capacity, such as an ungrooved, stationary seal.

8 Input eccentricities result in negative film thickness.

This warns the user that the prescribed displacement and tilt exceed allowable values and should be reduced.

9 Attempt encountered to exceed maximum allowable grid points in z direction.

The values of NRSUB must be reduced.

10 Matrix inversion error encountered in pressure solution.

This error would occur in the highly unlikely event that a singular matrix was encountered in during the column method solution for the pressures.

11 Maximum dimensions for fine grid solution would be exceeded.

This error will occur if IACC=1 and the grid size for the course grid solution falls within allowable limits but one or both of the dimensions required for the fine grid solution is too large. Reduce N or the NRSUB values appropriately.

12 Illegal length, clearance, viscosity, pressure or speed encountered.

Check inputs and correct error.

13 Maximum number of circumferential grid points exceeded.

Reduce N accordingly.

14 Maximum number of allowable regions exceeded.

Reduce NREG.

>100 Coarse grid solution returned due to error in fine grid solution specified by last 2 digits.

If IACC=1 and the course grid solution is completed without error but errors are encountered while obtaining the fine grid solution a 3 digit error code will result. The first digit will be 1 and the second 2 digits will correspond to the error codes given above.

15 Unable to open input file: SPIRAL.INP

The input file "SPIRAL.INP" was not found.

16 Invalid output filename. Make sure namelist variable: OUTFIL is defined.

The namelist variable "OUTFIL" which defines the output filename is missing or misspelled.

8. References

1. Vohr, J.H. and Pan, C.H.T., *"On the Spiral Grooved Self Acting Gas Bearing"*, MTI-63TR52, Mechanical Technology Incorporated, Latham, NY, (1962)

2. Vohr, J.H. and Pan, C.H.T., *"Design Data: Gas Lubricated Spin-Axis Bearings for Gyroscopes"*, MTI-68TR29, Mechanical Technology Incorporated, Latham, NY, (1968)

3. Smalley, A.J., *"The Narrow Groove Theory of Spiral Grooved Gas Bearings: Development and Application of a Generalized Formulation for Numerical Solution"*, ASME J. Lub. Tech., V 94, 1, (1972), pp. 86-92

4. Castelli, V. and Pirvics, J., *"Review of Methods in Gas Bearing Film Analysis"*, Trans. ASME, (1968), pp. 777-792

5. Press, W.H., Flannery, B.P., Teukolsky, S.A. and Vetterling, W.T., *"Numerical Recipes"*, Cambridge University Press, (1986)

6. Artiles, A.,A., Walowit, J.A. and Shapiro, W., *"Analysis of Hybrid Fluid Film Journal Bearings with Turbulence and Inertia Effects"*, Proc. ASME Symposium in Advances in Computer-Aided Design, (1982), pp. 25-52

7. Castelli, V., *"Design of Gas Bearings - Volume 1, Part 4: Numerical Methods"*, Gas Bearing Course Notes, Mechanical Technology Incorporated, Latham, NY, (1971)

8. Shapiro, W., *"Computer Code SPIRALP for Gas-Lubricated Spiral-Groove Bearings and Seals"*, MTI 88TM2, Prepared for NASA under Contract No. NAS3-24645, (1988)

9. Sato, Y., Ono, K. and Iwama, A., *"The Optimum Groove Geometry for Spiral Groove Viscous Pumps"*, ASME J. Tribology, V 112, 2, (1990), pp. 409-112

APPENDIX A

SOURCE LISTING
OF
SPIRAL AND SUPPORTING SUBROUTINES

Supplied Under Separate Cover

MTI 92TM1

The source listing of SPIRAL and supporting subroutines
were released as LEW–16582 in 1998.

APPENDIX B

SOURCE LISTING
OF
PROGRAM SPIRALG AND SUPPORTING SUBROUTINES

Supplied Under Separate Cover

The source listing of Program SPIRALG and supporting subroutines were released as LEW–16582 in 1998.

REPORT DOCUMENTATION PAGE

Form Approved
OMB No. 0704-0188

1. AGENCY USE ONLY (*Leave blank*)	2. REPORT DATE	3. REPORT TYPE AND DATES COVERED
	October 2005	Final Contractor Report

4. TITLE AND SUBTITLE

Users' Manual for Computer Code SPIRALG
Gas Lubricated Spiral Grooved Cylindrical and Face Seals

5. FUNDING NUMBERS

WU–506–42–31–00
WU–590–21–11–00
NAS3–25644

6. AUTHOR(S)

Jed A. Walowit

7. PERFORMING ORGANIZATION NAME(S) AND ADDRESS(ES)

Mechanical Technology, Inc.
968 Albany Shaker Road
Latham, New York 12110

8. PERFORMING ORGANIZATION REPORT NUMBER

E–13621

9. SPONSORING/MONITORING AGENCY NAME(S) AND ADDRESS(ES)

National Aeronautics and Space Administration
Washington, DC 20546–0001

10. SPONSORING/MONITORING AGENCY REPORT NUMBER

NASA CR—2003-212361
91TM11

11. SUPPLEMENTARY NOTES

Jed A. Walowit, Jed A. Walowit, Inc., 4 Cypress Point, Clifton Park, New York 12065 for Mechanical Technology, Inc. Project Manager, Anita D. Liang, Aeropropulsion Projects Office, NASA Glenn Research Center, organization code P, 216–977–7439.

12a. DISTRIBUTION/AVAILABILITY STATEMENT

Restriction changed to Unclassified/Unlimited on July 27, 2005, by authority of the NASA Glenn Research Center, Structures Division.

Export Administration Regulations (EAR) Notice

This document contains information within the purview of the Export Administration Regulations (EAR), 15 CFR 730–774, and is export controlled. It may not be transferred to foreign nationals in the U.S. or abroad without specific approval of a knowledgeable NASA export control official, and/or unless an export license/license exception is obtained/available from the Bureau of Industry and Security, United States Department of Commerce. Violations of these regulations are punishable by fine, imprisonment, or both.

Unclassified-Unlimited
Subject Category: 34
Available electronically at http://gltrs.grc.nasa.gov
This publication is available from the NASA Center for AeroSpace Information, 301–621–0390.

12b. DISTRIBUTION CODE

13. ABSTRACT ***(Maximum 200 words)***

The computer codes developed predict the performance characteristics of gas lubricated cylindrical and face seals with or without the inclusion of spiral grooves. Performance characteristics include load capacity, leakage flow, power requirements and dynamic characteristics in the form of stiffness and damping coefficients in 4 degrees of freedom for cylindrical seals and 3 degrees of freedom for face seals. These performance characteristics are computed as functions of seal and groove geometry, load or film thickness, running speeds, fluid viscosity, and boundary pressures. A derivation of the equations governing the performance of gas lubricated spiral groove cylindrical and face seals along with a fairly detailed description of their solution is given, followed by a description of the computer codes including an input description, sample cases, and comparisons with results of other codes.

14. SUBJECT TERMS	15. NUMBER OF PAGES
Face seals; Seals; Cylindrical seals; Leakage; Gas Lubricated; Spiral-grooved; Turbulent; Users' manual	90
	16. PRICE CODE

17. SECURITY CLASSIFICATION OF REPORT	18. SECURITY CLASSIFICATION OF THIS PAGE	19. SECURITY CLASSIFICATION OF ABSTRACT	20. LIMITATION OF ABSTRACT
Unclassified	Unclassified	Unclassified	